Surging glaciers in Svalbard: Observing their distribution, characteristics and evolution

William D. Harcourt*[1,2], Danni M. Pearce[1,3], Wojciech Gajek[4], Harold Lovell[5], Erik S. Mannerfelt[6,7], Andreas Kääb[6], Douglas I. Benn[8], Adrian Luckman[9], Richard Hann[10], Jack Kohler[11], Tazio Strozzi[12], Rebecca McCerery[13], Bethan J. Davies[14]

[1]School of Geosciences, University of Aberdeen, Aberdeen, United Kingdom
[2]Interdisciplinary Institute, University of Aberdeen, Aberdeen, United Kingdom
[3]Faculty of Environmental Sciences and Natural Resource Management, Norwegian University of Life Sciences, Ås, Norway
[4]Institute of Geophysics, Polish Academy of Sciences, Warsaw, Poland
[5]School of the Environment and Life Sciences, University of Portsmouth, Portsmouth, United Kingdom
[6]Department of Geosciences, University of Oslo, Oslo, Norway
[7]Arctic Geology, The University Centre in Svalbard, Longyearbyen, Norway
[8]School of Geography & Sustainable Development, University of St Andrews, St Andrews, United Kingdom
[9]Department of Geography, College of Science and Engineering, Swansea University, Swansea, United Kingdom
[10]Department of Engineering Cybernetics, UAV Icing Lab, Norwegian University of Science and Technology, Trondheim, Norway
[11]Norwegian Polar Institute, Fram Centre, Tromsø, Norway
[12]GAMMA Remote Sensing AG, Gümligen, Switzerland
[13]Department of Geography and Environmental Science, Northumbria University, Newcastle Upon Tyne, UK
[14]School of Geography, Politics and Sociology, Newcastle University, Newcastle Upon Tyne, UK

*Corresponding author: William D. Harcourt (william.harcourt@abdn.ac.uk)

Abstract

Glacier surges are episodes of significantly increased ice flow due to ice-dynamical feedbacks, and are often repeated in a quasi-periodical manner. Ice mass is redistributed during a surge, which leads to surface lowering at high elevation as ice is transferred down-glacier and thickening nearer the terminus. In this paper, we review different approaches for monitoring and detecting glacier surges in Svalbard, one of the most prominent global clusters of surge-type glaciers. Current surge detection is mainly based upon tracking the speed of glaciers over time, measuring elevation and frontal changes, and more recently automatically detecting surface changes such as increased crevassing. Thermal and hydrological changes near the glacier bed drive surge dynamics and can be measured using geophysical sensors such as ground-penetrating radar (GPR) and seismometers. When glaciers surge, they often produce diagnostic landforms in subglacial and proglacial environments, allowing historical surging to be identified even if surges have not been directly observed.

Through this review, we have compiled an updated database of surge-type glaciers in Svalbard and find that 36% of glaciers display surge-type behaviour, which accounts for 75% of the total glacier area on Svalbard. Only 10% of all glaciers have been directly observed to surge, yet account for 48% of the total glacier area on Svalbard. Svalbard surge-type glaciers have gentler slopes, are generally longer, and extend across a larger elevation range compared to non surge-type glaciers across the archipelago. We find that the behaviour of surge-type glaciers is variable and more closely resembles a continuum from glaciers that do not surge to those which redistribute mass in a single event of strongly enhanced ice flux. We can describe the variability in surge behaviour using the concept of enthalpy and a six-stage surge model that characterises the build-up of energy at the glacier bed driven initially by thermal change and then ice acceleration which is prompted by changes in subglacial hydrology. Observations of glacier surges have improved significantly with routine mapping from satellites such as Sentinel-1, Sentinel-2 and the Landsat satellite series. Furthermore, an increasing number of geophysical measurements is enabling an improved understanding of subglacial processes before, during and after a surge, which is crucial for improving models of surge behaviour. As our observations of surges continue to improve, we expect to uncover new elements and details of surge behaviour, reaffirming the need to rethink the binary classification of glaciers as either ‘surge-type’ or ‘not surge-type’ in Svalbard and across the world.

Keywords: Glacier surging; satellite remote sensing; geophysics; palaeo-glaciology; continuum of behaviour

Highlights

- Approximately 36% of glaciers in Svalbard have been observed to surge or show clear evidence of having surged in the past, accounting for 75% of the total glacier area on Svalbard.
- Surges can be readily identified from satellite data, landforms representative of fast flow (e.g. crevasse squeeze ridges), and geophysical sensors.
- Svalbard surges may be described by a six-stage model from gradual speed-up, ice acceleration and then peak velocity, before a slow dissipation of energy and glacier slow-down.
- There is a continuum of glacier dynamical behaviour: full catchment surges, pulses of tributary glaciers, partial acceleration, and no surge behaviour.
- Key knowledge gaps include understanding the surge potential of small valley glaciers, the relationship between surges and mass balance, and the evolution of surge-type glaciers and surging from the Little Ice Age through to the present day and into the future.

1. Introduction

1.1. Glacier surges

Surge-type glaciers undergo quasi-periodical changes in their flow regime from accelerated velocities during an ‘active’ surge to low velocities during quiescence (Benn et al., 2019a). This behaviour contrasts to the flow dynamics of non-surging glaciers, which are governed by the ongoing adjustment to the difference between mass accumulation at higher elevation and ablation at lower elevation (i.e. the balance velocity), with short-term velocity variations (e.g. diurnal, seasonal) superimposed on this long-term pattern. The surge cycle between fast and slow flow results from internal dynamical instabilities, whereby fast flow initiates due to frictional feedbacks (Thøgersen et al., 2019; 2024) and may be expedited by external factors such as dynamic thinning from enhanced surface melt (Sevestre et al., 2018). The subsequent enhanced down-glacier discharge of ice can increase the mass loss over short time periods during a multi-year active surge (McMillan et al., 2014; Dunse et al., 2015; Morris et al., 2020) and subsequently expose more ice to higher air temperatures leading to enhanced surface melting (Oerlemans, 2018). In addition, the influx of freshwater into the ocean/fjord caused by a glacier surge may impact circulation and stratification, whilst also affecting downstream marine and terrestrial ecosystems through local changes in biogeochemistry (Hopwood et al., 2020). Conversely, the link between surge-type glaciers advancing into proglacial permafrost terrain and disrupting methane stores is less clear, but high subglacial water pressure may increase this flux (Kleber et al., 2025), and is therefore relevant to consider in the context of surging. Surges may last months to years and can occur over full catchments or along individual tributaries, hence the impact of these quasi-periodical events will vary spatially and temporally (Raymond, 1987). Glacier surges can also cause a number of hazards through the direct impact of their advance on land and infrastructure, the increased flux of icebergs into the ocean, river damming and flooding, and ice avalanching (Truffer et al., 2021; Kääb et al., 2021; Lovell et al., 2026). On Svalbard, a key impact of glacier surging is through enhanced crevassing that makes travel routes dangerous or at least more complicated.

Glacier surges involve changes in subglacial conditions (Meier and Post, 1969; Kamb et al. 1985; Benn et al., 2019a). Traditionally, surges were thought to be governed by one of two potential mechanisms: the ‘thermal switch’ and the ‘hydrologic switch’. In the ‘thermal switch’ model (Clarke, 1976; Fowler et al., 2001), surges begin and end due to a change in basal temperature that leads to an increase or loss of meltwater availability for basal sliding. In contrast, in the ‘hydrologic switch’ mechanism (Kamb, 1987; Fowler et al., 1987), surges initiate due to a change in the configuration of the subglacial hydrological system from a channelised system to a distributed one. This increases subglacial water pressure and consequently enhances basal slip, leading to glacier acceleration during a surge.

Recent studies have suggested that surge cycles can be explained by oscillations in the coupled mass and basal enthalpy (thermal energy and water) budgets, which occur when glaciers are unable to settle on a stable steady state (Benn et al., 2019a). The enthalpy balance model can explain both the broad evolution of glacier surge dynamics and the occurrence of surge-type glaciers in climatically controlled clusters. In its current form, it takes a simplified approach to representing basal friction and hydrology and adopts a lumped (non-spatial) framework and thus cannot represent the details of individual surges. Thøgersen et al. (2019; 2024) aimed to explain oscillatory dynamics such as surges through a rate and state friction framework, whereby basal shear stress evolves as subglacial cavities expand due to an increase in subglacial water pressure. As a glacier gains mass, basal shear stress increases and ice velocity 'strengthens' to a point at which subglacial cavities form and the glacier surges. During a surge, mass is redistributed leading to a reduction in basal shear stress, the velocity 'weakening' regime. In this phase, there is a negative feedback between basal friction and subglacial cavity formation beneath hard-bedded glaciers (Gilbert et al., 2022). For a glacier to move back into a velocity 'strengthening' regime, glacier sliding must then incorporate subglacial sediments, or the glacier margins become cold-based so that subglacial cavities can persist. After surge termination, mass will build up and the basal shear stress increases again, hence the cycle between velocity 'strengthening' and 'weakening' continues quasi-periodically. This model was developed for hard beds but has since been extended to include sliding over deformable sediments (Minchew and Meyer, 2020; Thøgersen et al., 2024). However, coupling enthalpy changes to sliding remains difficult. Terleth et al. (2021) suggested combining both the enthalpy and basal sliding theories by considering the transient nature of friction and deformation at the bed as the fundamental component, with enthalpy as the forcing component. Resolving the causes, drivers, and triggers of glacier surges may yield insights into the fundamental physics that govern ice flow, and in particular processes at the glacier base, where direct observations are scarce due to its inaccessibility.

The presence of unstable ice flow raises a pertinent question: why do some glaciers surge and others do not? Sevestre and Benn (2015) found that surge-type glaciers are located in geographical clusters with specific temperature and precipitation regimes optimal for surge-type ice flow cycles to exist. In the Arctic, a ring of surging glacier clusters can be found extending from Alaska-Yukon to Novaya Zemlya, also including the Canadian Arctic Archipelago. The 'Arctic ring' encapsulates Svalbard, an archipelago with a long history of glaciological observations and consequently measurements of glacier surges. Around 56% of the Svalbard archipelago area is covered by 1,583 glaciers and ice caps (RGI 7.0, 2023; Figure 1). Furthermore, there are three primary regions with bases in Svalbard:

central (Longyearbyen and Barentsberg), northwest (Ny Ålesund), and southwest (Hornsund) Spitsbergen. All three locations can be accessed all year round either by air, boat or snowmobile, making field measurements cost-effective and logistically possible. As a result, many of Svalbard's glaciers located around these central research hubs have long-term records of glacier changes, with more sites being added as more of the archipelago becomes accessible via improved logistics. Using these observations alongside remote sensing data is enabling a better understanding of the physical processes driving glacier surges. Svalbard is therefore an ideal natural laboratory for studying glacier surges, their drivers, and their changes in the past and into the future. Here, we review the current knowledge of Svalbard surges, including the main techniques used for detecting and monitoring surges, and provide an update on the spatial and temporal distribution of surge-type glaciers and glacier surges.

FIGURE 1

1.2. Surging glaciers in Svalbard

Svalbard is an Arctic archipelago located between 76°N and 81°N. It is approximately 700 km east of Greenland and 300 km west of the Russian Arctic. There is a large climatic gradient across the archipelago (Hanssen-Bauer et al., 2019) as Svalbard is located at the boundary between warm Atlantic waters to the west, which travel northwards along the Fram Strait, and the cold Polar waters in the Barents Sea to the east. Warm Atlantic water is transported along the west coast of Svalbard via the West Spitsbergen Current, releasing heat and moisture that leads to higher temperatures than average found at this latitude. In comparison, the East Spitsbergen Current transports colder water from the Arctic Ocean into the Barents Sea, which leads to the formation of seasonal sea ice (Rieke et al., 2023). The formation of sea ice in western Svalbard is generally limited to the fjords (e.g. Swirad et al., 2024). The presence of sea ice to the north and east of Svalbard (Onarheim et al., 2018) limits available moisture sources and hence average precipitation rates are low, averaging less than 700 mm per year (Hanssen-Bauer et al., 2019).

Spitsbergen is the largest island in Svalbard with an area of 40,000 km^2 and is covered by ice fields in the northwest, northeast and south, with many smaller glaciers and ice masses found in valleys in between. The second largest island is Nordaustlandet to the northeast where the two largest ice caps in Svalbard, Austfonna (8,100 km^2) and Vestfonna (2,500 km^2), are located. Kvitøya, covered almost completely by the Kvitøyjøkulen ice cap, is located a further 90 km east. The islands of Barentsøya and Edgeøya are located to the southeast of Spitsbergen where several large ice caps and valley glaciers can be found. During the last glacial maximum, the Barents Sea Ice Sheet extended from mainland Russia to Franz Josef Land and then to the continental shelf break to the west of Svalbard (Ingólfsson and Landvik, 2013). At the start of the Holocene, ice in Svalbard was restricted to the archipelago (Farnsworth et al., 2020), after which there was a rapid deglaciation (12.0-10.5 ka) before several episodes of re-advances culminating in the Little Ice Age. Between 1936 and 2010, Svalbard glaciers lost mass at a rate of ~8 Gt per year (Geyman et al., 2022), and this rate has increased to ~14 Gt per year in the more recent period between 2000 and 2023 (Zemp et al., 2025). This accelerated mass loss is a result of the Svalbard and the Barents Sea region warming up to 6 times faster than the rest of the planet (Isaksen et al., 2022; Rantanen et al., 2022). Future simulations by Geyman et al., (2022) suggest that glaciers will lose mass 2-4 times the historical rate by 2100.

The number of surge-type glaciers in Svalbard has been estimated to range between 10% and 90% depending on the classification technique used and the amount of data available for each compilation (Lefauconnier and Hagen, 1991; Jiskoot et al., 1998; Sevestre and Benn, 2015; Kääb et al., 2023; Koch et al., 2023). Therefore, although Svalbard is considered to have a large share of surge-type glaciers compared to other regions, not all glaciers have displayed this behaviour, suggesting local factors may control the ability of a glacier to surge. Jiskoot et al. (1998; 2000) found that glacier geometry (width, thickness, surface and bed slope) has a significant influence on the likelihood of a glacier to be of surge type. This is in agreement with Sevestre and Benn (2015), who found that surge-type glaciers globally tend to be longer, have lower slopes and have larger catchment sizes. In Svalbard, most surge-type glaciers are most likely to overlay deformable sedimentary bedrock (Hamilton and Dowdeswell 1996; Jiskoot et al., 2000). Complex glacier configurations (i.e. the presence of multiple tributaries feeding into a larger glacier, or multiple flow-units within a glacier system) may also partly control Svalbard surges (Jiskoot et al., 2000; Sevestre and Benn, 2015).

To better understand the causes, triggers and impacts of glacier surges in Svalbard, improved monitoring is required and new techniques developed to extend the observational record of active surge dynamics. Observations of sediment-landform assemblages formed by past surging have partially bridged this gap (Farnsworth et al., 2016; Flink et al., 2018; McCerery et al., 2024; 2025), particularly when combined with absolute dating methods (Kempf et al., 2013; Flink and Noormets, 2018; Lovell et al., 2018b), but such records can be compromised by erosion and sedimentation. Historical aerial photographs and archival maps have revealed past surges as far back as 1850 (Lefauconnier and Hagen, 1991; Hagen et al., 1993; Geyman et al., 2022) but these are intermittent observations and do not document surge velocities, terminus advance rates, mass transfer, triggers or subglacial conditions. Even in the satellite era, with dense observations that can be used to detect active surges (Kääb et al., 2023; Koch et al., 2023), only in situ geophysical observations are capable of directly studying subglacial drivers of a surge (Sevestre et al., 2015; Bouchayer et al., 2024). The influence of environmental factors such as calving and surface melt has been less studied with only a few studies (e.g. Dowdeswell et al., 1995; Sevestre et al., 2018; Benn et al., 2022) commenting on the potential causes of surge initiation. Consequently, the lack of detailed long-term surge observations has also inhibited our understanding of their impact on regional glacier mass balance, which may be significant (e.g., McMillan et al., 2014; Dunse et al., 2015).

1.3. Aims of review

The primary aim of this paper is to review the techniques used to observe surges and the distribution of surge behaviour in Svalbard. Through this review, we will highlight research gaps and opportunities for future research. Our specific objectives are to:

1) Review the techniques used to detect glacier surges, monitor their characteristics, and measure their causal processes.

2) Compile existing databases of surge-type glaciers in Svalbard to generate an updated estimate of their distribution across the archipelago.

3) Evaluate the role of the different monitoring techniques to advance our knowledge of surge behaviour in Svalbard and their causal mechanisms.

4) Identify key gaps in process knowledge and monitoring capabilities to inform future research priorities.

2. Previous compilations of surge-type glaciers in Svalbard

One of the first reliable sources of a glacier surge in Svalbard is linked to the 1838 French La Recherche Expedition, which painted Recherchebreen as extensively crevassed, and mapped the terminus position to an extent that far exceeded both previous and subsequent maps (Figure 2). Since then, and with ever more observations of glacier surges, there have been several attempts to compose a database of surge-type glaciers in Svalbard based on different methodologies. Lefauconnier and Hagen (1991) compiled a detailed list of surge-type glaciers in eastern Svalbard that were marine-terminating and discharged icebergs into the Barents Sea, concluding that 90% of glaciers in Svalbard were likely to be surge-type. Hagen et al. (1993) developed the first Svalbard-wide inventory of surge-type glaciers, documenting recorded surges from historical observations, satellite imagery and archival aerial photographs. In comparison, statistical analysis of variables that control surging (e.g. bed lithology, glacier geometry) have suggested that only 13% of Svalbard's glaciers are surge-type (Jiskoot et al., 1998; 2000). Sevestre and Benn (2015) compiled a global database of surge-type glaciers from ice flow velocities, detected terminus advances and geomorphological evidence (see section 4). They also compiled a list of glaciers that are possibly surge-type after showing signatures of past surge behaviour, and glaciers very likely to be surge-type that display several well-preserved surge features but have not been directly observed to surge. An updated version of this database is currently available in the Randolph Glacier Inventory (RGI) version 7 (RGI 7.0 Consortium, 2023). In this database, Sevestre and Benn (2015) estimated that 17% (n=263) of glaciers in Svalbard have shown past surge activity, of which only 8% (n=125) have been directly observed to surge.

FIGURE 2

Other studies have suggested that the presence of diagnostic landforms associated with surging, such as crevasse-squeeze ridges (CSRs; Sharp, 1985; Evans and Rea, 1999), represent evidence of past surge activity. Farnsworth et al. (2016) interrogated centimetre resolution aerial imagery and found that 431 forefields in Svalbard contained CSRs, which equates to 43% of glaciers in Svalbard (although only 27% of the Randolph Glacier Inventory (RGI) 7.0 glaciers, see section 5). The absence of CSRs does not necessarily mean that a glacier has not previously surged as these landforms may not be well preserved due to erosion, weathering, sedimentation, or deposition in water. Other landforms diagnostic of surging have been recognised, such as glaciotectonic moraines and mud-aprons (Croot, 1988; Kristensen et al., 2009; Lovell and Boston, 2017; Lovell et al., 2018b), and these can also be used to assess Svalbard-wide prevalence of surges.

Because of the difficulty in directly observing glacier surges before the satellite era, statistical models have been developed to classify the probability of a glacier being surge-type based on the correlation of local geometric and climatic factors with known surge-type glaciers. Hamilton and Dowdeswell (1996) found that Svalbard glaciers had a higher probability of being surge-type as their centrelines were generally longer than other glaciated regions. This finding is in agreement with other studies using logit regression (Jiskoot et al., 1998; 2000), which found length and surface slope to be key determinants of surge prevalence in Svalbard and suggested 13% of glaciers were surge-type. More recently, advanced machine learning techniques have been employed to map the probability of glaciers across the archipelago being surge-type. Bouchayer et al. (2022) trained several models with data on mass balance, glacier geometric features and climatic data and found that 17% of all glaciers larger than 1km^2 could be of surge-type, although when considering glaciers of all size classes, this equates to 10%. Whilst these statistical models give new insights into the potential local environmental drivers of surging and the possibility of currently unidentified surge-type glaciers, they do not represent direct observations.

To complement these existing inventories, we now review the techniques used to monitor past and present glacier surges and their processes in Svalbard. This review focuses on five key characteristics: 1) ice velocities; 2) mass redistribution; 3) ice front changes; 4) surge drivers; and 5) subglacial conditions. These techniques inform the creation of a new Svalbard surge database, which is described in section 5, and contributes to the discussion of surge behaviour in section 6.

3. Monitoring glacier surges

3.1. Observational pyramid

Comprehensive monitoring of surges in Svalbard and their associated processes relies upon remote sensing at multiple scales. The observational pyramid provides a conceptual framework for integrating the various technologies used to monitor glacier surges in Svalbard (Figure 3). It spans satellite remote sensing, airborne platforms, and ground-based and uncrewed maritime systems, each contributing observations at different spatial and temporal scales. Satellites offer long-term, large spatial coverage through sensors such as optical imagers and synthetic aperture radar (SAR). Medium-resolution satellite sensors (e.g. Landsat, Sentinel satellites, ASTER) typically have coarse (5-50 m) spatial resolution. In comparison, commercial satellite systems (e.g. SkySat, Planet, ICEYE, Capella) can offer spatial resolution imagery down to 30 cm and acquire data when tasked by an end-user. Uncrewed aerial vehicles (UAVs), by contrast, capture high-resolution (down to a few cm) data at lower altitudes, using a range of sensors to focus on specific areas such as glacier fronts, or to map entire glaciers with more complex missions. Geophysical sensors, such as seismometers and ground-penetrating radar (GPR), enable detailed observations of subsurface features such as the presence of pooled or flowing water, englacial layering, and lithology below the glacier. Boreholes can be constructed using hot water drills (Makinson and Anker, 2014) to access the glacier bed and directly measure subglacial water pressure, sliding rates and basal temperature (Porter and Murray, 2001; Murray and Porter, 2001; Bouchayer et al., 2024). These subsurface features are otherwise inaccessible, yet crucial for understanding subglacial conditions driving surges. Marine uncrewed systems—including autonomous and remotely operated underwater vehicles (AUVs and ROVs)—extend observational capabilities below the terminus for marine-terminating glaciers, enabling the study of calving fronts, meltwater discharge, subglacial outflows and the former glacier bed that are otherwise difficult to access (Howe et al., 2019; Inall et al., 2024). The observational pyramid allows for coordinated observations to improve observations of glacier surges, whereby coarse-scale satellite data can guide the targeted deployment of close-range or subsurface sensors, whilst in situ measurements can validate and refine interpretations of remotely sensed signals.

FIGURE 3

3.2. Satellite Earth Observation (EO)

3.2.1. Overview

The earliest surges in Svalbard were identified using EO satellite data. Whilst the first EO satellites were launched in the 1960s (e.g. TIROS-1), as well as several spy satellites (e.g. CORONA), satellite EO expanded significantly in the 1970s with the launch of the first Landsat satellites. These observations were infrequent up to the 1990s, hence only large surges with pronounced surface changes could be detected. In the 1990s, several satellites with optical imaging and SAR payloads (e.g. ERS-1, ERS-2, RADARSAT-1, Landsat 7, ASTER) enabled routine mapping of glaciers in Svalbard. The launch of CryoSat-2 in 2010 improved spaceborne monitoring of glacier volume changes, while the density of satellite measurements has increased dramatically since 2014 with the launch of several new NASA satellites (Landsat 8 and 9), and the initiation of the Copernicus satellite programme launching Sentinel-1 (SAR) and Sentinel-2 (optical). Both Sentinel-1 and Sentinel-2 were designed as a two satellite constellation, phased 180° apart so that they share the same orbital plane but are positioned on opposite sides of the Earth. Sentinel-1 imagery offers revisit periods of 1-2 days in extra-wide swath mode (EW) and 6-12 days in interferometric-wide swath mode (IW), whilst Sentinel-2 has almost daily coverage in Svalbard between March and October. Meanwhile, the long time series of Landsat imagery is key for detecting surges back to the 1970s (e.g. Dowdeswell et al., 1991). The major benefits of satellite EO is their ability to continuously and systematically monitor the dynamics of glacier surges over time and therefore detect anomalous changes associated with unstable ice flow, whilst doing so across the whole archipelago. However, these sensors can only detect surface changes, and do not provide direct data on subglacial conditions.

EO monitoring of surges in Svalbard has transformed our understanding of their distribution, scales and dynamics, relationship to mass balance, and detection capabilities, but these methods struggle to observe surge dynamics of smaller glaciers with lower ice fluxes. Small satellite constellations (e.g. ICEYE, Planet, Capella) might fill this gap in the observational pyramid but this requires financial investment (the data is not free to use) and the development of new computational tools.

3.2.2. Glacier Velocity

An active glacier surge in Svalbard typically undergoes a multi-year speed-up and then decelerates gradually (Figure 4). Although the magnitude of this pattern differs between glaciers, the premise is that velocity data can be used to detect an active surge from continuous satellite monitoring. Techniques such as feature-tracking and radar interferometry (InSAR) are employed to measure the surface displacement between image pairs, enabling the detection of surge events (Murray et al., 2003b; Koch et al., 2023). Before 2000, velocity maps were restricted to image pairs covering limited spatial regions in Svalbard due to the longer revisit periods (Dowdeswell and Collin, 1990; Rolstad et al., 1997). In the 2000s, velocity data were primarily acquired from satellites such as ERS-1/2, ENVISAT, RADARSAT-1/2 and ASTER (Murray et al., 2003a,b; Mansell et al., 2012), often with variable revisit periods which detected only large surges of glaciers with extensive catchments. In the case of ERS-1/2, the revisit times over Svalbard were either too short (1-3 days) to capture the displacement of surface features or too long (35 days) causing surface decorrelation, despite the images being of high quality. Older Landsat 1-5 imagery had lower quality (e.g. spatial and radiometric resolution) compared to more recent Landsat 7-9 imagery, resulting in larger geolocation errors and lower contrast between surface features, which hinder the image matching during feature-tracking. Despite the relative paucity of appropriate SAR images over Svalbard, InSAR has successfully been used to detect unstable ice flow, such as during the surges of Fridtjovbreen (Murray et al., 2003b) and Monacobreen (Luckman et al., 2002). Also, with the open release of historical satellite imagery, it is now possible to generate long-term velocity time series (e.g. Strozzi et al., 2017), enabling the detection of previously unidentified surges (Figure 5). In addition, extracting velocity data from satellites such as ALOS PALSAR has enabled a more complete understanding of complex surge dynamics, such as those at Nathorstbreen in southern Spitsbergen Svalbard (Nuth et al., 2019). Finally, high-resolution TerraSAR-X images have been used to capture the evolution of two major surges at Aavatsmarkbreen and Wahlenbergbreen (Sevestre et al., 2018), demonstrating the benefits of high-resolution velocity time series for understanding surge dynamics.

FIGURE 4

FIGURE 5

Since 2014, the density of ice velocity observations has significantly increased primarily due to the simultaneous orbits of Sentinel-1, Sentinel-2, Landsat 8 and Landsat 9, leading to the development of open access glacier velocity databases (Friedl et al., 2021; Lei et al., 2022; Gardner et al., 2025). The velocity time series in Figure 4 is taken from ITS_LIVE, which contains glacier velocity maps for individual image pairs and annual mosaics for most glacier regions (https://its-live.jpl.nasa.gov/), and demonstrates the simplicity of tracking large surges in near real-time. The dense time series of ice velocity measurements in Svalbard has led to the development of automated anomaly detection methods for surge identification (Koch et al., 2023). The higher temporal resolution also enables tracking of surge dynamics in more detail, such as the impact of seasonal ice flow variations which may be imprinted on the surge velocity pattern (Benn et al., 2022). These observations have been used to test glacier surge theories (Benn et al., 2019b) and assess drivers of surges (e.g., Sevestre et al., 2018), aiding advancement towards a general theory of surge behaviour. However, these methods encounter difficulties when detecting anomalous flow patterns on smaller valley glaciers where flow rates are typically much slower. The surge of Scheelebreen (Figure 4b) is somewhat of an anomaly, as it is a glacier flowing into a small, narrow valley yet experienced a rapid acceleration from 0.5 m/d to ~9.5 m/d in a short time period when measured by ITS_LIVE, although velocity mapping from higher resolution SAR imagery suggests its velocity reached 30 m/d at its peak.

3.2.3. Glacier Elevation

Whilst the velocities can be used to track ice discharge and frontal ablation (Dunse et al., 2015; Luckman et al., 2015), glacier mass balance requires mapping of volume changes associated with a surge (Figure 7). Ice accumulates in the reservoir zone during quiescence but is redistributed down-glacier during a surge, leading to increased thinning at high elevation and thickening at low elevation, often with an advance of the terminus. DEM differencing has been used to measure ice build-up before a surge and the subsequent transfer of mass down-glacier towards the margin (Sund et al., 2009; Murray et al., 2012; Sevestre et al., 2018). Longer time series of surge activity have been derived from historical maps created by explorers in the 1900s (Melvold and Hagen, 1998; Ottesen et al., 2008), but these are of lower quality compared to modern-day sensing systems. Similar to the velocity data, surface elevation mapping of surging glaciers in Svalbard increased significantly after 2000 with the availability of repeat stereoscopic satellite imagery (ASTER, ArcticDEM), laser altimeters (ICESat, ICESat-2) and radar altimeters (CryoSat-2, ENVISAT).

FIGURE 6

ASTER has a revisit period of 16 days and can be used for detailed analysis of geometric changes during a surge. Nuth et al. (2019) used ASTER stereoscopic pairs with 2-4 year intervals to map the geometric evolution of the Nathorstbreen system during its multiple phases of surge activity and compared it to earlier DEMs from 1936 and 1990. This long-term elevation mapping has been used by other studies (Sund et al., 2009; Rolstad et al., 1997; Sund et al., 2014; Sevestre et al., 2018) and has revealed the mass redistribution resulting from a surge. More recently, Huggonet et al. (2021a) derived glacier surface elevation changes across Svalbard between 2000 and 2019 using the entire ASTER catalogue over the archipelago. Although the data are averaged within four temporal epochs (2000-2004, 2005-2009, 2010-2014, and 2015, 2019; data available at Hugonnet et al., 2021b), the data may be used to detect anomalous surface elevation changes related to glacier surges.

Coarser resolution CryoSat-2 data have been instrumental in acquiring Svalbard-wide elevation changes and has been used to quantify the mass loss of the large Basin-3 surge in Austfonna (McMillan et al., 2014; Morris et al., 2020). However, the 500 m resolution of CryoSat-2 products inhibits quantification of volume changes on smaller glaciers. More recently, the release of 2 m resolution ArcticDEM data has been used to assess elevation changes alongside other DEMs from ASTER and Tandem-X (Figure 7; Haga et al., 2020; Kavan et al., 2022). Since 2003, regional surface elevation maps have been available covering the entire archipelago and derived from ICESat (Nuth et al., 2010), CryoSat-2 (Morris et al., 2020) and more recently ICESat-2 (Sochor et al., 2021). Although these do not specifically target the detection of surges and are generally coarser compared to ASTER, aerial photos and ArcticDEMs, the measurements have high temporal resolution and enable detailed mapping of elevation changes suitable for monitoring geometric changes of glaciers during a surge. Combined with similar repositories of terminus changes (Li et al., 2024; 2025), mass balance can be quantified and the impact of surges assessed, but this remains to be analysed fully. The multi-modal elevation data sets can be used to generate a coarse time series of geometric changes during surge activity after 2000, but large gaps further back in time hinder more detailed understanding of past surge activity.

3.2.4. Glacier Surface Features & Terminus Change

Visible changes to the glacier surface can be observed during the active phase of a surge where the ice flow acceleration leads to pervasive surface crevassing due to the high strain rates induced by the sudden discharge of ice down-glacier. For downward propagating surges with a surge bulge, crevasses are initially longitudinal as compressional flow dominates, after which transverse crevasses dominate as the surge transitions to extensional flow. Longitudinal crevasses may also be produced in a playing surge lobe at the glacier terminus as it advances during an active surge (e.g. Lovell et al., 2015b). Upward propagating surges typically only experience extensional flow and therefore transverse crevasses dominate (Murray et al., 2012). Unstructured, chaotic crevasse networks dominate as the glacier accelerates rapidly during a surge (Hodgkins and Dowdeswell, 1994; see Figure 8). Early studies detected glacier surges when large, transverse crevasses could be identified across a large proportion of a glacier or crescentic crevasses could be found in the upper basin suggesting the glacier was decoupling from bedrock due to fast flow (Lefauconnier and Hagen, 1991). Furthermore, several studies have used optical imagery from satellites and airborne platforms to observe the progressive increase in surface crevassing before and during a surge. For example, Dowdeswell et al. (1991) observed the initiation of crevassing on the surface of Osbornebreen using sequential Landsat images between 1986 and 1988, Sund (2006) observed the upglacier propagation of transverse crevasses on Skobreen between 1990 and 2005, whilst Murray et al., (2003b) detected crevasses on Fridtjovbreen during its surge in 1996. More recently, the upward propagation of the Aavatsmarkbreen terminal crevasse field was mapped using repeat Landsat and TerraSAR-X scenes (Sevestre et al., 2018), showing in particular the propagation of transverse crevasses illustrating extensional flow as the surge initiated. It is now possible to also track changes in crevasse heights from ICESat-2 data to map the expansion of crevasse fields and variations in the stress regime during a surge (Trantow and Herzfeld, 2025), but currently only large and deep crevasses >10 m may be detected.

The heavy crevassing observed on the surface of surging glaciers leads to a change in surface texture which is visible between satellite images taken before and during a surge. This is particularly pronounced in SAR imagery as the heavy crevassing increases surface roughness and consequently radar backscatter (Figure 6). Leclerq et al. (2021) found that by differencing SAR imagery between 2018 and 2019, locations of increases in radar backscatter can be related to surge activity. They identified 11 ongoing surges in Svalbard using this approach. Kääb et al. (2023) extended this analysis to between 2017 and 2022, enabling detection of 26 surges in Svalbard during this time period, thus more than doubling the initial estimate by Leclerq et al. (2021). Mannerfelt et al. (2025) further developed this technique to delineate interferometric coherence changes in sequential Sentinel-1 images and found that several surges were preceded by surface changes multiple years before such changes could be detected within optical images. This has been combined with data on ice velocity, surface elevation changes, climate reanalysis and glacier outlines to identify 31 glacier surges between 2000 and 2024 (Guillet et al., 2025). The extension of this technique to other satellite time series (e.g. ERS-1/2, JERS-1, ENVISAT, ALOS-1, RADARSAT-2) is expected to yield even further information on historical glacier surges. While texture changes in optical imagery have not yet been explored in Svalbard, they hold potential as a tool for monitoring and detecting glacier surges (Trantow and Herzfeld, 2018).

FIGURE 7

In most cases, the increased ice flux during a glacier surge leads to an advance of the terminus that can be detected in satellite imagery. Lefauconnier and Hagen (1991) utilised repeat historical maps

(1858-1901), repeat aerial photos (1936-1971) and early Landsat images (1985-1986) to identify 82 surges along the east coast of Svalbard based on the incidence of surface crevassing and terminus advances when repeat data sets were available. Use of early Landsat images also enabled Dowdeswell (1986) to identify surges from outlet glaciers of the Vestfonna ice cap (e.g. Bodleybreen) during the period 1969 to 1981, during which time all glaciers around Austfonna were either static or retreating, hence not considered to be surging. Similar observations of a terminus advance were made at Osbornebreen using SPOT and Landsat imagery from 1987 and 1988 (Rolstad et al., 1997), whilst ASTER imagery was used to measure a 2.8 km advance during the surge of Skobreen between 2003 and 2005 (Kristensen and Benn, 2012). A time series of terminus positions may be derived from frequent satellite revisits and used to assess temporal patterns of advance during a surge (e.g. Mansell et al., 2012). Sevestre et al. (2018) reconstructed the frontal position of both Aavatsmarkbreen and Wahlenbergbreen using 1976-2013 Landsat imagery to quantify quiescent phase terminus changes before their respective surges were initiated. Although the majority of surges in Svalbard have an observable terminus advance, glaciers such as Uvêrsbreen (Figure 7b) did not undergo any significant advance. In these situations, the ice flux is of a similar magnitude to ablation and despite the increase in ice speed, the glacier front remains stationary. Furthermore, Li et al. (2025) derived calving front positions between 1985 and 2023 for 149 marine-terminating glaciers in Svalbard using a deep learning approach (Li et al., 2024), enabling the tracking of frontal advances for large surges (e.g. Negribreen, Basin-3). They also showed that active surges also display seasonal behaviour in terminus position, undergoing retreat/fixed position in winter and an advance in summer. Whilst the new terminus change data set of Li et al. (2024; 2025) opens up the possibility to evaluate terminus change patterns before, during and after tidewater glacier surges, less is known about the patterns on land-terminating glaciers and remains a key knowledge gap.

3.3. Airborne remote sensing

Aerial images using crewed aircraft are a crucial tool for surge identification, which has previously been adopted to show an apparent variable surge frequency on the Svalbard archipelago (Dowdeswell et al., 1995). Aerial image campaigns by the Norwegian Polar Institute started in 1936 (Geyman et al., 2022) and have since been performed in recurring intervals of at most 30 years, with the most notable campaigns near the years 1960, 1990 and 2009/2011, accompanied by sporadic campaigns of smaller extent in between. Using photogrammetric techniques, these aerial images can be used to generate DEMs, although complications arise across homogenous surfaces such as in the accumulation zone where suitable features for tying overlapping image pairs together may be absent (Eiken and Sund, 2012). Instead, lidar sensors may be used as an alternative to map glacier surface elevation (e.g. Bamber, 1989; Bevan et al., 2007).

Long-term changes in Svalbard's ice volume can be readily quantified by differencing a modern-day digital elevation model (DEM) with a 1930s DEM generated from historical aerial photographs (Geyman et al., 2022; Mannerfelt et al., 2024), enabling the quantification of almost 100 years of ice volume changes across Svalbard. In addition, a DEM generated from 1990s aerial imagery also offers a baseline year to study elevation changes from which surge activity can be detected (Rolstad et al., 1997; King et al., 2016). However, the infrequent repetition interval of about 30 years means that many smaller events (e.g. glacier surges with a slow ice flux, slow active phase, or no terminus change) are missed altogether. Furthermore, large surges could occur in between airborne campaigns and any changes due to the surge (e.g. terminus advance, surface crevassing, volume change) may not be detected with certainty. This leads to a temporal bias, especially in inland regions, in detecting surges around these acquisition dates. Despite these challenges, the benchmark airborne campaigns available in Svalbard have successfully been used to track the terminus position (e.g., Ottesen et al., 2008, Lovell et al., 2018b) and volume changes (Mannerfelt et al., 2024) of surging glaciers.

To improve the temporal sampling of surge monitoring, some glaciers have been mapped during dedicated airborne field campaigns, such as Fridtjovbreen before and after its surge in the 1990s (Murray et al., 2012) and Finsterwalderbreen during quiescence (Nuttall et al., 1997), enabling a better understanding of geometric changes as a surge cycle evolves. More recently, there have numerous airborne flights covering smaller regions in Svalbard, including: hyperspectral surveys using the Dornier aircraft in 2020 (https://sios-svalbard.org/AirborneRS) and 2021 (https://sios-svalbard.org/AirborneRS_Call2021), sea ice surveys by the Alfred Wegener Institute (AWI) that also covered glaciers in Svalbard (Haas et al., 2023; Kolar et al., 2025), and opportunistic flights using a helicopter (e.g. Girod et al., 2017). Compiling available airborne data covering Svalbard surge-type glaciers would generate a useful data set to fill gaps in satellite time series.

3.4. Close-range sensing

Satellite sensors can detect large-scale patterns in glacier surge activity in Svalbard, such as seasonal speed-ups or terminus advance/retreat. However, to capture detailed surface processes associated with a surge, such as iceberg calving, surface melt, and flow patterns, close-range sensors are required. Terrestrial laser scanners (TLS), surface-mapping radars, such as the GAMMA Portable Radar Interferometer (GPRI) (Werner et al., 2008; Strozzi et al., 2017) and millimetre-wave radar (Harcourt et al., 2022), provide high-resolution data but are relatively costly to build. However, UAVs with visible imager payloads and time-lapse cameras are relatively inexpensive, although to date their application to understanding surge behaviour is limited.

UAVs are successfully and increasingly commonly applied to monitor glacier surges with very high spatial resolution (Hann et al., 2021, Hann et al., 2022). Typically relying on Red-Green-Blue (RGB) cameras, UAVs use photogrammetric methods (Smith et al., 2016) to extract DEMs and orthomosaics (Figure 8). These data sets have been used to detect surface elevation changes, flow velocities, calving rates, and the spatial extent and structure of crevasses (e.g. Dachauer et al., 2021 and Karušs et al., 2022). Commercial off-the-shelf multirotor systems (e.g. DJI), are relatively inexpensive and logistically straightforward to deploy. These systems offer valuable data, particularly for short-range surveys over smaller glaciers or discrete areas of interest. More sophisticated UAV platforms, such as fixed-wing and vertical take-off and landing (VTOL) systems, allow for larger-area coverage and more complex mission profiles, often with increased endurance, payload capacity, and autonomy (Solbø and Storvold, 2013). However, they come with significant operational challenges, including more complex logistics, specialised training requirements, certification, and permits from aviation authorities. In general, most UAV operations in Svalbard are also constrained by regulatory restrictions, particularly within national parks or protected areas, which limit deployment without special permits (Hann et al., 2023).

FIGURE 8

The use of TLS for monitoring surges is limited despite showing significant potential for 3D monitoring of tidewater calving fronts (Pętlicki et al., 2015; Köhler et al., 2019). The limited application of this technique may be due to the potential for signal absorption of visible and infrared wavelengths into pure ice, but the rougher surface of a highly crevassed surging glacier may suggest TLS instruments are better suited to monitoring surface conditions during unstable ice flow. Time-lapse photography is the most commonly used close-range sensor for monitoring glacier surges in Svalbard. It has been used to generate dense observations of terminus conditions during an active surge, such as at Paulabreen in 2005 (Kristensen and Benn, 2012) and Nathorstbreen in 2008 (Sund and Eiken, 2010). Furthermore, when two or more cameras are deployed to take images of the same field of view at different angles, orthomosaics may be produced using photogrammetric processing (Eiken and Sund, 2010). For surging glaciers, time-lapse photography is especially useful as it can capture fast and transient changes that are often missed by other monitoring techniques e.g. satellite sensors. These advantages also mean surges can be tracked from quiescence to an active surge (Vallot et al., 2018) whilst they may also be employed in a network to track surface melt, iceberg calving and surface flow patterns (How et al., 2017). While time-lapse photography can enable automated long-term monitoring, the presence of snowfall, rainfall, fog, low cloud cover and periods of darkness can introduce significant gaps in the time series.

Close-range sensors are not currently widely used for monitoring the dynamics of glacier surges. A reason for this is the unpredictability of surges and an inability to plan and fund the deployment of close-range sensors during the short time window of a surge. Permanent installations at glacier systems that are known to surge relatively frequently (e.g. Nathorstbreen glacier system, Paulabreen, Tunabreen) or are predicted to surge soon (e.g. Kongsvegen, Edvardbreen) might enhance monitoring efforts. An improved strategy for deploying close-range sensors at surging glaciers is required, e.g. a portable observing system for detailed monitoring of glacier surges.

3.5. Geophysical measurements: surface

Global navigation satellite systems (GNSS) are used to measure 3D surface changes on glaciers over time at specific geographic points. Offering higher temporal resolution (seconds) and greater accuracy than satellite-derived displacement (millimeters to 1 cm; Still et al., 2023; Pickel and Howley, 2024), GNSS is particularly effective at detecting subtle movements, such as anomalous flow at the onset of a surge when velocities remain near quiescent levels, or vertical displacement, for instance from changes in subglacial hydrology or surface bulging (e.g. Nanni et al., 2025). This capability proved crucial in identifying the activation of a surge at Basin-3, Austfonna (Figure 9; Dunse et al., 2012; 2015) and is currently being used to study the slow surge initiation at Kongsvegen (Bouchayer et al., 2024; Nanni et al., 2025). Similarly, Nuttall et al. (1997) measured annual and seasonal velocity variations using stakes on Finsterwalderbreen and detected a reduction in ice flux consistent with mass accumulation in the reservoir zone. GNSS data can also be used to validate satellite measurements of ice velocity and confirm the existence of ice flow acceleration during a surge (Pohjola et al., 2011). Furthermore, GNSS can track elevation changes associated with surge activity, including the down-glacier progression of a surge bulge. For example, Hodgkins et al. (2007) measured ice accumulation on Finsterwalderbreen during quiescence and subsequent downwasting in the ablation zone, revealing the mass gradient imbalance associated with the quiescent-stage phase of the surge cycle. Similar processes have been observed at Kongsvegen (Eiken et al., 1997; Hagen et al., 2005), highlighting the ability of GNSS to bridge the temporal resolution gap left by satellite data.

However, the deployment and maintenance of GNSS instruments on surging glaciers is challenging due to their highly deformable and fractured surfaces, often rendering suitable deployment sites inaccessible. Even when successfully installed, GNSS units face significant risks of damage or loss. Similar to other close-range sensing methods, deploying GNSS sensors in advance of a surge requires accurate predictions of surge active phase timing. This may be feasible for glaciers with multiple surge-type tributaries, such as Nathorstbreen or Paulabreen/Bakaninbreen, but logistical and financial constraints make it impractical to cover the entire archipelago. A strategic sampling approach is therefore necessary, whereby glaciers with signatures of an imminent surge are prioritised. This might include, but are not limited to, early signs of surface changes from interferometric decoherence maps (Mannerfelt et al., 2025), the formation of a surge bulge at higher elevation, or an increase in surface velocity. Alternatively, internal GNSS data produced from any GNSS-equipped field instrument (e.g., seismic stations) can provide information about sliding velocity while avoiding the need to install multiple instruments on a surging glacier surface. Although the positional information has lower accuracy (40 cm or more in the case of Gajek et al., 2025) it may still be used to determine the dynamics of speed up at the onset of a surge.

FIGURE 9

3.6. Geophysical measurements: subsurface

3.6.1. Ground-penetrating radar (GPR)

Ground-penetrating radar (GPR) is a non-invasive method that uses low microwave frequency electromagnetic waves (most often from tens to hundreds MHz in glaciological context) to penetrate and image the subsurface. These capabilities make GPR a useful technique for studying surge-type glaciers as changes at the bed (e.g. presence of meltwater, drainage configurations, thermal regime, lithology) are key to understanding glacier evolution throughout a surge cycle (Kamb et al., 1985; Benn et al., 2019a). Land-based GPR systems are usually manually operated, requiring the radar antenna to be dragged or towed over surfaces (Figure 10b). As a result, land-based GPR surveys are relatively slow and can be challenging or dangerous to apply in steep or heavily crevassed areas, particularly during ongoing glacier surges. However, it may be possible if glacier surfaces can be navigated safely, which was the case for the GPR survey of the actively surging Vallåkrabreen in 2022 (Figure 11a). In comparison, airborne GPR systems, traditionally mounted on helicopters, are now increasingly deployed on UAVs (Figure 10a, López et al., 2022), enabling rapid surveys over extensive areas, especially in remote or inaccessible regions. Recently, multi-rotor UAVs have gained popularity for GPR surveys (Jenssen et al., 2024), offering improved flight path precision, denser spatial sampling, and lower operational costs compared to helicopters, albeit with reduced range. However, while effective for large-scale surveys, airborne GPR typically offers lower spatial resolution than land-based methods due to limited spatial sampling and is more reliant on favorable weather conditions (Bamber, 1989; Dowdeswell and Bamber, 1995), such as moderate winds and gusts. An alternative approach is to deploy an Autonomous phase-sensitive Radio Echo Sounder (ApRES) at a fixed location to measure subtle changes in the distance between the radar and reflective targets (such as ice layers, bedrock, or subglacial water) over time. ApRES has been successfully applied in

Antarctica (Kingslake et al., 2014; Lok et al., 2014) and Greenland (Gillet-Chaulet et al., 2011) but has only recently been applied to study glacier surges in Svalbard (Harcourt et al., 2024).

FIGURE 10

Englacial and subglacial scattering of electromagnetic waves is strongly influenced by the glacier thermal regime (Björnsson et al., 1996), with warm ice typically scattering more than cold ice. This is typically driven by ice thickness and pressure melting (Murray et al., 2000), with thick ice over 100 m usually leading to warm basal ice, and thinner ice being cold-based due to conductive heat losses. GPR data has revealed the presence of a basal layer of temperate ice overlain by cold ice in polythermal surge-type glaciers (Ødegård et al., 1992; Björnsson et al., 1996; Sevestre et al., 2015; Figure 11). At the snout of surge-type glaciers, a cold ice dam extending the full ice thickness can block outflow of subglacial water, although it may be removed through iceberg calving (Sevestre et al., 2015) leading to the presence of warm ice across the whole glacier bed. The thermal regime of Bakaninbreen during and after its 1985-1995 surge was extensively studied with GPR (Murray et al., 1998; 2000; Smith et al., 2002). Murray et al. (2000) interpreted an internal reflecting horizon (IRH) with 60 MHz GPR data acquired at Bakaninbreen to show the position of the surge front where the thermal regime transitioned from warm to cold, which was subsequently confirmed by borehole and seismic data (Murray and Porter, 2001; Smith et al., 2002). The presence of ice lenses below the bed indicated the presence of permafrost-trapped meltwater in a thin ice-bed interface (Murray et al., 2000), from which it was inferred that the slow leakage of water through pores in the permafrost and through fractures in the basal ice was responsible for gradual surge termination. Similar thermal characteristics have been observed at land-terminating surge-type glaciers such as Hørbyebreen (Małecki et al., 2013) and Von Postbreen (Sevestre et al., 2015; Delf et al., 2022). GPR has also been used to uncover changes in thermal conditions associated with surge-like behaviour. Several small valley glaciers that were previously warm-based have been shown to now be predominantly cold-based and frozen to their beds (Hodgkins et al., 1999; Bælum & Benn, 2011; Lovell et al., 2015a; Sevestre et al., 2015), suggesting mass loss has reduced the ability of these smaller glaciers to undergo dynamic ice flow (Mannerfelt et al., 2024).

FIGURE 11

The presence of englacial or subglacial liquid water is similarly important when considering the role of subglacial drainage configurations on surge cycles (Kamb 1987; Fowler et al., 1987). Because water has a significantly different dielectric permittivity compared to ice, its presence can be observed in GPR data as a strong contrast in radar backscatter. This contrast, in turn, can be used to map the extent of warm and cold ice (Björnsson et al., 1996; Ødegård et al., 1997; Sevestre et al., 2015

Kachniarz et al., 2025) or to infer water accumulations at depth. Barrett et al. (2008) detected distributed scatterers in GPR data at the bed of Bakaninbreen representing the presence of large water bodies. Furthermore, bright reflectors within Von Postbreen were interpreted as small water bodies that stored meltwater all year round (Delf et al., 2022) and often held more water than the bed. Crevasses that form during an active surge will close up during surge termination and quiescence as the glacier decelerates. Meltwater located within the crevasses will refreeze and lead to the formation of superimposed ice layers that can be detected within GPR surveys (Brandt et al., 2008). The detection of such features may indicate the presence of past surge activity.

Both land-based and airborne GPR systems can reveal detailed internal structures to reveal past dynamics related to surging (Murray et al., 1998; Woodward et al., 2003) and internal stratigraphy (Dunse et al., 2009; Barzycka et al., 2019; Barzycka et al., 2020). Saturated sediment is squeezed and deformed into basal fractures that open during surges, which can be detected in GPR data (Murray et al., 1998; Woodward et al., 2003; Murray and Booth, 2010; Temminghoff et al., 2019). Linear bands of 'dark' internal layering that were dipping 45º relative to the bed were found in both Bakaninbreen (Murray et al., 1998) and Kongsvegen (Woodward et al., 2003) and interpreted to be sediment thrust faults formed during surging. The presence of debris-rich englacial structures, which are also often exposed at the margins of surge-type glaciers and melt-out to form diagnostic geometrical ridge networks and crevasse-squeeze ridges (Glasser et al., 1998; Lovell et al., 2015b; Lovell and Fleming, 2023), provides strong evidence for past unstable ice flow. These features are particularly useful in determining whether smaller valley glaciers have previously surged (Lovell et al., 2015a; Sevestre et al., 2015) and determining the changing distribution of surging behaviour across the archipelago. The formation of surface crevasses below snow and firn may also be identified using GPR surveys and indicate the initiation of glacier acceleration (Dunse et al., 2015). In addition, the scattering properties of different zones on the glacier (e.g. superimposed ice) can also be used to infer melt and refreezing properties (Langley et al., 2007; 2009), aiding the interpretation of mass build-up and enthalpy production.

Importantly, GPR surveys are essential for mapping ice thickness and bedrock topography, both of which are critical for modelling surge-type behaviour (Benn et al., 2019a; Thøgersen et al., 2019). Several studies have mapped subglacial topography in Svalbard (Smith et al., 2002; Saintenoy et al, 2013) and quantified ice volumes (Navarro et al., 2014; Sevestre et al., 2018; Karušs et al., 2022), whilst recent compilations of existing data using ice flow models have improved coverage in recent years (Fürst et al., 2018; van Pelt and Frank, 2025). Furthermore, GPR measurements of the glacier bed may also reveal the lithology of the subglacial environment, which may help to determine the likelihood that a glacier will surge (Jiskoot et al., 1998; Murray and Porter, 2001). An overview of all publicly available GPR data sets in Svalbard can be found in Van Pelt and Frank (2025), highlighting in particular the dense surveys around Ny Ålesund, Nordenskiöld Land, Hornsund and on the Austfonna ice cap, with scarce measurements across other parts of the archipelago. Therefore, additional GPR surveys across the poorly sampled regions of the archipelago are required, focusing in particular on the thermal regime of quiescent phase surge-type glaciers, meltwater conditions at the bed of actively surging glaciers, and the lithology at the glacier bed to further test the link between surging and bedrock types.

Although GPR is a powerful tool for glacier monitoring, challenges remain. Glacier ice is a favorable medium for electromagnetic wave propagation due to its limited number of internal scatterers (Woodward and Burke, 2007). However, surveying actively surging glaciers remains difficult due to the presence of surface crevasses (e.g., Dunse et al., 2015). Land-based GPR provides denser and more controlled spatial sampling but is restricted in spatial range and accessibility. Moreover, its use is often limited to spring months, when snow cover facilitates faster data acquisition with antennas towed behind snow machines (Figure 10b). In contrast, airborne GPR enables surveys across larger areas regardless of snow cover, but its spatial sampling is less controlled, particularly with helicopter-mounted systems, due to the influence of wind conditions on aerial systems. Furthermore, the presence of crevasses diffracts signals from airborne antennas, which reduces signal penetration through the surface layers.

Furthermore, data resolution remains a challenge. Due to the physical principles governing wave propagation, a trade-off exists between resolution and depth penetration (Navarro and Eisen, 2009). For instance, GPR systems with GHz antennas can only image the first meters of the subsurface but with centimetre-scale resolution. Conversely, obtaining information from the glacier bed requires longer wavelengths using lower frequency antennas (e.g., 10 MHz), but this reduces the resolution to metres despite the gain in penetration depth. In temperate ice, scattering bodies necessitate even longer wavelengths, further lowering resolution. Airborne systems tend to use lower-frequency antennas compared to land-based systems to reduce the impact of atmospheric attenuation, which compromises hence vertical depth resolution.

Future research should aim to combine these methods to enhance overall data quality and coverage, focusing not only on active (wherever accessible) but also quiescent phase of the surge cycle. One promising technical advancement is spectral GPR, which acquires a wide range of frequencies within a single cycle, effectively integrating the advantages of different frequency antennas into a single device (Dyrda et al., 2023). Additionally, combining GPR data with remote sensing and other geophysical techniques, such as seismic surveys and GNSS measurements, can provide a more comprehensive understanding of glacier surges and their controlling factors. Studies of the Bakaninbreen surge used GPR data to better constrain the source of seismic events at the bed of a glacier (Smith et al., 2002; Stuart et al., 2005), enabling an understanding of the processes leading to surge termination. The use of data on ice velocity and elevation changes would further improve geophysical data collection strategies and provide an holistic understanding of how bed conditions translate to ice-dynamical and geometric changes during a surge.

3.6.2. Seismology

Seismological methods have been used to study glaciers for decades (Crary, 1955; Röthlisberg, 1955; Hatherton & Evison 1962; Weaver & Malone, 1979), including in Svalbard (Lewandowska & Teisseyre, 1964; Cichowicz, 1983; Górski & Teisseyre, 1991) and is now recognized as the field of cryoseismology. Seismic instruments such as geophones or seismometers are used to record ground shaking. Installing them in the vicinity of, or directly on, glaciers (drilled in the ice, Figure 10d) may provide information about the dynamics of glacier surge processes, particularly processes at the bed, especially when installed in deep (close to glacier thickness) boreholes (Köpfli et al., 2022; Nanni et al., 2025). Cryoseismology may complement traditional glaciological observations from fieldwork or remote sensing by operating independently of visibility conditions, including the polar night, providing wide spatial imaging beyond single observation points and achieving high temporal resolution on the sub-second scale (e.g., Bartholomaus et al., 2012). Furthermore, it enables systematic analysis of continuous seismic records from permanent stations, facilitating the study of long-term trends and seasonal patterns of cryoseismicity over years or even decades (e.g., Köhler et al., 2016; Gajek et al., 2017). Seismological findings can also complement GPR surveys (e.g. Smith et al., 2002) to cross-validate interpretations of subglacial conditions, including surge-related changes at the glacier bed (Zhan, 2019).

Short-term and multi-season deployments of seismometers in close proximity to, or directly on, surging glaciers provide detailed insights into various englacial phenomena. For example, analysis of recorded seismic events enable the study of ongoing crevassing by mapping thousands of surface icequakes per day (Mikesell et al., 2012; Walter et al., 2015). Studying basal icequakes has enabled the inference of frictional processes at the glacier bed (Gräff & Walter, 2021), while analysis of shear-wave splitting from the same events has revealed daily expansion and contraction of englacial channels (Gajek et al., 2021). Analysis of long-lasting monochromatic tremors can be used to infer moulin formation (Röösli et al., 2014; Walter et al., 2015) and quantify subglacial discharge (Bartholomaus et al., 2015). In addition, ambient noise can be used, for instance, to observe the development of subglacial channels (Zhan, 2019; Nanni et al., 2020) and provide estimates of subglacial channel geometries and efficiency (Gimbert et al., 2016; Bouchayer et al., 2024). Comprehensive reviews, such as those by Podolskiy & Walter (2016) and Aster & Winberry (2017), as well as the 2019 SESS Report ‘CRYOSEIS’ focusing on cryoseismology in Svalbard (Köhler et al., 2020), illustrate its value as a powerful method for advancing our understanding of glacier surge dynamic processes and measuring englacial and subglacial conditions.

Despite its potential, seismological studies of glacier surges are scarce due to the difficulties in deploying instruments on heavily crevassed surging glacier surfaces (Raymond and Malone, 1986), but a few case studies from Svalbard exist. A study of Bakaninbreen (Stuart et al., 2005) identified near-field seismic signals associated with an ongoing surge, while Köhler et al. (2015) observed exceptional far-field surge-related variations in long-term seismic emissions from Tunabreen and Nathorstbreen (Figure 12). At Kongsvegen, the subglacial hydraulic gradient and the radius of the channelized subglacial drainage system were inferred from the power of recorded seismic signals (Bouchayer et al., 2024). Most recently, seismology has been employed to monitor the ongoing surge of Borebreen (Harcourt et al., 2024, Gajek et al., 2025). These examples highlight the importance of seismology in monitoring surge-type glaciers and their driving processes.

FIGURE 12

New technologies, such as Distributed Acoustic Sensing (DAS), which consist of kilometres long fibre-optic cables used as seismic receivers (Figure 10c) offer great potential for surge monitoring. Ice-surface DAS applications has already proven to be effective in studying icequakes in alpine glaciers (Walter et al., 2020) and Antarctic ice streams (Hudson et al, 2021), providing unprecedented insight into dynamic processes due to the sensor density and spatial sampling down to the metre scale. The first on-ice installation of DAS in Svalbard took place in 2023 on Hansbreen (Gajek et al., 2024), but the potential of DAS for surging glaciers has not been explored yet. Notably, DAS may be installed underwater in the proximity of the terminus enabling insights into calving front dynamics (Gräff et al., 2025) or in boreholes (Fichtner et al., 2025). Another way to install underwater seismic stations is to use Ocean Bottom Seismometers (OBS) which, after being dropped and sunk in the glacial fjord, record seismic waves at a single location at the seabed. Such stations installed close to the terminus are less hazardous to maintain and offer less noisy recordings than surface sites. Podolskiy et al. (2021) have demonstrated that OBS data may be used to monitor calving rates and to use seismic noise as a proxy for glacial sliding velocity, even when using a single station. The ability of these new techniques to provide high-resolution cryoseismological data, and the potential to use pre-existing fibres (e.g., ocean bottom telecom cables) suggests they should be seriously considered for future monitoring of surges.

3.6.3. Boreholes

Boreholes are constructed to directly measure glacier bed conditions related to surge behaviour, such as subglacial water pressure, thermal conditions, lithology and till deformation rates. Although the glacier bed may be exposed towards the margins, boreholes must be constructed using electrothermal, electromechanical or hot-water driller systems to directly access the bed below the faster flowing glacier trunk. Once established, boreholes can host surface-wired or wireless geophysical instruments for several years (Hart et al., 2006; Porter, 2011), protecting them from melting out whilst being sheltered from surface conditions. Boreholes have been used to measure several important glacier characteristics related to surge behaviour, such as subglacial hydrological properties, glacier thermal regime, subglacial deformation rates, and englacial layering to calibrate GPR surveys.

Observing hydrological processes at the glacier bed, such as subglacial drainage configurations, water pressure, and the relationship of these parameters to ice velocity is key to understanding the drivers of a glacier surge. Direct measurements of subglacial water pressure can be obtained by installing transducers at the base of a borehole that reaches the bed. These borehole instruments were used to measure subglacial conditions during the Bakaninbreen surge between 1985 and 1995 (Murray and Porter, 2001; Porter and Murray, 2001; Kulessa and Murray, 2003). The observations showed that the bed of Bakaninbreen was partially floating towards the end of the surge (1994-1995) due to high subglacial water pressures, but no relationship was found between sliding and till strength indicating water pressure variations dominated the velocity variations (Murray and Porter, 2001; Porter and Murray, 2001). In comparison, several boreholes have been constructed to reach the bed of Kongsvegen as it builds up to a surge (Bouchayer et al., 2024; Nanni et al., 2025). For example, Bouchayer et al. (2024) found that the bed of Kongsvegen evolved transiently to abrupt water supplies from the surface which promotes the development of hydraulically connected regions and local weakening of the ice-bed coupling. Similarly, Nanni et al. (2025) found that high surface melt rates enable more water to reach the bed, leading to increased basal water pressures and sliding. On glaciers with no direct measurements of surging but evidence of having surged in the past (see section 5), water pressure sensors have measured transient events such as the reactivation of the subglacial drainage system due to rainfall events at Kronebreen (How et al., 2017), the activation and stagnation of sliding due to changes in subglacial permafrost active layer thickness below Tellbreen (Alexander et al., 2020b) and water pressure variations below Hansbreen (Jania et al., 1996).

The lithology below the glacier is also crucial because basal friction may vary when there is a layer of deformable sediment at the bed. Boreholes may directly sample this sediment (Murray et al., 1997;

Bouchayer et al., 2024) or have instruments directly installed in the till layer (Porter, 2011). Murray and Porter (2001) used ploughmeters, sliding sensors, thermistors and pressure transducers to understand the role of the deformable sediment layer below Bakaninbreen in modulating sliding rates, which may have been up to 60 cm thick (Smith et al., 2002). Through calculations of yield strength (Porter et al., 1997) and strain rates (Porter and Murray, 2001), they concluded that the soft bed assisted in promoting glacier sliding during the end of the surge active phase. It was also noted that sediments down-glacier of the surge front were frozen, suggesting sliding via deformation of the till layer was thermally regulated. Kulessa and Murray (2003) found a high hydraulic conductivity below Bakaninbreen that suggests sediments were dilated during its surge, whilst low hydraulic conductivities below Midtre Lovénbreen, likely a non-surge-type glacier (Hansen, 2003), suggests it is underlain by permafrost and is therefore less likely to surge, with such measurements corroborated by permafrost underlying other small valley glaciers (Alexander et al., 2020b). Similar measurements have been conducted at Kongsvegen using ploughmeters, leading Bouchayer et al. (2024) to conclude that the basal till behaves as a Coulomb plastic material i.e. it deforms at a rate dependent on effective pressure (i.e. due to ice and water pressure) and sediment cohesion. Borehole videos may also be used to understand subglacial till and sedimentation processes (e.g. Roberson and Hubbard, 2010), although such measurements are scarce on surge-type glaciers in Svalbard.

Beyond understanding sliding processes, thermistors may be installed within boreholes to measure temperatures along the vertical profile of a borehole to infer the thermal regime of a surge-type glacier. Surge-type glaciers in Svalbard are typically polythermal with a two-layer structure of cold surface ice underlain by warm basal ice and this structure has been found through direct borehole measurements at several surge-type glaciers (Kotlyakov and Macheret, 1987; Ødegård et al., 1992; Björnsson et al., 1996; Ødegård et al., 1997). This two-layer thermal structure has also been inferred in GPR measurements where an IRH has been found demarcating the cold to warm ice transition (Kotlyakov and Macheret, 1987; Ødegård et al., 1992; Björnsson et al., 1996; Ødegård et al., 1997; Murray et al., 2000; Smith et al., 2002). However, borehole measurements have also found a similar IRH to represent a layer of a debris-rich basal ice (Murray et al., 1997) or the transition of low to high water content (Jania et al., 1996), hence the IRH in GPR data may not always represent the cold-warm ice transition below surge-type glaciers.

Although borehole measurements have been integral in our understanding of how subglacial hydrology, thermal regime and till deformation impacts surge behaviour, the construction of boreholes remains logistically challenging and costly. Furthermore, they are at risk of damage due to the deformation of both the glacier ice and subglacial sediment layers, particularly during an active glacier surge when the glacier velocity is much higher than during quiescence. The use of autonomous, wireless subglacial probes, such as the supraglacial drifters used by Alexander et al. (2020a) or the cryoegg / cryowurst instruments developed by Prior-Jones et al. (2021), reduce the risk of damage as these instruments can rely on natural boreholes such as moulins to enter the subglacial environment. However, they require antennas to be installed directly above the sensor in order for data to be received at the surface, hence future work should investigate the potential for sensor data to be transmitted across a wider field of view to reduce the risk of data loss.

4. Identifying historical and paleo-glacier surges

Reconstructing long-term surge histories is essential for contextualising contemporary surge observations. Extending surge records beyond the remote sensing era relies on two primary approaches: investigations of sediment-landform assemblages formed during surges, and interrogations of historical observations and archival evidence of surge activity.

The dynamic glacier flow during surges shapes the subglacial and proglacial environment producing sediments and landforms that can be linked to surge processes (Evans and Rea, 1999). Where these sediment-landform assemblages are revealed and preserved during quiescent phase ice stagnation and retreat, they provide diagnostic geomorphological evidence for past surging - often extending far beyond the observational record (e.g., Flink et al., 2018; Lovell et al., 2018b). This approach is particularly valuable in Svalbard, where glaciers have often experienced multiple surges separated by decades to centuries (Dowdeswell et al., 1991), and where some glaciers may have surged in the past but are no longer capable of doing so (e.g., Lovell et al., 2015a; Mannerfelt et al., 2024). As a result, geomorphological investigations have identified past surge activity in numerous glaciers that have not been directly observed to surge (e.g., Farnsworth et al., 2016; Ottesen et al., 2017; Aradóttir et al., 2019; Ben-Yehoshua et al., 2023; Mannerfelt et al., 2024; Osika and Jania, 2024). These approaches require comprehensive understanding of surge-associated sediments and landforms, and typically integrate field mapping, visual observations, sediment logging, and sample measurements with remote sensing techniques (i.e., mapping using aerial and UAV photography and satellite imagery within a GIS framework) (Chandler et al., 2018).

Geomorphological investigations commonly focus on the best-preserved sediment-landform assemblages. For surge-type glaciers, the clearest evidence is typically associated with a glacier's most-recent surge. For many Svalbard glaciers this corresponds temporally with the Little Ice Age (LIA) Neoglacial maximum, dated approximately to the late 1800s and early 1900s (Mannerfelt et al., 2024). However, where repeated surges have reached successively less-extensive positions, it can be possible to explore preserved sediment-landform assemblages associated with multiple surges (e.g.

Ottesen et al., 2008; Flink et al., 2015). Combined with a well-constrained geochronology, this can allow surge timings to be reconstructed beyond the immediate observation period (i.e., during the LIA), further back into the Holocene (e.g., Hald et al., 2001; Kempf et al., 2013; Flink et al., 2017; 2018; Flink and Noormets, 2018; Larsen et al., 2018; Lovell et al., 2018b; Lyså et al., 2018; Streuff et al., 2018), and can even allow surge-like behaviour of ice streams within the Barents Sea Ice Sheet during the glaciation to be identified (e.g., Andreassen et al., 2014; Bjarnadóttir et al., 2014; Kurjanski et al., 2019). Sedimentary archives recorded in proglacial lakes have significant potential to provide insights on past surging of land-terminating glaciers (e.g., Striberger et al., 2011; Larsen et al., 2015). In Svalbard, such records have allowed glacier dynamics to be reconstructed (e.g., Røthe et al., 2015) but are yet to be directly linked to surging. This represents an exciting avenue for future research.

4.1. The surging glacier landsystem

The sediments and landforms associated with surging have been documented in both terrestrial and marine settings in Svalbard (Ottesen and Dowdeswell, 2006; Ottesen et al., 2008, 2017; Flink et al., 2015; Streuff et al., 2015; Farnsworth et al., 2016; Lovell et al., 2018a,b; Osika and Jania, 2024; McCerery et al., 2025). To interpret these landscapes, a 'landsystems' concept is typically employed (Figures 13 and 14). This approach seeks to identify, describe, and interpret the diverse range of sediments and landforms observed in glacial environments to reconstruct processes and thus the dynamics of the ice that previously covered the terrain (cf. Evans, 2005; Evans and Rea, 1999). Surging glaciers produce rapid, extensive modifications to the landscape that leave behind a specific suite of landforms. Surging glacier landsystems are most accessible in terrestrial settings (Figure 15), which can be investigated in the field and from remote imagery, but preservation of features can be heavily impacted by fluvial and gravitational reworking processes during ice stagnation. In contrast, landforms associated with marine-terminating glacier surges are often excellently preserved on the seafloor (Figure 16), but analysis of these is reliant on the availability of high-resolution bathymetry data (Ottesen and Dowdeswell, 2006; Ottesen et al., 2017). However, in most cases, marine-terminating glacier surges also leave behind landform evidence on the adjacent terrestrial fjord margins that can be utilised instead (Bennett et al., 1996; Lovell et al., 2018b).

FIGURE 13

FIGURE 14

FIGURE 15

FIGURE 16

4.2. Key components of the surging glacier landsystem

Glaciotectonic moraines: In Svalbard, the maximum extent of a surge is sometimes delineated by a large moraine system (Croot, 1988; Boulton et al., 1999; Lovell and Boston, 2017; Ottesen et al., 2017). These are most common in a marine setting, where they typically have a low-gradient debris flow lobe extending from the distal flank (e.g. Ottesen and Dowdeswell, 2006; Flink et al., 2015; Ottesen et al., 2017; Aradóttir et al., 2019) (Figure 16c). In terrestrial settings, the moraine systems often have multiple ridge crests, forming complexes known as composite ridge systems (Croot, 1988; Hart and Watts, 1997; Boulton et al., 1999; Lovell and Boston, 2017; Lovell et al., 2018a) (Figure 15a,b). These features have also been referred to as 'push moraines/complexes', although these terms can be ambiguous since they are employed for a broad range of landforms at various scales. In both terrestrial and marine settings, these moraine systems are formed by glaciotectonic deformation as the glacier advances rapidly into unconsolidated sediment in the proglacial zone.

Crevasse-squeeze ridges (CSRs): CSRs form when highly-saturated, deformable subglacial sediment is squeezed into a highly fractured glacier base (Evans and Rea, 1999; Rea and Evans, 2011). During recession, CSRs melt out in situ to form a system of cross-cutting ridges composed of diamicton that are typically aligned transverse or subparallel (i.e., 40-60°) to ice-flow, mimicking surface crevasse patterns (Figure 15c,d). During the early parts of the quiescent phase following a surge, CSRs can often be observed emerging from crevasses in terrestrial settings. The required conditions for their formation are (1) a saturated subglacial environment, (2) a glacier base fractured by extensive ice flow, and (3) ice mass stagnation following the surge in order to promote their preservation, making CSRs arguably the most diagnostic landform evidence for surging (Farnsworth et al., 2016). CSRs are found in both terrestrial and submarine settings (Figures 15c,d and 16b) and have been studied extensively in Svalbard (e.g., Bennett et al., 1996; Boulton et al., 1996; Woodward et al., 2002; 2003; Rea and Evans, 2011; Flink et al., 2015; Lovell et al., 2015b; Farnsworth et al., 2016; Ben-Yehoshua et al., 2023, Osika and Jania, 2024). They form a key line of evidence for identifying past surges when there is no direct observational data (e.g., Farnsworth et al., 2016; Ben-Yehoshua et al., 2023). Because CSRs form beneath surging glaciers, in situ geotechnical measurements could provide a valuable data set on stresses and strains in the subglacial environment right before the stagnation of surges.

Flutes: Flutes are streamlined ridges of sediment formed subglacially and are often found in front of surging glaciers in Svalbard, both in terrestrial and marine settings (Figures 15e and 16a). Their formation during surges is associated with rapid advance causing flow-parallel deformation of the underlying basal sediments. In marine settings they can be over 1 km in length (e.g., Borebukta, Ottesen and Dowdeswell, 2006). Flutes often form in a close geomorphological association with CSRs, with both forming in the subglacial environment (e.g., Christoffersen et al., 2005).

Eskers: Eskers are sinuous ridges of sand and gravel that form in channelised subglacial or englacial meltwater systems, which can be preserved in the foreland during glacier retreat. Their formation is not uniquely linked to surging, but eskers are often found as part of the Svalbard surging landsystem (e.g., McCerery et al., 2024; 2025). In some cases, geometrical ridge networks similar to CSRs but composed of sand and gravels have been reported (Evans et al., 2022) (Figure 15f). These likely reflect pressurised meltwater exploiting the heavily fractured glacier towards the end of a surge and are probably similar to ‘zig-zag’ or ‘concertina’ eskers reported from some surging glacier forelands in Iceland (Evans and Rea, 1999). Morphologically, such eskers are hard to distinguish from CSR networks without detailed sedimentological investigations. Large sinuous seafloor eskers are often revealed during quiescent-phase retreat of marine-terminating eskers (e.g., Ottesen et al., 2008, 2017).

Quiescent phase stagnation and retreat: Most landforms associated with surging form during the active phase due to the combination of fast ice flow, frontal advance and a highly saturated glacier bed. The geomorphological signature of the quiescent phase is typically less diagnostic of surging but can still be identified. In terrestrial settings, the cessation of surging leads to widespread stagnation and subaerial downwasting of the over-extended glacier front. Surging glaciers often transport large volumes of debris, creating extensive areas of ice-stagnation topography in the form of ice-cored hummocky moraine (e.g., Schomacker and Kjaer, 2008). Debris flows and kettle holes are common as buried ice degrades over time, which, together with extensive glaciofluvial erosion, can impact the preservation of landforms such as CSRs and flutes. At tidewater surging glaciers, annual retreat moraines can form on the seafloor during quiescent phase retreat (e.g., Ottesen and Dowdeswell, 2006; Flink et al., 2015) (Figure 16d), whilst subaerial stagnation terrain will likely be common along their terrestrial fjord margins (e.g. Lovell et al., 2018b).

4.3. Historical observations and archival evidence for surging

Nineteenth and early 20th century expeditions to Svalbard produced a wealth of maps, photographs and written observations (e.g., Hamberg, 1894; Conway, 1897; Gregory et al., 1897; Garwood and Gregory, 1898; Hoel, 1914; Gripp, 1929), which both directly and indirectly provide an important insight into the state of glaciers at that time. The end of the 18th century featured substantial improvements in topographic mapping techniques (Holmlund and Martinsson, 2016), meaning the geographical accuracy of maps became reliable enough for intercomparisons. In some cases, maps, qualitative observations, and subsequently photographs, strongly suggest that glaciers were actively surging. For example, one of the first reliable sources of a surge was by the 1838 French La Recherche Expedition, who painted the glacier Recherchebreen as extensively crevassed (Figure 2) and mapped its terminus to an extent that far exceeded both previous and subsequent maps and is corroborated by modern observations of a submerged moraine (Zagórski et al., 2023). Other events such as the ~1908 surge of Wahlenbergbreen was captured through repeated mapping campaigns showing a ~6.6 km advance between 1896 and 1908 (Figure 17), with accompanying photographs detailing its highly crevassed surface (de Geer, 1910). While these unique data points are useful for historical accounts of surging, they are strongly biased towards large events along the coast. The quality of these historical maps and observations prohibits the detection of small (<1km) scale events, and most studies were carried out from a ship, with very few exceptions to this rule.

FIGURE 17

One of the only historical sources of non-coastal observations is from the Conway Expedition of 1896 crossing of Spitsbergen (Conway 1897, Gregory et al., 1897, Garwood and Gregory, 1898). They walked eastward from Adventalen (where Longyearbyen has since been established) and photographed "Booming Glacier" (today Drønbreen), noting its "aggressive front" (Figure 18; Gregory et al., 1897). They also passed other glaciers such as Rieperbreen, Foxbreen, Ayerbreen and Scott Turnerbreen and provided observational and photographic leads to infer the ongoing or imminent surges (Mannerfelt et al., 2024). Additional Norwegian photography and mapping campaigns between 1906 and 1928 yield further potential for detecting inland surges (Figure 18d), but not all of these thousands of archived photographs have been analysed and published. Photographic and observational evidence is invaluable for further understanding the past dynamics of terrestrial glaciers in Svalbard, but information is sparsely distributed along the path of the associated expeditions, leading to the need for extrapolation to establish a wider picture.

FIGURE 18

5. Svalbard surge-type glacier database

5.1. Database structure

We have developed a new database of surge-type glaciers in Svalbard (Harcourt et al., 2025b) by combining existing compilations and reviewing studies examining surge dynamics, many of which have been discussed in the previous sections. Through this literature review we have documented, where they exist, years of surge onset and termination, active and quiescent velocities, and terminus changes. We record these characteristics using the RGI 7.0 digital glacier database (RGI 7.0 Consortium, 2023). Observations of surges are generally limited to the period ~1850-2025 (time of writing), which broadly corresponds to the end of the LIA through to the present, but some palaeo-glaciological evidence for surging may relate to activity occurring prior to this.

Our compilation of existing Svalbard-wide glacier surge databases is sourced from several studies: Lefauconnier and Hagen (1991) [LH1991]; Hagen et al. (1993) [H1993]; Sund et al., 2009 [SU2009]; Sevestre and Benn (2015) [SB2015]; Farnsworth et al. (2016) [F2016]; Kääb et al. (2023) [KA2023]; Koch et al. (2023) [KO2023]; Guillet et al. (2025) [GU2025]; and Strozzi et al. (2025) [ST2025]. The compilation of LH1991 only covers eastern Svalbard and mostly focuses on marine-terminating glaciers but is included as it contains details on surge characteristics. H1993 is the original database of glaciers across Svalbard and similarly contains details of historical surges. The current RGI 7.0 database defines the 'surge status' of each glacier according to Sevestre and Benn (2015): (0) no evidence of surging; (1) possible surge, (2) probable surge, and (3) observed surge. Most of the evidence for surge behaviour in this database has been verified through independent studies. The F2016 compilation was manually translated into the RGI 7.0 database. The glacier names described in F2016 often referred to tributaries which are now combined into single glacier catchments (e.g. Nuddbreen / Strongbreen), hence we manually combined these entries. The compilations from SU2009, KA2023, KO2023, GU2025, and ST2025 were manually transcribed from tables in PDF files or online repositories.

The KA2023 data are based on manual surge identification from annual Sentinel-1 interferometric wide-swath (IW) satellite radar backscatter differences between 2017 and 2022 (Kääb et al. 2023). For the present review, we updated the data by mapping more recent surges from winter-to-winter differences 2022-2023, 2023-2024, and 2024-2025 using new IW data. Before 2017, we use 2015-2016 and 2016-2017 extended wide-swath (EW) data instead, acknowledging that these coarser data (compared to IW) might lead to less detailed surge identification, or overlooking of surges of small glaciers or surges accompanied by only limited backscatter changes. Based on these additional data, we are also able to update some surge information contained in the original KA2023, for instance concerning surge start and end years, and by adding the last year of strongly enhanced backscatter (before backscatter reduction). The new 2015-2025 backscatter-derived surge inventory over Svalbard now contains 39 surging glaciers (the 2017-2022 KA2023 contained 26 surging glaciers).

We complement these compilations with our own literature review to generate the most comprehensive database to date of surge-type glaciers in Svalbard. In the following sections, we provide details of the new database and compare it to existing compilations.

5.2. Directly observed surges

Direct observations of glacier surges are defined here as those where studies have presented evidence of glacier velocity changes an order of magnitude above quiescence, surface changes (e.g. heavy crevassing), large iceberg production in imagery, ice mass redistribution as detected through surface elevation changes, or inferred clear evidence of terminus advance from modern imagery or historical maps. Glaciers which have both accelerated (e.g. Sveabreen, Esmarkbreen) and have demonstrable evidence of surging in the past (e.g. presence of CSRs in their foreland) are considered to have been directly observed to surge. Of the compilations used here, only the F2016 database is not used as it infers surges from the landform record. A total of 157 surges have been directly observed in Svalbard (Lefauconnier and Hagen, 1991; Hagen et al., 1993; Sund et al., 2009; Kääb et al., 2023; Koch et al., 2023; Guillet et al., 2025; Strozzi et al., 2025), which accounts for 10% of all glaciers (Table 1) and 48% (16,141 km^2) of the total glacier area on Svalbard (Table 2). Of those directly observed surges, 59% are marine-terminating (Table 1). Figure 19 shows the spatial distribution of the directly observed surges. Most of the direct observations cover glaciers with large catchments, particularly where they terminate into the ocean. Dynamical changes on large glaciers can be more easily detected using satellite data and historical imagery, whilst a large advance of a marine-terminating glacier can increase iceberg production which can be detected in historical imagery (e.g. Lefauconnier and Hagen, 1991). Surges on smaller glaciers (e.g. <1 km^2) have generally not been detected, especially across Andrée Land (Figure 19b) and Nordenskiöld land (Figure 19c). This may be due to the inability of a smaller glacier to discharge large volumes of ice over a short period of time but could also be due to an inability of current sensing systems to detect lower magnitude changes in velocity or surface elevation. Many direct observations come from historical records (Lefauconnier and Hagen, 1991; Hagen et al., 1993) and were biased towards the eastern margins of the archipelago due to interests in calving glaciers and their impact on offshore structures and shipping routes. Direct observations of historical surges are mostly based on archival aerial imagery and identifying known features of surges (e.g. crevassing, steep surface slopes), whilst after the 1990s satellite measurements have mostly been used due to improvements in mapping glacier velocity changes and terminus advances during a surge. The reliance on these methods likely means smaller surges are missed from this compilation.

FIGURE 19

TABLE 1

5.3. Indirectly observed surges

Glacier surges interpreted from the landform record or historical maps (see section 4.3) are classified as 'indirectly observed surges'. Here, we do not differentiate between 'possible' and 'probable' surge-type glaciers as used by Sevestre and Benn (2015) and the current RGI7.0 database to avoid potential subjectivity in our database. Here, most evidence is taken from the F2016 database (Farnsworth et al., 2016) although there are several additional studies which have detected surges at outlets not mentioned in Farnsworth et al. (2016) (Sund et al., 2009; Robinson and Dowdeswell, 2011; Flink et al., 2018). We have identified a total of 535 glaciers with evidence of past surging behaviour, representing 34% of all glaciers in Svalbard (Table 1) and 65% (22,003 km^2) of the total glacier area on Svalbard (Table 2). This is undoubtedly an underestimate, as Farnsworth et al. (2016) focused on the terrestrial landform record and therefore did not explore marine-terminating glacier forefields, such as several of the outlets in Austfonna, Vestfonna and Kvitøyjøkulen. Strikingly, many glaciers never previously considered to be surge-type contain CSRs in their foreland, suggesting these glaciers may have very long quiescent periods towards the upper end of the spectrum in Svalbard (e.g. over 150 years) or have lost the ability to surge. This includes glaciers with long-term observational records (e.g. Kronebreen, Nordenskiöldbreen) which have explicitly been categorised as not surge-type (e.g. Błaszczyk et al., 2021; Kavan et al., 2024). Until recently, Hansbreen in southern Spitsbergen was also not considered to be surge-type, but archival photographs and geomorphological mapping now suggests it underwent a surge in the late 1800s (Osika and Jania, 2024). Furthermore, 23% (n=124) of the glaciers with past evidence for surging (indirect) have been directly observed to surge. This finding suggests that we will uncover more evidence for glacier surges across the archipelago as we continue to study glacier dynamics in Svalbard.

The larger number of surge-type glaciers identified through indirect evidence increases the spatial coverage of surge-type glaciers across Svalbard (Figure 20). Many smaller glaciers across Andrée Land and Nordenskiöld Land have evidence of past surge behaviour, particularly through the presence of CSRs in their foreland. The dynamics of these smaller glaciers is difficult to monitor using satellite methods and so geomorphological evidence for past unstable ice flow is usually the only way to detect past surges. Figure 20 demonstrates that many smaller glaciers across the large ice fields of Spitsbergen in the northwest, northeast and south have evidence for past surge behaviour. Direct evidence for surging has mostly been found on the eastern edges of these three subregions. In comparison, past evidence for surging extends from these eastern regions to the warmer Atlantic side along the west coast of Spitsbergen, and also across Ny-Friesland. There is a distinct lack of geomorphological evidence for surging across the northeast of Svalbard which is likely due to the sparse bathymetry data available to analyse submarine glacial landforms and confirm the presence of past fast flow related to a surge, whilst the geology of this region is also different which may alter surge behaviour as well as CSR formation through differences in sediment supply. Although these observational gaps are being filled through the acquisition of new bathymetric data (e.g. Flink et al., 2018), more surveys are needed to increase spatial coverage in this area and also around Kvitøya. We find that 21% (n=33) of glaciers directly observed to surge do not have evidence for past surge behaviour. This is most likely due to scarce observations rather than the behaviour representing a different type of flow regime other than a surge, although this remains to be tested. For example, there was no evidence to suggest Monacobreen was a surge-type glacier before its surge in the 1990s (Murray et al., 2003a). Further analysis of historical data sets and the expected continuation of satellite EO time series suggests that we will uncover many more surge-type glaciers in Svalbard. Finally, we encourage further analysis of geomorphological (e.g. Farnsworth et al., 2016; McCerery et al., 2025) and glaciological evidence to understand past surge behaviour across the archipelago. Recent studies (e.g. Mannerfelt et al., 2024) are beginning to fill this knowledge and observational gap.

FIGURE 20

5.4. All surges

Compiling both the direct and indirect databases together, we estimate that 36% (n=565) of glaciers in Svalbard are surge-type (Table 1), which accounts for 75% (25,496 km^2) of the total glacier area on Svalbard (Table 2). We note here that if a glacier has been both 'directly' (e.g. velocity changes) and 'indirectly' (e.g. through the presence of CSRs) observed to surge, it is only counted once in the 'All Surges' category. Of these directly observed glaciers, 24% are marine-terminating and 76% are land-terminating. Comparing to all glaciers in Svalbard, 73% of all Svalbard's marine-terminating glaciers are surge-type, whilst 31% of all land-terminating glaciers are surge-type (Table 1). In other words, there is proportionately more surge-type marine-terminating glaciers than there are surge-type land-terminating glaciers. Figure 21 shows the spatial distribution of surge-type glaciers across Svalbard. The ice fields in northwest, northeast and south Spitsbergen contain several large glacier catchments many of which have exhibited surge behaviour, with only a collection of outlets showing no evidence of past surge behaviour. Regions with many small valley glaciers (Figure 21b and 21c) generally have fewer surge-type glaciers but as discussed previously, this pattern may be due to slower dynamics related to surge behaviour with lower ice fluxes that are difficult to detect in historical archives, palaeo-glaciological landforms and modern-day sensing systems. Surge observations in Vestfonna and Austfonna are more limited, most likely due to fewer in situ observations of palaeo-glaciological landforms on the seafloor. We expect that several of the outlets from both ice caps may surge in the future given the past history of surging in the region (Robinson and Dowdeswell, 2011). Finally, there appears to be little evidence for glacier surges across the western coast of Albert I Land in northwest Spitsbergen despite there being several large tidewater glaciers in this region (e.g. Raudfjordbreen, Smeerenburgbreen, Svitjodbreen). Larusbreen, a small glacier in this region that terminates partially on land and in the ocean, was heavily crevassed in 2016 and partially advanced, which suggests it might have been surging but further work (e.g. by mapping velocity changes) is required to confirm this. Future work should target these less studied regions to better understand glacier dynamics and past evidence for surging (e.g. through historical archives and the landform record).

FIGURE 21

Surge-type glaciers in Svalbard range in size: 9.5% (n=54) are <1 km^2, 45.4% (n=258) are 1-10 km^2, 33.4% (n=190) are 10-100 km^2, 11.3% (n=64) are 100-1,000 km^2, and 0.4% (n=2) are 1,000-10,000 km^2. The smallest glacier that has been directly observed to surge is U/Storknausen E by Hagen et al. (1993) with a surface area of 0.86 km^2, whilst the smallest glacier with evidence of past surge activity (excluding detached tributaries of larger surging glaciers) has a surface area of 0.16 km^2 and is an unnamed valley glacier (RGI2000-v7.0-G-07-00706) located in western Nathorst Land (Farnsworth et al., 2016). Smaller glaciers may be unable to build up the mass required for a surge and thus could be treated as not a surge-type glacier, as in previous studies (e.g. Bouchayer et al., 2022). Moreover, they are thin (Bahr et al., 2015) which typically means they are cold-based due to conductive heat losses and, therefore, cannot build up enthalpy at the glacier bed to initiate fast flow. Despite this, 54 glaciers with a surface area smaller than 1 km^2 were found to be surge-type in our compilation. Some of these are former tributaries of larger surge-type glaciers (e.g. Esmarkbreen, Wahlenbergbreen) or once formed part of a larger lobe (e.g. Smaubreen-Berrklettbreen-Vallotbreen). However, there are some isolated valley glaciers such as Meyerbreen and Purpurbreen in Andrée Land, Dumskoltbreen in Sørkapp Land, and Saksbreen in Wedel Jarlsberg Land which have CSRs present in their foreland (Farnsworth et al., 2016) and are therefore likely to have surged in the past. This suggests that small valley glaciers in Svalbard have previously been able to surge and may be undergoing very long quiescence periods and their active surge is yet to be observed. Alternatively, these smaller valley glaciers may have surged in the past when they were larger but are now unable to due to excessive thinning leading to a thermal regime switch to predominantly cold-based (Mannerfelt et al., 2024). For example, it has been suggested that Midtre Lovénbreen transitioned to a non surging state due to a prolonged period of negative mass balance which inhibited sliding due to the presence of cold-based ice at its bed (Hansen, 2003). The physical relationship between glacier size, thermal regime and surging potential, alongside the relative importance of thinning and meltwater production (e.g. Nuth et al., 2019) over time has not yet been tested and requires further study.

5.5. Characteristics of Svalbard surges

It has been suggested that surge-type glaciers in Svalbard have different characteristics from their non-surging counterparts (e.g. Jiskoot et al., 1998; 2000; Bouchayer et al. 2022). Here, we compare our new database of surge-type glaciers in Svalbard with glacier characteristics from the RGI7.0 database (Figure 22). We choose to compare six characteristics available in the RGI7.0 database (i.e. area, elevation range, mean elevation, slope, length, aspect) that have previously been suggested to influence a glacier's ability to surge (Jiskoot et al., 1998; 2000; Bouchayer et al. 2022). We note that we are comparing glaciers with evidence of surging behaviour with the entire list of glaciers in Svalbard, many of which may be surge-type but with no demonstrable evidence. Therefore, this analysis may be more accurately described as a comparison between glaciers with a higher probability of surging compared to those in long quiescent phases that may or may not be surge-type. We find that the average elevation range, slope and length (Figures 22b,d,e) differs between surge-type and non-surge-type glaciers. This means that compared to non-surge-type glaciers, surge-type glaciers have slopes that are 3.5° shallower (9.7° compared to 13.2°), are 4.4 km longer (5.6 km compared to 2.7 km), and extend across a 152.8 m larger elevation range (629.4 m compared to 476.6 m). We also find that the area of surge-type glaciers is 6 km^2 larger compared to non-surge-type glaciers, although there may be an element of bias due to our ability to more easily observe surges of larger glaciers both now and in the past. In contrast, we find no clear relationship between surge classification and both aspect and mean elevation (Figures 22c,f).

It has been previously suggested that local environmental factors may influence the propensity of a glacier to surge (Clarke et al., 1986; Clarke, 1991; Sevestre and Benn, 2015) and similar observations have been made in Svalbard (e.g. Jiskoot et al., 1998; 2000; Bouchayer et al. 2022). Despite the bias in surge observations towards large glacier catchments, the larger surface area of surge-type glaciers compared to non-surge-type glaciers (Figure 22a) has been observed in previous studies (Sevestre and Benn, 2015). This is consistent with the notion that temperate conditions at the glacier bed can only be sustained through thick ice to avoid conductive heat losses. Larger glaciers are also likely to be longer (Figure 22e; Hamilton and Dowdeswell, 1991; Jiskoot et al., 1998; 2000). Longer glaciers have a greater longitudinal stress coupling between the upper glacier regions and its terminus, which enhances the propagation of fast flow on both upward and downward propagating surges. This leads to greater mass transfer during a surge compared to smaller and shorter glaciers. Furthermore, larger and longer glaciers may accumulate more mass compared to smaller and shorter glaciers. This is corroborated by the fact that surge-type glaciers are found over a greater elevation range (hypsometry; Figure 22b), which might suggest that these glaciers can also reach elevations cold enough to retain accumulated mass whilst ablation rates remain high down-glacier. Therefore, long glaciers with shallower slopes that cover a wide elevation range may be expected to have both high accumulation and ablation rates, leading to a steepening surface profile that, possible at some critical threshold, induces oscillatory surge behaviour as the glacier builds up mass (quiescence), redistributes it during a surge (active) and then builds up mass again (quiescence). Ultimately, these factors imply a scale-dependence on glacier surge behaviour in Svalbard.

FIGURE 22

Variations in the spatial distribution of Svalbard surges over time is shown in Figure 23. We note that several surges in the historical record have not been accurately dated and there may be errors. We split the time series into three time steps: the LIA maximum (1800-1930), early air photo record (1930-2000), and the dense contemporary observational period (2000-2025). During these time periods, we have identified 57 (1800-1930), 80 (1930-2000), and 52 (2000-2025) observed surges. This equates to 0.44 (1800-1930), 1.16 (1930-2000), and 2.1 (2000-2025) surges per year. Multiple surges have been observed at 26% (n=41) of all glaciers directly observed to surge. The greater number of surges per year identified since 2000 likely reflects the denser range of observations available from satellite data. The fewer observations before 1930 similarly probably reflects our reliance on historical archives and geomorphological analyses. Some glaciers, such as Bodleybreen, are likely to have experienced more than once surge during the Holocene (Flink et al., 2017) but it is currently not possible to date these historical surges. Therefore, whilst the spatial and temporal variability likely reflects limitations in our current observational capacities, we can draw some early conclusions from their patterns.

FIGURE 23

The spatial distribution of identified surges is remarkably similar over the three time periods with evident clusters in Oscar II Land and Olav V Land where there are glacier surges present in all three epochs. These two regions are dominated by large surges e.g. Negribreen in Olav V Land. There was a cluster of surges in northwest Isfjorden in both 1800-1930 and 2000-2025 and their apparent synchronicity might suggest their behaviour is partly driven by a common mechanism. In southern Spitsbergen, the Paulabreen system has been active in all three time periods and continues to be in the present day (Kääb et al., 2023; Koch et al., 2023; Lovell and Fleming, 2023). The most prominent surge activity in southern Spitsbergen can be found in van Keulenfjorden (1800-1930 and 2000-2025) where Nathorstbreen and its tributaries are located. In the time period 1930-2000, this system did not appear to be active and instead surges were mostly found along the east coast of Sørkapp Land.

Surges on Edgeøoya have been mostly dominated by several advances of the large Stonebreen catchment.

The lack of evidence for many surges from Vestfonna and Austfonna likely reflects a lack of submarine data available to reveal past signatures of ice flow. We note that many of the surges identified with dates are marine-terminating despite representing a smaller percentage of the total number of Svalbard glaciers (Table 1). This possibly reflects the better preservation of past fast flow in the submarine geomorphological record. Therefore, our time series of spatial changes in surges is biased towards those with clear evidence of surge behaviour. If observational techniques had an increased sensitivity to smaller magnitude changes or we had more lines of evidence from geomorphological landforms and/or historical archives, many smaller magnitude surges may be uncovered. We therefore suggest that our current database is biased towards ice flow from larger glaciers. Unstable fast ice flow may take many different forms depending on glacier characteristics and other local environmental controls such as geological substrate, ocean boundary conditions, local climate and many more. Therefore, as our measurements improve, we expect to observe more complex behaviour related to glacier surging that is not captured in these plots which are binary in nature i.e. surge-type or not. We explore this concept in the next section.

6. Surge behaviour

6.1. Continuum of surging

As we acquire more observations of glacier surges in Svalbard using a diverse range of techniques that are becoming more accurate and increasingly sensitive to lower magnitude changes in ice dynamics, the more we observe a larger variability in surge behaviour across the archipelago. This challenges the assumption that we can simply classify a glacier as ‘surge-type’ or ‘not surge-type’, which has previously been suggested by several authors (e.g. Raymond, 1987; Jiskoot et al., 2000; Benn et al., 2019a). We therefore propose that Svalbard glaciers can be represented as a continuum of dynamical behaviours (Figure 24) that include: (1) full catchment scale surges; (2) pulses from valley glaciers with several tributaries; (3) low magnitude glacier speed-ups and slow-downs; and (4) glaciers which do not surge. There have been similar observations indicating a spectrum of surge behaviour from the Canadian Arctic (Van Wychen et al., 2020), Alaska (Herreid and Truffer, 2016), and the Karakoram (Quincey et al., 2015), suggesting this is a widespread occurrence. This spectrum of surge behaviour reflects differences in glacier characteristics (geometry, size, elevation range), spatial variability in subglacial enthalpy (Benn et al., 2019a), subglacial lithology, and local climatic conditions that influence rates of accumulation and ablation. All these features are likely typical of polythermal glaciers (Kristensen and Benn, 2012) where spatial variability in thermal regime leads to differences in surge behaviour. These factors ultimately influence the dynamics of a surge and whether it manifests as a surge bulge travelling down-glacier (Sund et al., 2009) or is initiated from the terminus (e.g. Sevestre et al., 2018) which leads to longitudinal stretching of the ice. Both may lead to mass redistribution and glacier terminus advance, but the magnitude of these changes depends on where the glacier is positioned along this continuum, with a higher likelihood of terminus advance when positioned nearer the full-catchment scale surge.

FIGURE 24

We consider a large, full-catchment scale surge of a glacier to represent an extreme end-member of this continuum. The surge of Basin-3 in Austfonna (e.g. Dunse et al., 2015) that started in 2012 and remains ongoing at the time of writing in 2025 is the best contemporary example of such an event. A surge of this magnitude can be readily detected through velocity and elevation changes in remote sensing data and typically leave behind strong indicators of past fast ice flow e.g. CSRs. Negribreen's surge since 2016 (Figure 4a; Benn et al., 2022; Trantow and Herzfeld, 2025) is also an example of this end-member type. Ordonnansbreen, which is a tributary of Negribreen, was not active during this surge. It should be noted that a 'catchment-scale surge' is defined by the RGI7.0 glacier outlines and often combines tributaries into a single catchment, such as Negribreen and Ordonnansbreen, therefore neglecting the potential for tributaries to surge independently. At the other end of the spectrum, glaciers that may not be able to surge are typically those that are cold-based and small (Sevestre et al., 2015; Mannerfelt et al., 2024). For a glacier to become this end-member type, mass accumulation does not lead to pressure melting, whilst conductive cooling evacuates any subglacial water transported to the bed from the surface via moulins, hence the bed remains cold-based, inhibiting sliding. In Svalbard, small valley glaciers across Nordenskiöld Land, Dickson Land and Andrée Land may be characterised by this end-member type although this is conjecture without additional data on thermal regime and ice dynamics.

Between these end-member types, Svalbard surges exhibit a wide variety of behaviours. For a glacier system consisting of multiple tributaries, such as Nathorstbreen and Paulabreen, the fjord where these glaciers coalesce into a single unit often undergo 'pulses' of advance in response to surges of individual tributaries (e.g. Nuth et al., 2019). The pulses of several tributaries might reflect the storage and release of energy locally within a glacier catchment, reflecting local variations such as bedrock topography and lithology, or even the surface slope of individual catchments. Therefore, spatial variability in enthalpy at the glacier bed may play a critical role in the behaviour of glacier surges across Svalbard. How the individual processes at a single glacier are interconnected across a wider system is less well known, although it has been previously suggested that surges are more prevalent from catchments with a higher degree of ‘branchiness’ (Jiskoot et al., 2000). Furthermore, surge propagation may be restricted by the presence of subglacial conduits incised into the bed (i.e. Nye channels; Benn et al., 2009), enabling the evacuation of meltwater and therefore reducing enthalpy. Neighbouring glaciers that are seemingly disconnected may also display apparent synchronicity in their surge timing but with different ice dynamics. For example, whilst Comfortlessbreen surged and underwent a 700 m advance in 7 years (Sund and Eiken, 2010; King et al., 2016), the speed-up of the adjacent Uvêrsbreen was barely noticeable on satellite data due to a lack of a considerable terminus advance (Figure 7b). Across the northern coast of Isfjorden, several glaciers have either surged (Sevestre et al., 2018; Harcourt et al., 2024) or accelerated in recent years. Although these are two isolated cases, the synchronicity in surge behaviour suggests there may be a shared process driving glacier dynamics within sub-regions of Svalbard. Possible mechanisms include the initiation of fast flow due to ocean warming, increased atmospheric temperatures enhancing surface melt that eventually reaches the bed and initiates sliding, or possible ice piracy altering the ice flux between neighbouring catchments. These hypotheses require further testing.

Between the glaciers that surge and the cold-based glaciers which act as an end-member of this continuum, there are several glaciers which have exhibited fast ice flow of a lower magnitude compared to the aforementioned glaciers (Sund et al., 2009). The surge of Monacobreen between 2017 and 2020 is a prime example (Benn et al., 2022) having undergone a multi-stage pattern of speed-up following seasonal ice flow acceleration which led to an increase in terminus velocities four times relative to pre-surge conditions. Some glaciers have sped-up and slowed down in a cyclical manner, consistent with surge behaviour, yet the magnitude of the velocity change was small, only 1-2 m per day, such as Hinlopenbreen (Figure 25d), Hansbreen (Figure 25e), and Esmarkbreen (Figure 25f). Sveabreen, which terminates in northwest Isfjorden, appeared to speed up at the same time as Wahlenbergbreen’s surge but did not evolve into a full-scale surge. Finally, some glaciers appear to be completely out of sync with climate, such as Kvalbreen (Figure 25a); seasonal signals of ice flow on these glaciers are almost completely absent and instead appear to be undergoing ice flow regimes almost entirely driven by internal ice dynamics. On the other hand, Hinlopenbreen (Figure 25d) has been undergoing a long-term seasonal cycle that does not appear to be dampened by long-term climate. A similar trend is found at Stonebreen (Figure 25c). The velocity of Nordsysselbreen and Sefströmbreen has generally fluctuated around 1 m/day but accelerated rapidly to above 10 m/day during their recent surges in 2024. The ice acceleration of these glaciers would be considered a full-catchment surge. Finally, cold-based glaciers with past evidence of surging such as proglacial CSRs (e.g. Mannerfelt et al., 2024) may not be classified as an end-member type. Instead, these glaciers have the potential to surge again and lie somewhere in between ‘no surge’ and ‘slow acceleration’.

FIGURE 25

6.2. Surge cycles and causality

It has typically been thought that Svalbard surges undergo a three-stage cycle of change from quiescence, active surge and then a gradual slowdown back to quiescence (Dowdeswell et al., 1991; Sund et al., 2009). In this model, subglacial enthalpy builds up before frictional feedbacks lead to an active surge. This enthalpy, which is defined as the internal availability of glacier energy and is a function of ice temperature and meltwater (Aschwanden et al., 2012; Benn et al., 2019a), then dissipates after the redistribution of mass that results from a surge, and the glacier reaches a minimum in velocity. The quiescent phase is long due to the low precipitation rates of Svalbard that increases the time taken for mass to build up in the reservoir zone. Our database confirms that the quiescent phase length ranges between 40 and 150 years (Lefauconnier and Hagen, 1991; Hagen et al., 1993; Flink et al., 2015). In comparison, the active phase length is far shorter and estimated to be between 3-10 years (Dowdeswell et al., 1991) which can be verified by satellite measurements of modern-day surges, some of which have been presented in this review. For surges of large glacier catchments (e.g. Basin-3, Negribreen) the active phase appears to be longer, usually 5 or more years, which suggests that the length of the quiescent and active phases scale with glacier size.

However, observations of Svalbard surges indicate that this process is more complex (Figure 25; Strozzi et al., 2017; Benn et al., 2022) and instead surges typically move through six interconnected stages. During early-quiescence (Stage 1), enthalpy is completely dissipated, and the glacier surface slope will typically be shallower compared to that of an actively surging glacier. Subsequently, there is a slow build-up of subglacial enthalpy (Stage 2) as mass accumulates and ice near the bed reaches the pressure melting point, slowly increasing the area of basal temperate ice (Benn et al, 2019a). This initiates frictional feedbacks that lead to measurable ice flow changes (Benn et al., 2022) but are restricted due to the loss of enthalpy through basal refreezing, subglacial outflow through channels, leakage of meltwater through the subglacial groundwater system or other means (Murray et al., 1998). Therefore, thermal conditions and subglacial hydrology work in tandem to alter ice flow. At some critical point, the basal sliding regimes switches (Stage 3) from one driven by glacier thermal regime, such as a Weertman-style power law, to one that is dominated by hydrologically driven basal sliding, such as a regularised Coulomb sliding law which depends on basal water pressure (Weertman, 1957; Lliboutry, 1968; Schoof, 2005). A full-scale surge is initiated when a glacier speed-up transitions into ice acceleration (Stage 4), where glacier velocities increase by an order of magnitude over a short time period e.g. months. A short-lived peak in velocity (Stage 5) will occur at the point at which enthalpy conditions reach their maximum. This may last from days to weeks on smaller glaciers to months on larger glaciers. After a peak in surge velocity, enthalpy reduces, and the glacier decelerates back to quiescence (Stage 6).

Although the conceptual six-stage surge model for Svalbard is idealistic, it can be used to explain the processes driving surges with high velocities and large surface changes. In the years preceding the 2020 surge of Kvalbreen (Figure 25a), ice velocities cycled between low winter flow rates of 0.5 m per day to faster flow in summer of ~1 m per day. For both land- and marine-terminating glaciers, the slow buildup of enthalpy may last just a few months if the subglacial environment reacts quickly to frictional feedbacks, which appears to be the case at Kvalbreen, and therefore the seasonal velocity cycle may represent late stage quiescence (Stage 1). At larger glaciers (e.g. Negribreen, Basin-3), the slow enthalpy build-up (Stage 2) and velocity increase has been observed to last several years, reflecting slow enthalpy production and long response times to external enthalpy inputs (e.g. from supraglacial meltwater). Kvalbreen transitioned to an active surge in 2020 following ice flow acceleration (Stage 4) that lasted several months before reaching a velocity peak of ~6 m per day (Stage 5). Despite ice flow deceleration in winter 2020-2021 (Figure 6) suggesting a dissipation of subglacial enthalpy, Kvalbreen experienced a second velocity peak of ~5 m per day in 2021 (Figure 25a), and then a further low magnitude peak of ~1.5 m per day in 2022. The pattern of multiple velocity peaks during an active surge has been observed at other glaciers, such as Negribreen (Figure 4a). It reflects the glacier moving through Stages 3-6 of our six-stage model in a repeating pattern, starting in spring with a transition in the basal sliding regime (Stage 3), ice acceleration over summer (Stage 4), a peak in velocity (Stage 5) and then ice deceleration over winter due to a reduction in enthalpy (Stage 6).

It is likely that most glaciers will not pass through each stage of the six-stage model during a single surge cycle, potentially explaining why the broader range of surge-like behaviour observed in Svalbard is so varied (e.g. Figures 4, 5, 9, 25). The surge of Basin-4 in Austfonna that peaked at 3.5 m per day (Figure 25b) moved from quiescence (Stage 1) in 2015 to slow enthalpy build up (Stage 2) in 2016-2017, leading to a doubling of velocity to ~1.5 m per day. Ice flow acceleration (Stage 4) was observed in summer 2018 leading to a velocity peak (Stage 5). However, the velocity magnitude during these stages was around half that of Kvalbreen, suggesting that changes in the basal sliding regime did not activate the whole glacier catchment. Basin-4 then underwent a slow multi-year deceleration in 2019-2025, a pattern that can also be observed at Esmarkbreen (Figure 25f). Patterns of surface elevation change at Esmarkbreen suggest that a surge took place between 2009 and 2016 (Figure 6d) but only the final Stage 6 enthalpy dissipation is observable in the velocity time series. Ice flow deceleration of Svalbard surges is typically a multi-year process (e.g. Benn et al., 2022; Kääb et al., 2023; Koch et al., 2023), which may be due to several processes such as the development of an efficient subglacial hydrological system (e.g. Benn et al., 2019b), thermal regime changes due to changes ice mass distribution, and seepage of meltwater into the underlying permafrost (e.g. Murray et al., 2000), all of which reduce subglacial enthalpy. This implies that both hydrological and thermal changes contribute to enthalpy dissipation, which is typical of polythermal glaciers (Kristensen and Benn, 2012).

The style of surging and the pattern through which a glacier cycles through the six stage surge model reflects the competing impacts of internal and external forcing. Ice flow acceleration is usually restricted to a small spatial region that progressively expands in size. For example, acceleration may initiate in the reservoir zone and travel down-glacier as a surge bulge, or it may progressively propagate from the terminus upwards (e.g. Sevestre et al., 2018). This supports the notion that glacier acceleration is driven by subglacial cavity formation and their expansion over time (Thøgersen et al., 2019; 2024). Environmental conditions may accelerate the basal sliding regime change required to initiate ice acceleration (Stage 4). Dynamic thinning can induce glacier acceleration and promote surface fracturing that enables surface meltwater to penetrate to the bed and facilitate accelerated basal sliding (Sevestre et al., 2018). In addition, high melt years may lead to larger meltwater volumes reaching the glacier bed and increase basal water pressures leading to basal sliding (Flink et al., 2015). Other potential environmental factors could include glacier retreat past a subglacial pinning point, steepening of the glacier surface through increased melting in the ablation zone and mass build up in the accumulation zone, or changes in ocean thermal forcing. Rapid velocity fluctuations related to seasonal velocity changes that are not related to the internal dynamics of a surge may also be superimposed on surge velocities (e.g. Benn et al., 2019a; 2022). Ultimately, a glacier may cycle through all six stages to produce a typical surge with high velocities, but it may only enter a few stages, leading to the rise of more complex and varied glacier dynamical behaviour (e.g. Basin-4, Esmarkbreen) that can be explained by surge theory.

6.3. Future projections

Svalbard is located within the Arctic ring of surge-type glaciers (Figure 26a) which is defined by a climatic envelope described by a pair of linear equations relating mean winter precipitation (MWP), to mean summer temperature (MST) i.e. 2m air temperature in summer:

$$MST = 0.001MWP + 8.4 \quad (1)$$

$$MST = 0.0014MWP - 0.97 \quad (2)$$

where MST is in °C and MWP is in mm a^{-1} (Sevestre and Benn, 2015). Glaciers that sit between the bounds set by equations (1) and (2) are considered to have a high probability of being surge-type. We map the modern-day limits of this envelope in Figure 26a using monthly averaged ECMWF Reanalysis

5th Generation (ERA5) data from 2000 to 2009. We note that this envelope can also be defined by mean annual temperature (MAT) and mean annual precipitation (MAP) which may produce different results. Furthermore, this analysis also neglects differences between different versions of ERA reanalysis products (e.g. ERA1 and ERA5) as our focus is solely on the large-scale patterns. Figure 26a shows that Svalbard is currently at the edge of the surging climatic envelope which may partially explain the large variability in surge behaviour. In the future, we expect the climatic envelope to shift northwards as summer temperatures and the volume of liquid water precipitation both increase (Bintanja, 2018; McCrystall et al., 2021; Gutiérrez et al., 2021). By 2100, there are projected increases in MSTs by up to 5°C and MWP by 30% (Gutiérrez et al., 2021). Applying these crude estimates of change to Equations 1 and 2, we can estimate the future spatial distribution of the surging climatic envelope (Figure 26b). The changes suggest Svalbard will remain in this climatic envelope up to 2100 and hence surging activity is expected to remain prevalent across the archipelago. However, this interaction of a changing climate with surging prevalence is unlikely to be linear and the changes are expected to be more complex than the basic analysis presented here. Nonetheless, the changing overlap between the envelope and Svalbard might lead to changes in surge behaviour and also lead to surging of currently inactive ice masses such as Kvitøya. Post-LIA warming may have similarly altered the distribution of surge-type glaciers across Svalbard through changes in Svalbard's climate. Therefore, comparing past and present surge dynamics may yield insights into how future climate change will impact surging behaviour in Svalbard.

FIGURE 26

As changes in the prevalence of surge behaviour is driven by MST and MWP (Sevestre and Benn, 2015), it follows that the changing nature of surging is driven by surface melt and ice thickness changes. Where surface meltwater can reach the bed, enthalpy will increase and drive glacier acceleration during a surge. However, long-term increases in surface melt can enhance the channelisation of the subglacial drainage system and reduce ice velocity. This effect has been observed in Greenland (e.g. Tedstone et al., 2015) and could lead to a negative feedback cycle in Svalbard and inhibit surging. It is not known whether an increase in surface melting due to climate change (van Pelt et al., 2019) could accelerate this process in Svalbard. However, because the surging climatic envelope is expected to remain over Svalbard up to 2100 and likely beyond (Figure 26), higher surface melt rates will likely act to enhance enthalpy rather than reduce it. Furthermore, although MWP is projected to increase, increased surface melt will counteract this process and lead to Svalbard-wide glacier thinning (van Pelt et al., 2021), increasing conductive heat losses. For smaller glaciers, this will shift their thermal regime to predominantly cold-based (Sevestre et al., 2015; Mannerfelt et al., 2024). For larger glaciers, increased accumulation at higher elevation could increase the prevalence of subglacial meltwater generation and enhance sliding, whilst enhanced ablation near the terminus could steepen the glacier surface and promote faster flow, initiating frictional feedbacks (Thøgersen et al., 2019; 2024). The increasing prevalence of liquid precipitation in Svalbard (McCrystall et al., 2021) could also promote glacier sliding and surging. The impact of ocean thermal forcing on surging has not been studied but it is possible that regional warming could lead to synchronous glacier thinning and acceleration, initiating fast ice flow.

If the Arctic ring of surges is normally distributed, we would expect glaciers at the edges of the envelope to have a lower probability of surging compared to those near the centre. Svalbard is currently near the edge of the envelope (Figure 26a) but will progressively move to the centre as the envelope moves northwards. This might suggest enthalpy availability will increase and surge behaviour will change. In particular, a glacier will pass through each of the stages outlined in Section 6.2 at different times and at variable timescales, altering the length of the active and quiescent phases which are particularly sensitive to changes in meltwater inputs (Benn et al., 2019a). For example, the advances of Tunabreen during its multiple surges between the late 1800s and present day were progressively smaller as a result of smaller ice fluxes related to glacier mass loss (Flink et al., 2015). In comparison, Wahlenbergbreen and Borebreen have recently surged for the first time in ~100 years (e.g. Ottesen and Dowdeswell, 2006; Sevestre et al., 2018), demonstrating that the build-up of internal energy can still take several decades to accumulate despite ongoing climatic changes post-LIA. Finally, it is unclear whether movement in the position of the climatic envelope leads to an instantaneous change in the surge state of a glacier or whether there is a lagged response consistent with glacier response times. Unravelling the future behaviour of surges in Svalbard will rely upon understanding the response of surge-type glaciers to external forcing and how this relates to the build-up and release of energy during a surge.

7. Summary and outlook

Svalbard is a natural laboratory to study glacier surges given its high density of surge-type glaciers, ease of access in an Arctic context and availability of historical observations. When combined, this makes Svalbard surges arguably the best studied anywhere in the world. In this paper, we have reviewed the methodologies used to monitor glacier surges and compiled a new database of surge-type glaciers in Svalbard together with their characteristics. We estimate that 36% (n=568) of the 1,583 glaciers in Svalbard have demonstrable evidence for past surge behaviour, which represents 75% of the total glacier area on Svalbard. Of all the glaciers in Svalbard, only 10% (n=157) have been directly observed to surge, with the others being classified as surge-type based on glaciological or geomorphological evidence of past surging. We found that surge-type glaciers are generally longer, have shallower slopes, and can be found across a broader elevation range, in agreement with previous studies (e.g. Jiskoot et al., 2000; Bouchayer et al., 2024). Therefore, surge-type glaciers have specific characteristics that make them more likely to surge. Since the 1990s, observations of glacier surges have increased dramatically with the launch of several new satellites, and since 2014 the launch of the Copernicus Sentinel satellites has simplified continuous monitoring of glacier surges. Analysis of glacial landforms such as CSRs and historical archives including photographs and maps enables the detection of past surges which are critical for increasing the temporal coverage of surge records. In situ geophysical surveys using instruments such as GPR and seismometers enable the study of subglacial conditions but are difficult to conduct in challenging terrain such as heavily crevassed surfaces during an active surge. A more harmonised, integrated approach that combines each of these techniques through the 'observational pyramid' would enhance our capabilities to measure surges at different scales in Svalbard.

As observations of glacier surges increase in number and quality, we are beginning to understand that the phenomenon of a 'glacier surge' is more complex than previously thought and the binary classification of whether a glacier is surge-type or not starts to break down, as has been previously suggested (e.g. Raymond, 1987; Jiskoot et al., 2000; Benn et al., 2019). Instead, our database compiles glaciers with evidence for non-steady ice flow, which has been observed to take many forms. We find that the 3-stage model of Svalbard surges from quiescence-active-quiescence (Dowdeswell et al., 1991; Sund et al., 2009) fails when considering recent observations. Instead, up to 6 stages have been observed including: 1) quiescence; 2) a gradual multi-year velocity build-up; 3) a switch in basal sliding regime from thermal to hydrological; 4) rapid acceleration; 5) surge peak; and 6) gradual slowdown. These stages are typical of polythermal glaciers that are widespread in Svalbard (Sevestre et al., 2015). Furthermore, we note that some glaciers, such as Basin-3 in Austfonna, experience a full surge across their entire catchment whilst others have multiple tributaries or flow-units that surge independently as 'pulses', such as the Nathorstbreen glacier system. Additionally, some glaciers accelerate over multiple years, similar to the slow build-up phase we have identified, but then gradually slow down again. We suggest that Svalbard glaciers represent a continuum of behavioural characteristics beginning from a glacier with no apparent non-steady ice flow characteristics to a glacier that undergoes the traditional model of a Svalbard surge with a distinct acceleration, peak and then deceleration. The temporal evolution of surges can therefore be described by the 6-stage model whilst the spatial variability can be represented by the continuum approach.

To improve our understanding of the complex behaviour of surging in Svalbard, we suggest ten areas of research that should be prioritised:

1) *Long-term measurements*: There is an urgent need to generate a long historical time series of Svalbard glacier surges and their characteristics by bridging the gap between palaeo observations and the contemporary satellite record. This may be done by developing methods to detect surges in the historical record (e.g., developing a new 1960/61 DEM from available aerial imagery) as well as through new satellite observations.

2) *Documenting surge characteristics*: Initiate systematic cataloguing of fundamental surge behavioural parameters (e.g., surge onset year, surge termination year, terminus change, maximum velocity, mean velocity in quiescence, surge propagation rates). This will enable a better understanding of surge drivers, spatial and temporal patterns of surge behaviour across Svalbard, and an investigation into surge frequencies (e.g. Strozzi et al., 2025). This should combine existing monitoring results from different research groups and include analysis of satellite imagery, modelling studies, and artificial intelligence methods.

3) *Interaction between surges and glacier mass balance*: Improved quantification of the impact of surges on mass balance, e.g., combining close-range sensors with satellite observations of surface elevation change. This should also include studying the evolution of a glacier before and after a surge. Integrated field campaigns and combining simultaneous monitoring efforts will be critical in achieving this. Additionally, analysing how mass balance influences surge behaviour will improve our understanding of how surges are affected by regional climate. Modelling of these processes, such as ice discharge changes and surface elevation melt feedbacks (Oerlemans, 2018) should also be prioritised.

4) *Subglacial observations*: Direct observations of the subglacial environment during a surge are urgently needed to understand thermal and hydrological conditions. As discussed in this review, this is not simple due to the logistical complexities of deploying instruments over heavily crevassed surfaces and the issue of GPR signal attenuation. Interdisciplinary approaches and new measurement technologies (e.g. wireless subglacial sensors, drone-based GPR) are the recommended path.

5) *Past surges of small glaciers*: Studying the prevalence of past surges at smaller glacier catchments will help us to understand the impact of catchment size on surge distribution and the potential for smaller glaciers to undergo fast ice flow during a surge. This will also help us constrain the changing spatial distribution of surge-type glaciers across Svalbard. In particular, mapping their thermal regime, understanding their velocities and measuring volume changes could be quantified using in situ and remote sensing observations.

6) *Surge causality*: Improved analysis of the processes that lead to a surge is recommended. In particular, the distinction between events happening after a long succession of internal changes and events happening as the result of some distinct environmental ‘push’ such as intense surface melt, calving episodes, winter warm spells or surges of physically connected glaciers. Disentangling these processes is critical.

7) *Improved physical modelling*: To improve surge process understanding, it is critical to unify models with observations (e.g. Terleth et al., 2021). In particular, modelling glacier sliding and the influence of subglacial hydrology is considered a priority area to better understand surges. This will help to understand the drivers and causality of surges and their quasi-periodal cycles.

8) *Artificial intelligence (AI)*: New developments in artificial intelligence should be explored to: 1) identify glacier surges (e.g. Bouchayer et al., 2022) and their behaviour across the continuum of surges; 2) model the characteristics of glacier surges through data-driven approaches such as neural networks (NNs) and physics-informed neural networks (PINNs); and 3) improve the accuracy and sensitivity of current data products e.g. ice velocity, surface elevation change. AI may be used to fill observational gaps in time and space using both NNs and PINNs, as well as by fine-tuning foundation models pretrained on large training data sets (e.g. millions of data sets). The effectiveness of these approaches is still in its infancy but could lead to a step-change in our ability to understand past surge behaviour.

9) *Submarine measurements*: A significant observation gap for understanding glacier surges is the submarine environment, where subglacial outflow, iceberg calving processes, and fjord circulation patterns are key components impacting surge activity. Additionally, bathymetry data is essential for detecting past surge behaviour from submarine landforms. Measurements using AUVs, passive underwater acoustics, OBS / DAS systems can fill these gaps

10) *Research infrastructure*: We suggest that new and portable research infrastructure should be developed to enable rapid deployment on surging glaciers which often start surging abruptly and without warning. This will enable the measurement of these surges from the start to the end of a surge. The detailed specific recommendations for developing research infrastructure in Svalbard are outlined in a recent white paper on Svalbard surges (Harcourt et al., 2025a).

The future distribution of surge-type glaciers in Svalbard and their associated behaviours is likely to evolve as the spatial overlap between the surge climatic envelope and Svalbard changes as a result of climate warming. In particular, we expect that many of the smaller glaciers across the archipelago that have surged in the past can no longer surge due to thinning and a transition to a predominantly cold-based thermal regime. Continued monitoring from satellites and in situ geophysical sensors is critical to understand these evolving glacier instability processes.

Acknowledgements

This work was supported by the Research Council of Norway, project number 322387, Svalbard Integrated Arctic Earth Observing System – Knowledge Centre, operational phase 2022. AK acknowledges support from the European Space Agency projects Glaciers_cci and EarthExplorer 10 Harmony (4000127593/19/I-NB, 4000146464/24/NL/MG/ar). We would like to thank Berit Jakobsen from the University Centre in Svalbard (UNIS) for assisting in acquiring the historical paintings from the Recherche Expedition. We thank Torben Dunse for providing the Basin-3 Austfonna GPS data for Figure 9.

Data Statement

The database that has been created in this review is available via a zenodo repository: https://zenodo.org/records/18033216 (Harcourt et al., 2025b).

Tables

Table 1 Number of surge-type glaciers in Svalbard, split into marine- and land-terminating. Total number of glaciers in Svalbard is 1,583 based on RGI7.0. If a glacier has been both 'directly' (e.g. velocity changes) and 'indirectly' (e.g. through the presence of CSRs) observed to surge, it is only counted once in the 'All Surges' category.

	Total	**Marine-Terminating**	**Land-Terminating**
All Glaciers	1,583	190	1,393
Directly Observed Surges	157	92	65
Indirectly Observed Surges	535	119	416
All Surges	568	139	429

Table 2 Total and mean area of surge-type glaciers in Svalbard. Data taken from RGI7.0. If a glacier has been both 'directly' (e.g. velocity changes) and 'indirectly' (e.g. through the presence of CSRs) observed to surge, it is only counted once in the 'All Surges' category.

	Total Glacier Area (km^2)	**Mean Glacier Area (km^2)**
All Glaciers	33,841	21
Directly Observed Surges	16,141	10
Indirectly Observed Surges	22,003	14
All Surges	25,496	16

Figures

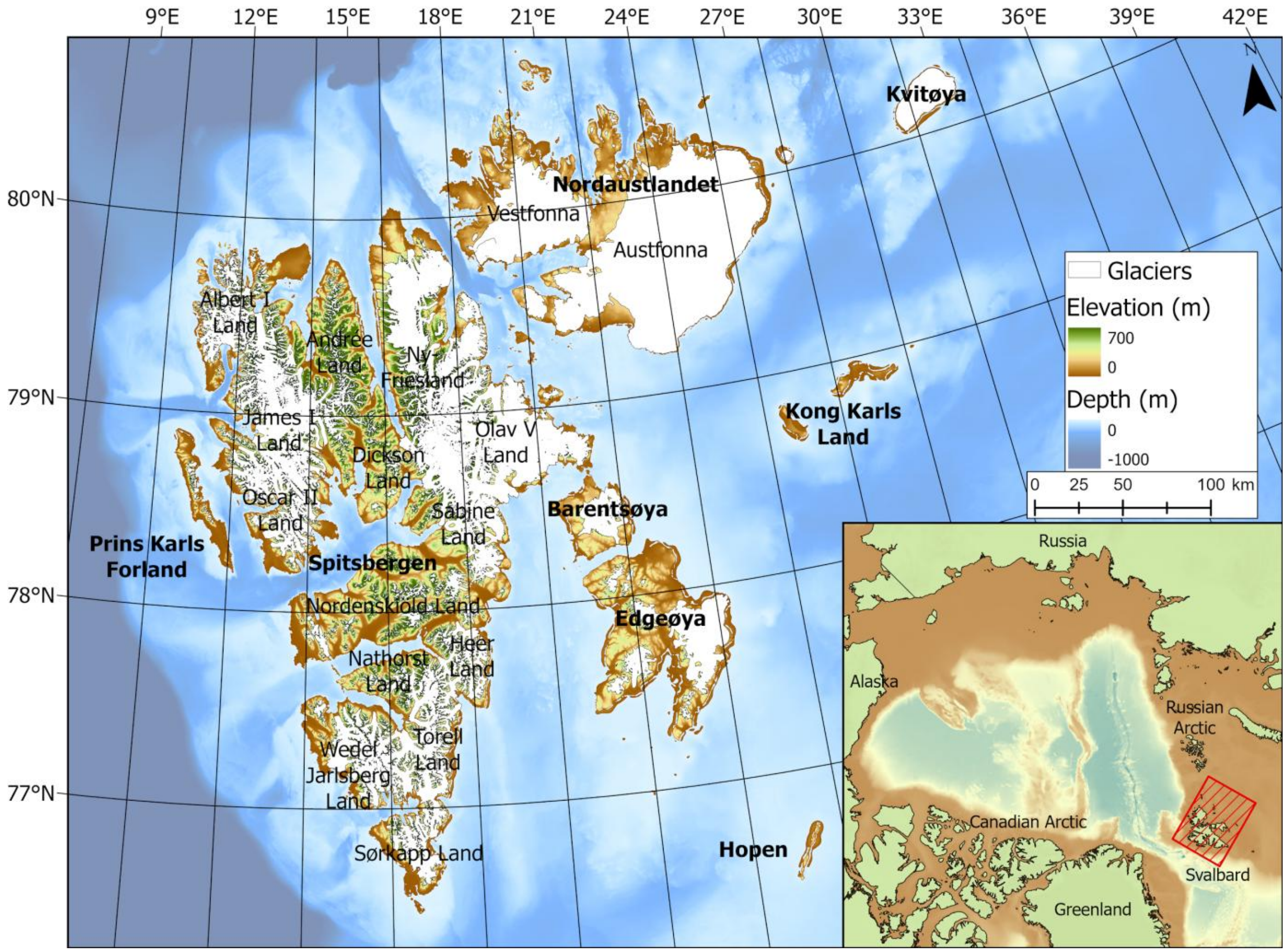

Figure 1 Location map of Svalbard and its position in the Arctic (highlighted in red within the inset panel). Names of different locations mentioned in the paper are highlighted. Land elevation and bathymetry are taken from the International Bathymetric Chart of the Arctic Ocean (IBCAO) (Jakobsson et al., 2024). Bold text indicates the locations of islands, whilst plain text represents different regions.

Figure 2 Painting of the terminus region of Recherchebreen (77.47°N, 14.73°E) from the ‘La Recherche’ Expedition between 1838 and 1840 (Commission scientifique du Nord, 1852).

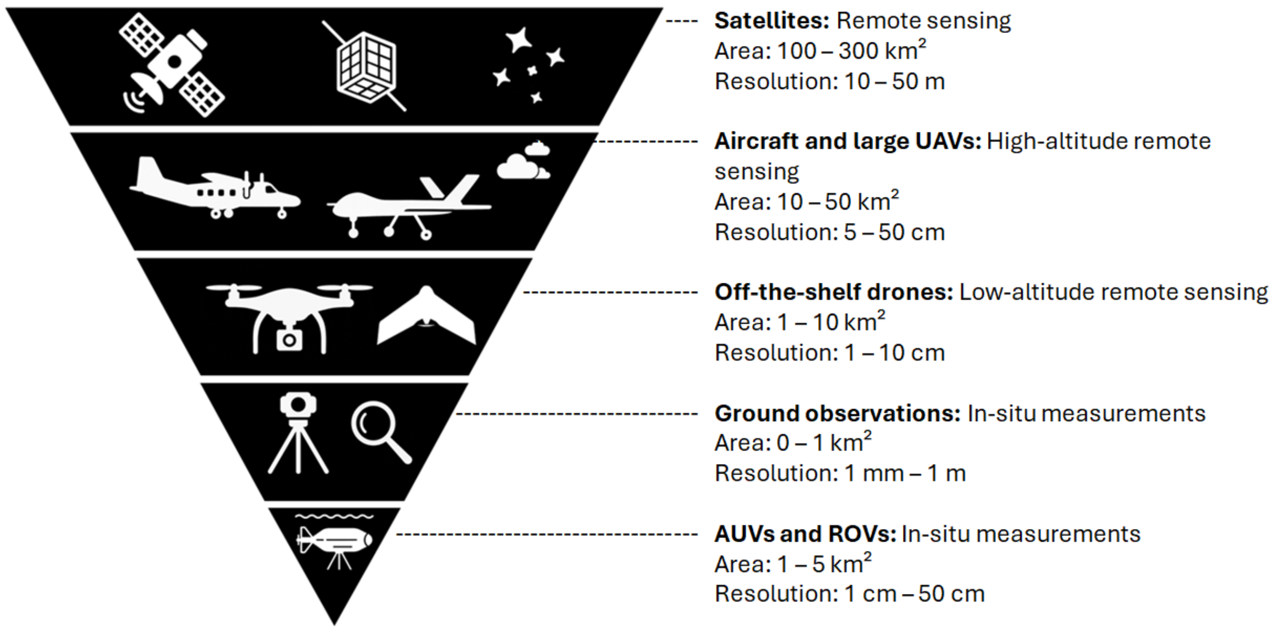

Figure 3 The ‘observational pyramid’ that is employed to monitor glacier surges in Svalbard at different scales. The lowest tiers, which include marine instruments such as AUVs and ROVs, relates only to marine or lake terminating glaciers.

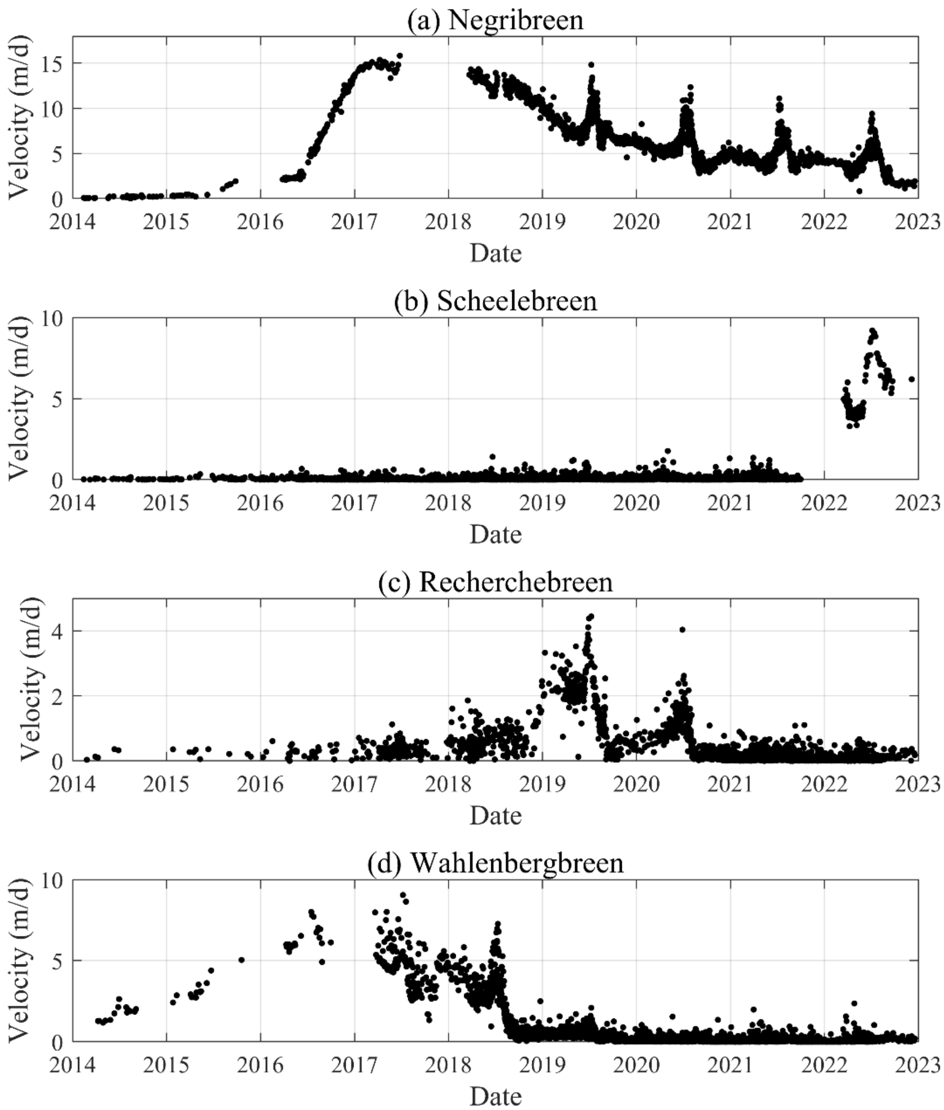

Figure 4 Velocity time series of selected surges that have taken place since 2014 at (a) Negribreen (78.57°N, 18.96°E), (b) Scheelebreen (77.75°N, 17.03°E), (c) Recherchebreen (77.47°N, 14.73°E), and (d) Wahlenbergbreen (78.47°N, 14.20°E). Data taken from the ITS_LIVE velocity catalogue (Lei et al., 2022). All plots were taken from a point near the terminus of the glacier.

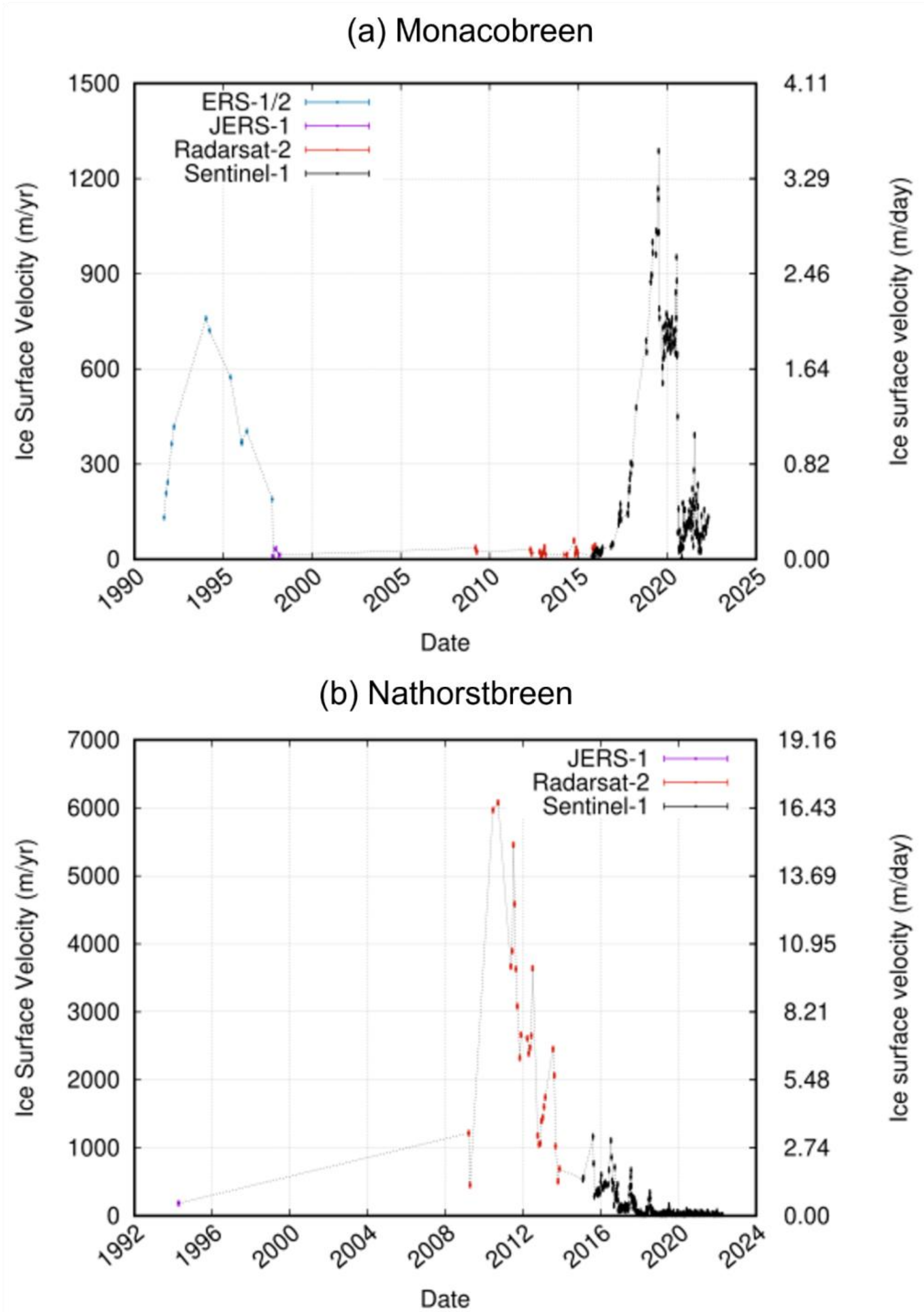

Figure 5 Velocity profiles of (a) Monacobreen (1990-2025; 79.50°N, 12.52°E) and (b) Nathorstbreen (1992-2024; 77.40°N, 16.22°E). All plots were taken from a point near the terminus of the glacier. These plots illustrate the availability of velocity data before and after the launch of the Copernicus Sentinel satellites.

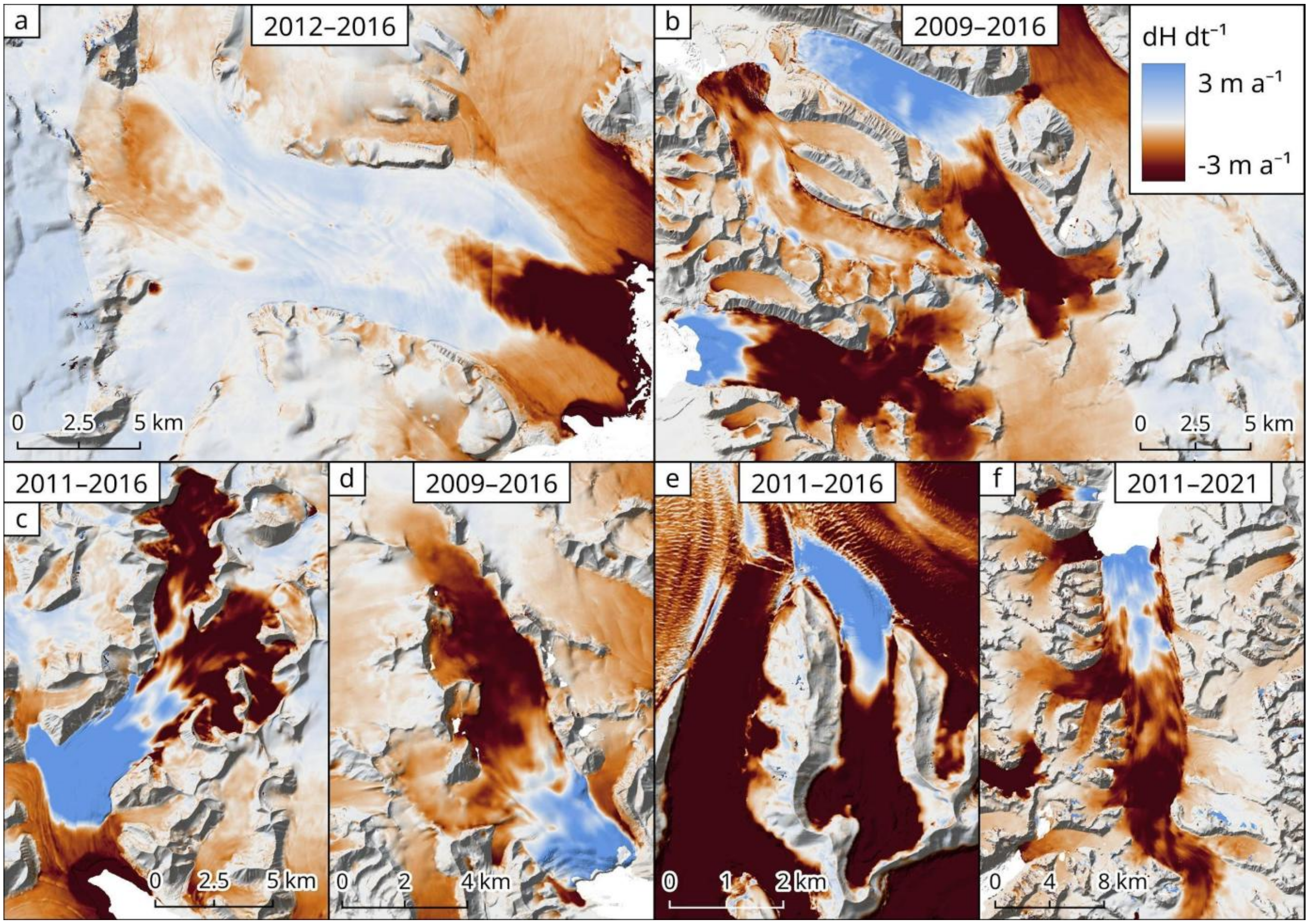

Figure 6 Elevation change rates (dH/dt) of surges in Svalbard: (a) Negribreen (78.57°N, 18.96°E), (b) Aavatsmarkbreen (bottom left; 78.71°N, 12.01°E) and Uvêrsbreen (top; 78.82°N, 12.23°E), (c) Moršnevbreen/Strongbreen (77.58°N, 17.55°E), (d) Esmarkbreen (78.31°N, 13.85°E), (e) Blankfjellbreen (tributary to Nathorstbreen; 77.27°N, 16.48°E), and (f) Monacobreen (center; 79.50°N, 12.52°E) and Emmabreen (top left; 79.55°N, 12.31°E). The maps were made by subtracting ArcticDEMs from the Norwegian Polar Institute 2008–2012 aerial image-derived DEMs. The background hillshade is from each respective ArcticDEM.

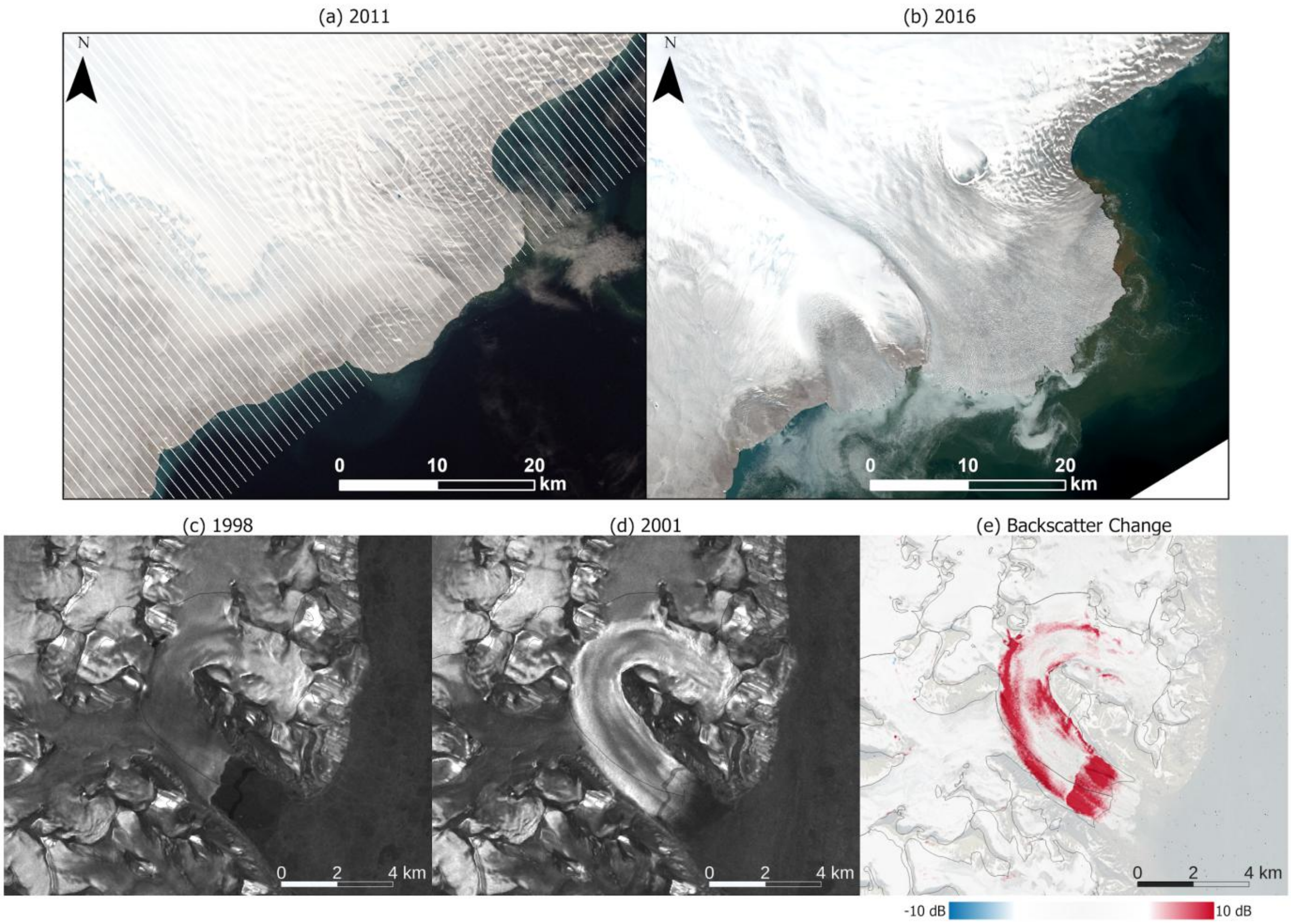

Figure 7 Surface conditions before and after a surge viewed from (a-b) optical and SAR (c-e) imagery. The optical true colour composite images show (a) a Landsat 7 scene of Basin-3 in Austfonna (79.42°N, 25.36°E) pre-surge and (b) a Landsat 8 image during its surge in 2016. ERS-1/2 average backscatter intensity images for descending orbits for data acquired between November and April from Ingerbreen (77.72°N, 18.16°E) are shown for (c) 1999 and (d) 2002, where the year marks the end of winter. Note the large increase in radar backscatter in panel (d), which is interpreted as increased crevassing (Kääb et al., 2023). (e) Radar backscatter change between the ERS-1/2 images.

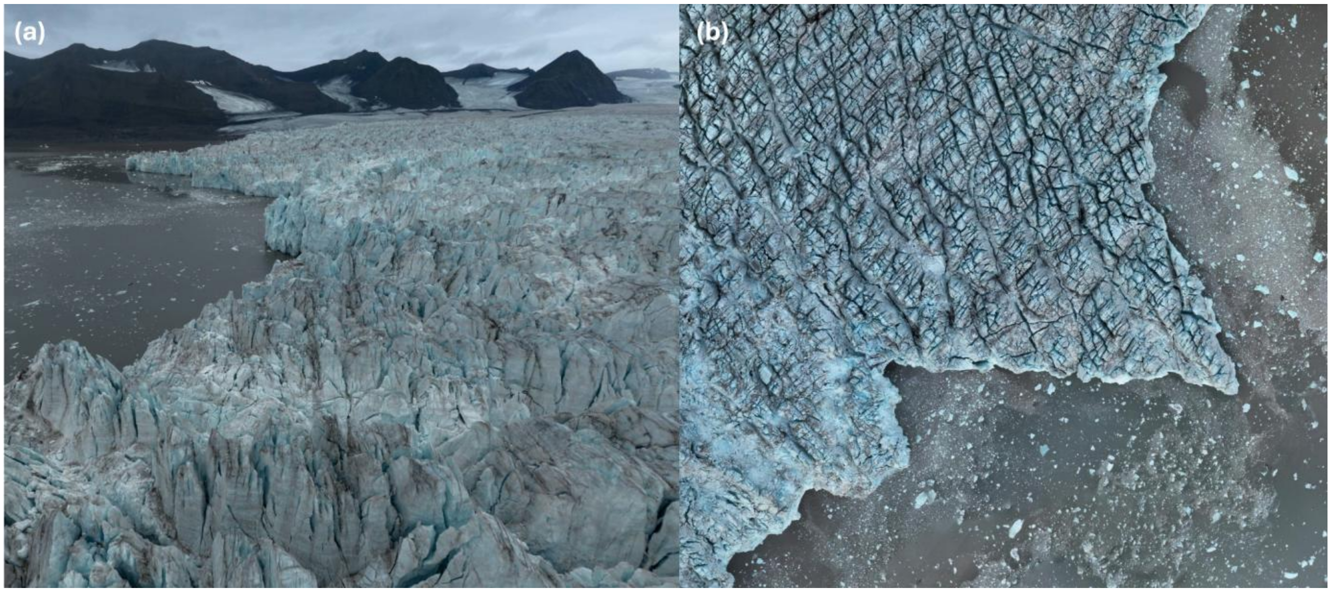

Figure 8 UAV imagery captured in (a) oblique and (b) nadir-looking geometry over Borebreen (78.42°N, 14.02°E) on 14th August 2024. Data taken from Hann et al. (2024).

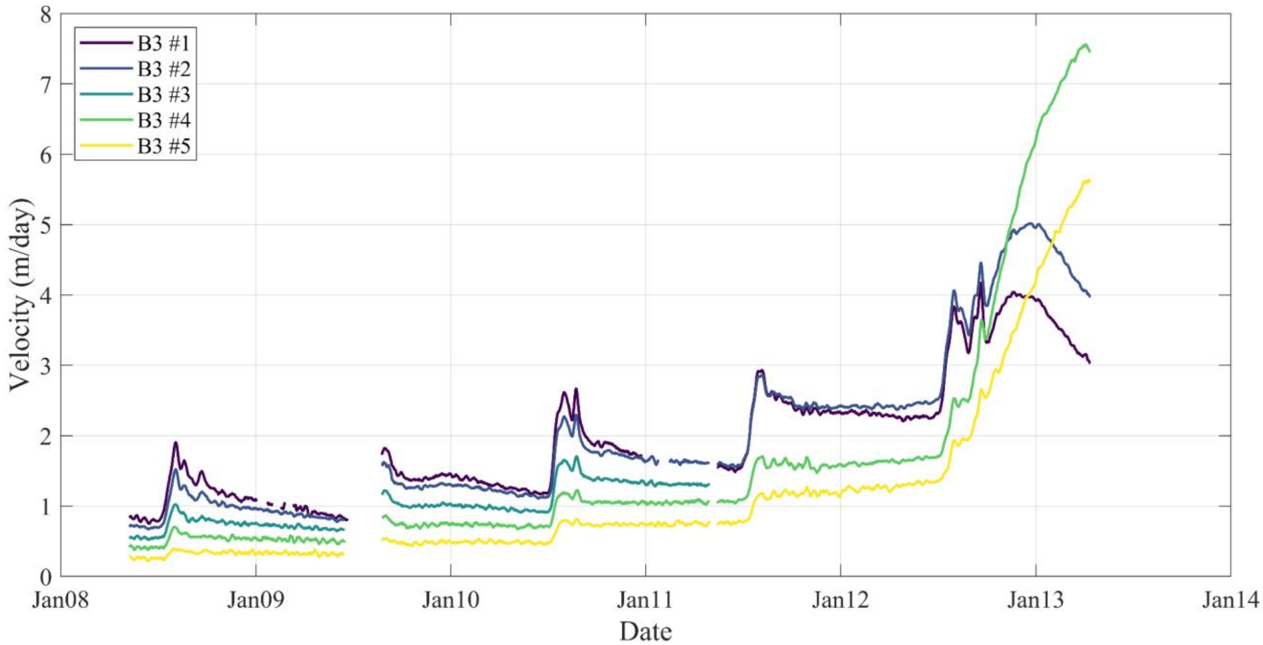

Figure 9 GNSS-derived flow velocities along the centreline of the fast-flow region of Basin-3, Austfonna (79.42°N, 25.36°E), between May 2008 and May 2013. GNSS stations are numbered from 1 at the lowest elevation to 5 at the highest. Data replotted from Dunse et al. (2015). Data credit: Torben Dunse.

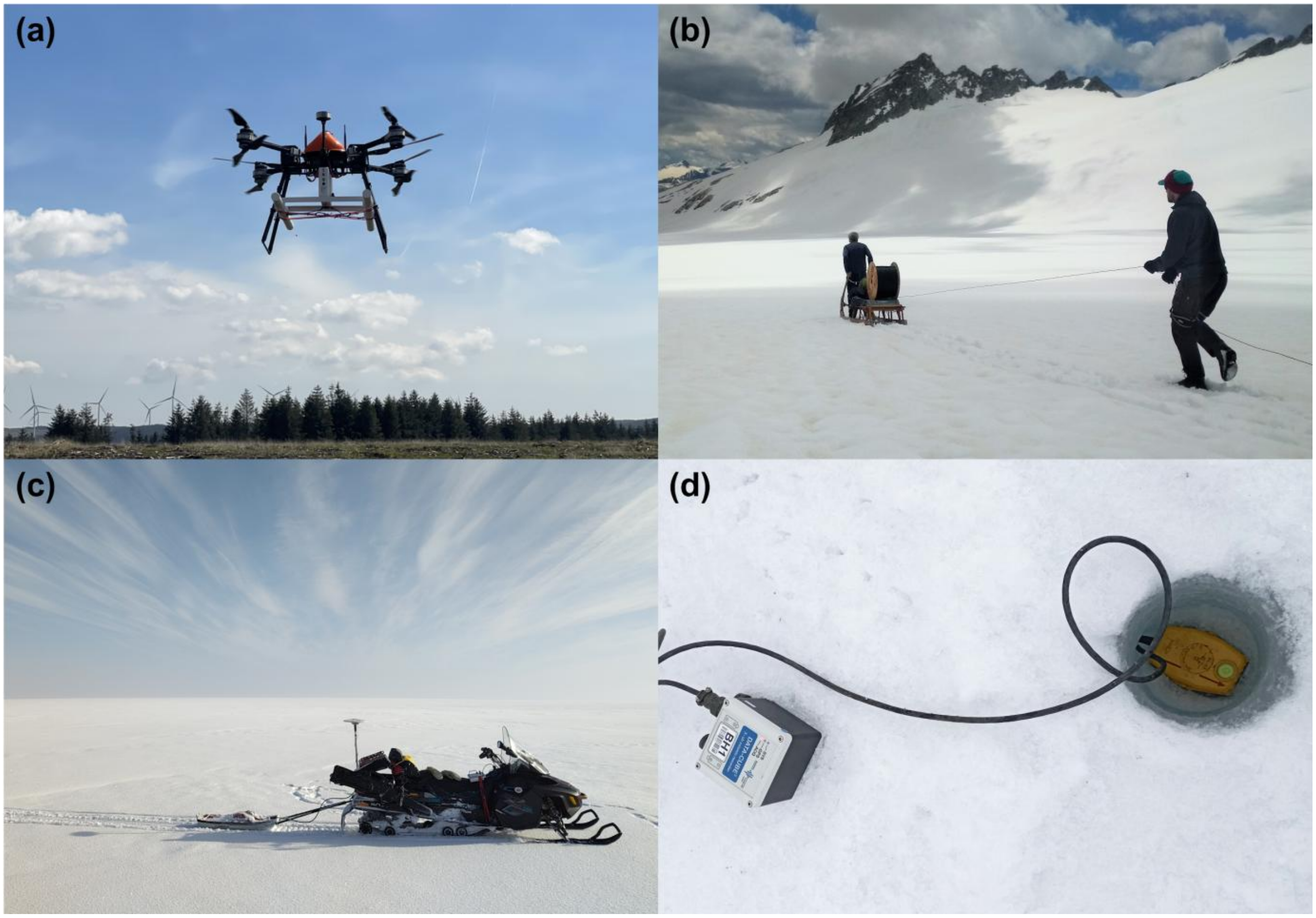

Figure 10 Examples of Ground Penetrating Radar (GPR) and seismic instruments in the field. (a) Airborne-GPR setup, GeoDrone 80MHz radar mounted on a Vulcan Harrier UAV flown in the Rhigos Mountains of South Wales, photo credit: Jon Walker (Swansea University); (b) A fibre-optic cable for Distributed Acoustic Sensing (DAS) being deployed on Rhônegletscher, Swiss Alps. The interrogator is located in the tent at the cable end. Photo by Wojciech Gajek; (c) Land-based GPR setup in Svalbard. The GNSS and radar unit are installed on the snowmobile while the antenna is towed behind it. Photo by Erik Mannerfelt; (d) Traditional seismological instrument: DIGOS DataCUBE recorder next to a 30cm deep borehole equipped with a 4.5 Hz 3-component geophone (to be enclosed with ice and snow) on Hansbreen, Svalbard. The DataCUBE is equipped with internal GNSS for time synchronisation and is powered with a pair of D20 batteries. Photo by Mateusz Olszewski.

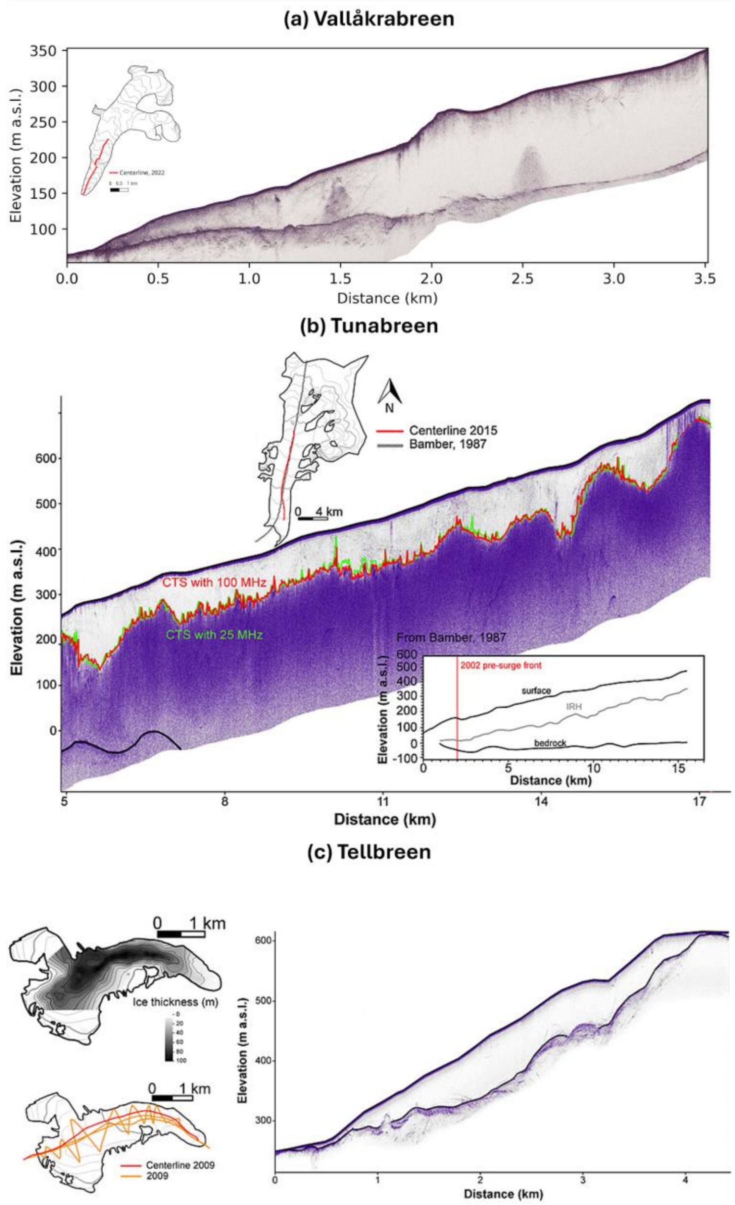

Figure 11 Examples of Ground Penetrating Radar (GPR) data collected for glaciers in Svalbard. (a) Survey over the surge bulge (at 2 km) of Vallåkrabreen (77.84°N, 17.08°E) collected in 2022 with a 100 MHz antenna. (b) Centerline radargram of Tunabreen (78.46°N, 17.41°E) collected in 2015 with a 100 MHz antenna. The top pick marks the glacier surface, while the bottom pick follows the bed reflector. The red line follows the Cold-Temperate transition Surface (CTS) picked on the data collected with the 100 MHz antenna, while the green line follows the CTS picked on data collected with the 25 MHz antenna along the same survey line. (c) Centreline radaragram collected in 2009 over Tellbreen (78.25°N, 16.20°E), corrected for elevation. The top pick marks the glacier surface, whilst the bottom pick follows the bed reflector. Panel (a) is an unpublished 2022 survey of Vallåkrabreen by Erik S. Mannerfelt. Panels (b) and (c) are from Sevestre et al. (2015).

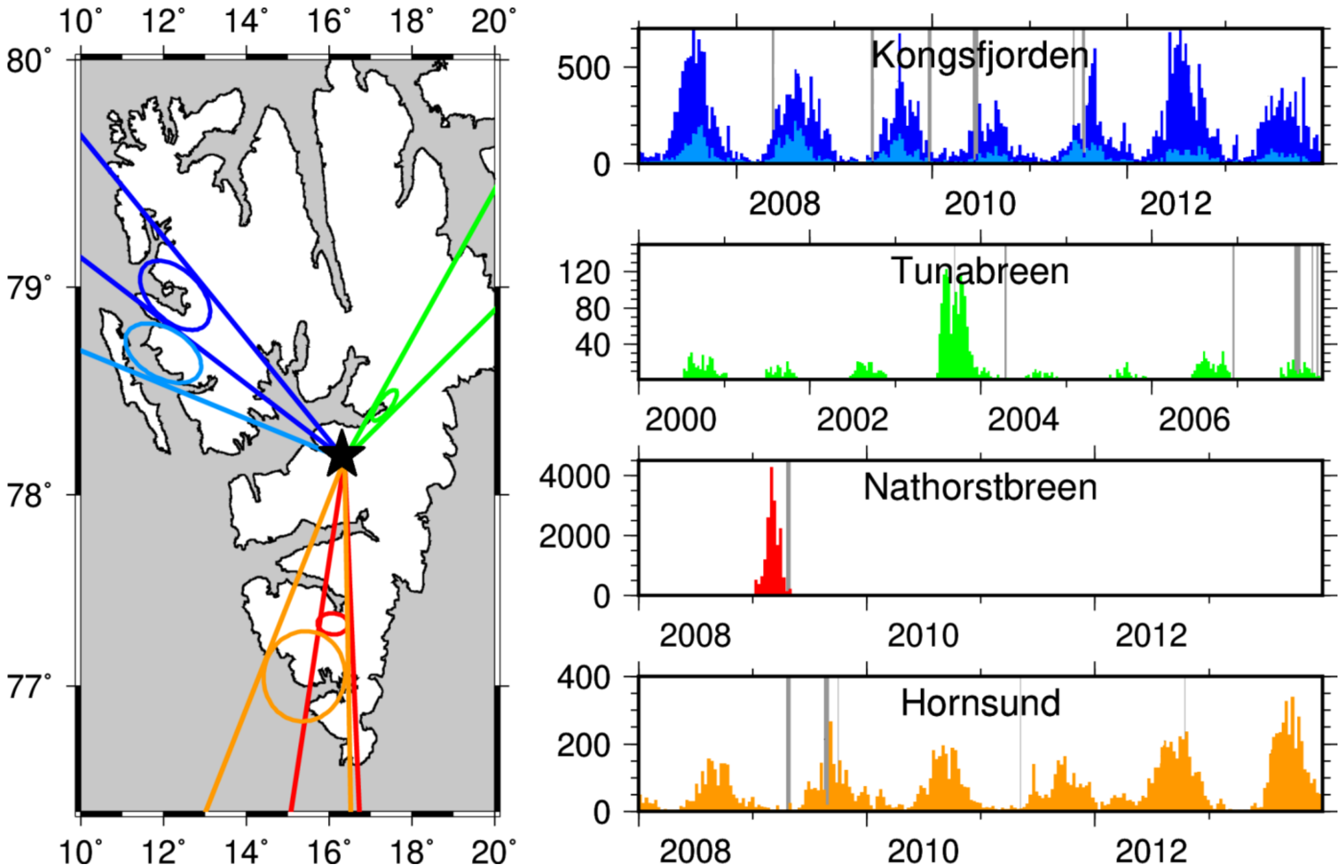

Figure 12 Temporal distribution of autonomous icequake detections obtained using regional seismic network stations. Lines and ellipses indicate individual source regions as seen in the data from the Spitsbergen seismic array (SPITS) marked as a black star. Temporal histograms present event counts per 10 days at each location. Light grey bars indicate days with data gaps. Seasonal temporal patterns at Kongsfjorden, Tunabreen and Hornsund are the result of glacier calving variability. High seismic activity at Nathorstbreen (2009; 77.27°N, 16.48°E) and Tunabreen (2003; 78.46°N, 17.41°E) was related to glacier surges. Modified from Köhler et al. (2015).

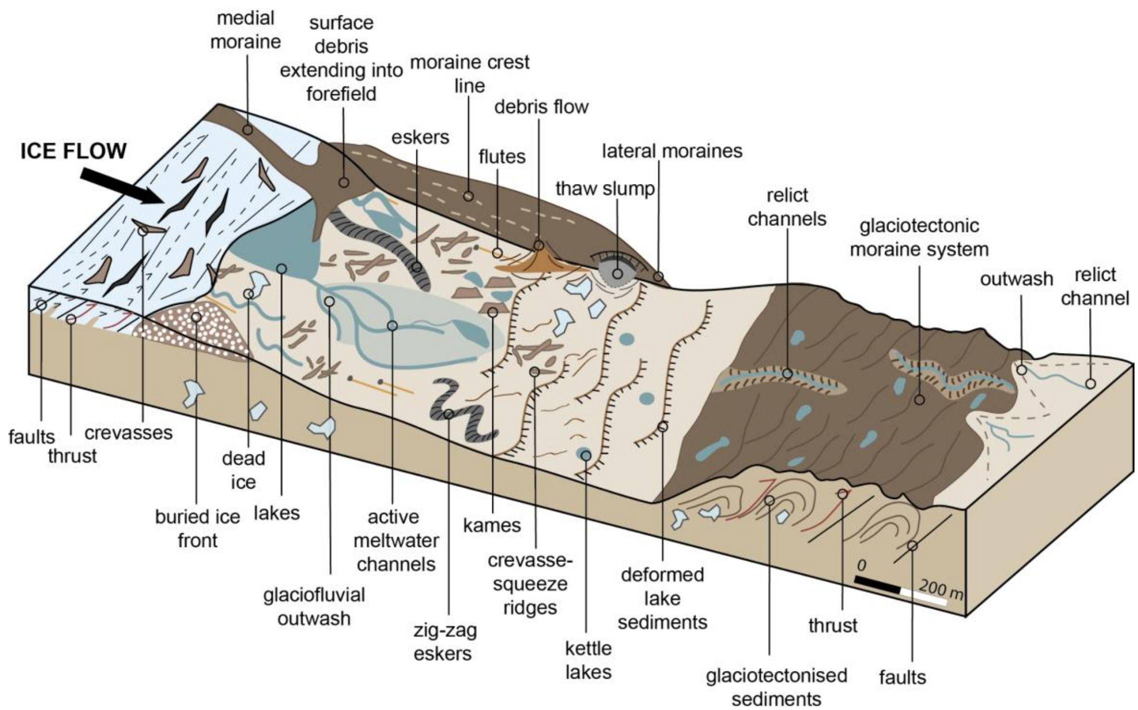

1771

1772 **Figure 13** Land-terminating surge-type glacier landsystem (from McCerery et al., 2025).

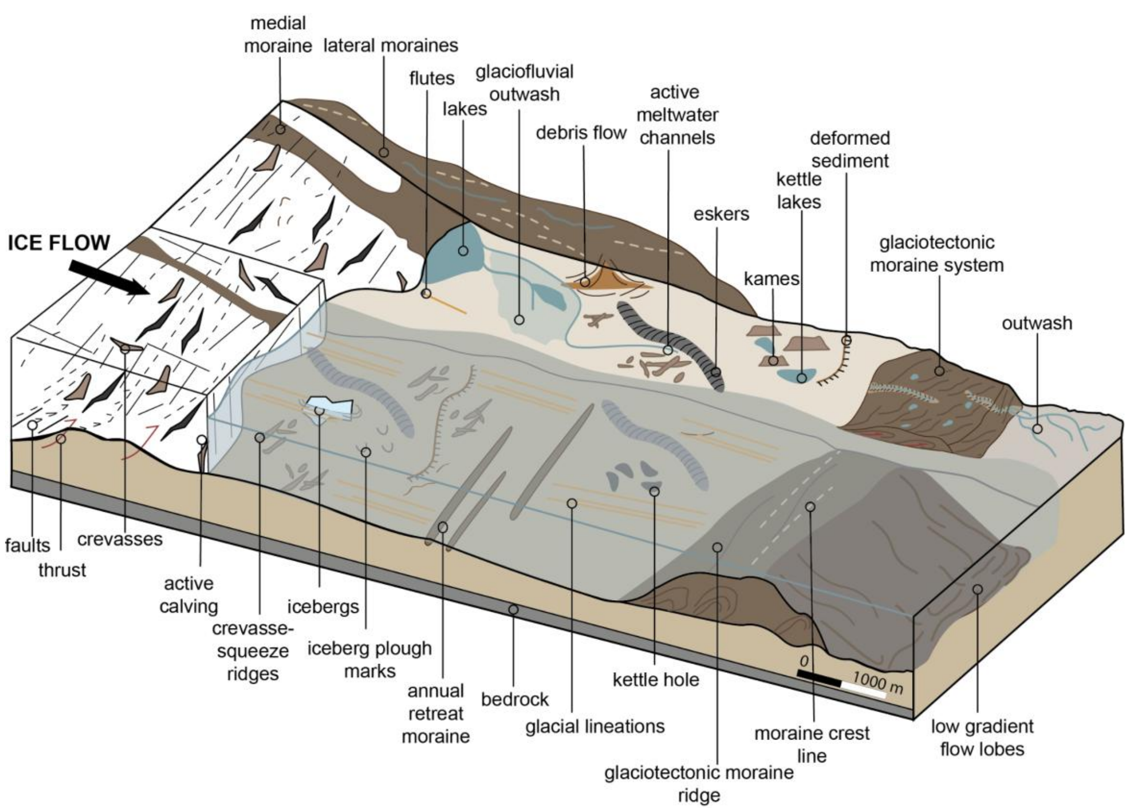

1773

1774 **Figure 14** Marine-terminating surge-type glacier landsystem (from McCerery et al., 2025). Note the
1775 fjord-adjacent terrestrial component where the surge extended on land (e.g. Aradóttir et al., 2019).

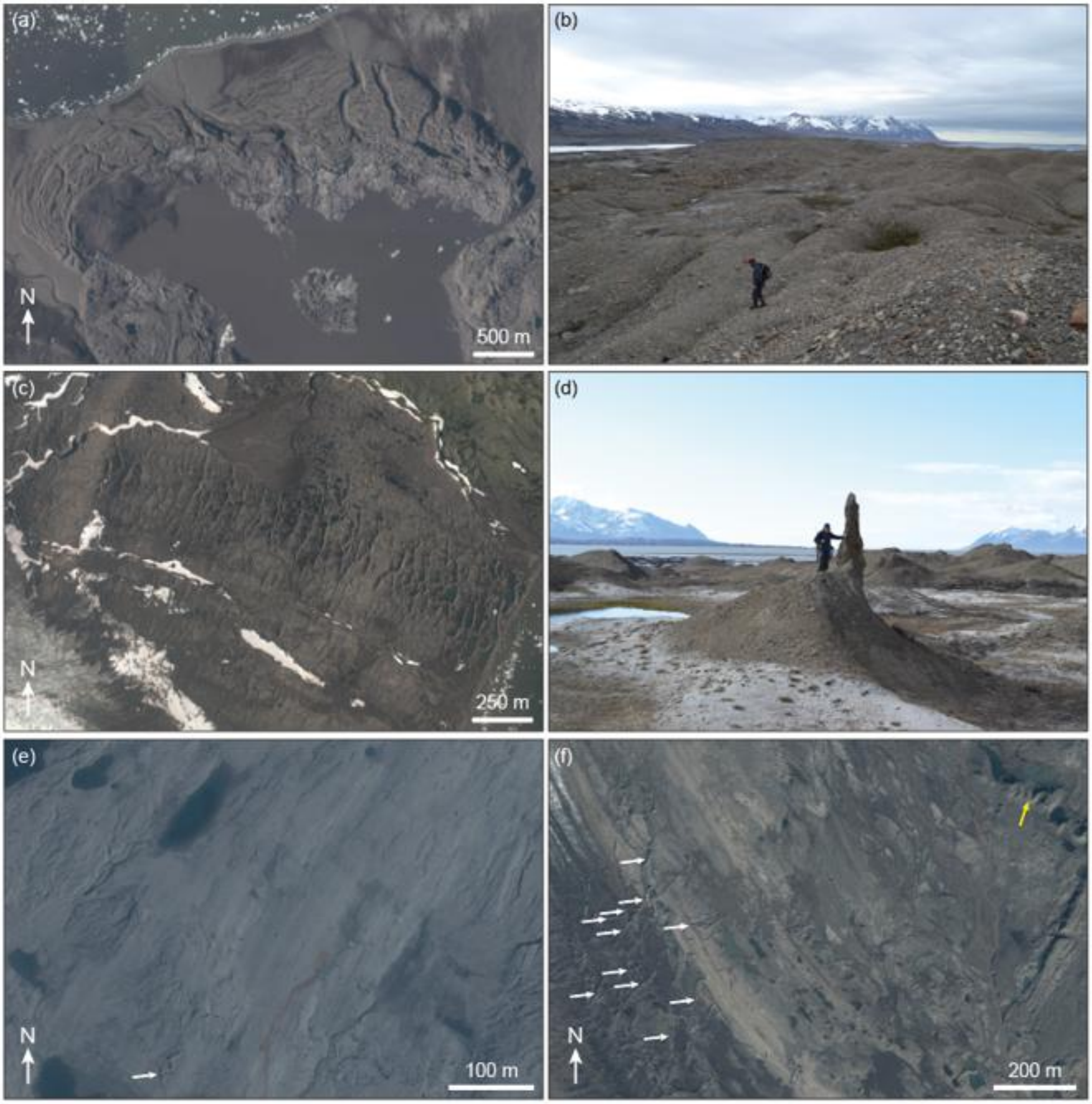

Figure 15 Surge landforms present at terrestrial glacier margins. (a) Glaciotectonic moraine system at Penckbreen (77.49°N, 15.61°E). Note the smooth surface of the moraine system compared to the rest of the exposed foreland, the multiple ridge crests oriented perpendicular to glacier flow (broadly from S to N), the channels cut through the ridges, and the large proglacial lake. Aerial photograph captured by Norwegian Polar Institute (NPI) in 2011 and accessed via TopoSvalbard (toposvalbard.npolar.no). (b) Photograph captured in 2012 looking west across the Penckbreen moraine system, with part of the proglacial lake visible in the left distance. Note the relatively homogenous gravel-sized surface sediment cover, which gives the smooth surface appearance seen in (a). Photo by Harold Lovell. (c)

Crevasse-squeeze ridge (CSR) network exposed in front of Pettersenbreen (77.48°N, 23.43°E). Note the cross-cutting ridges oriented perpendicular and sub-perpendicular to ice flow (broadly from NW to SE), mimicking surface crevasse patterns. Aerial photograph captured by NPI in 2011 and accessed via TopoSvalbard (toposvalbard.npolar.no). (d) Photograph captured in 2012 of pinnacle-like CSR on Nathorstbreen's Nordre Nathorstmorenen (77.50°N, 16.13°E). Note other CSRs visible in the background. Photo by Harold Lovell. (e) Flutes in front of Elisebreen (78.62°N, 12.09°E). Ice flow was broadly from NE to SW, parallel to flute orientation. Note the cross-cutting meandering ridges and ridges oriented perpendicular to ice flow, interpreted by Christoffersen et al. (2005) as infilled basal meltwater conduits and CSR, respectively. A zig-zag esker can also be seen in the centre-left at the bottom of the image (white arrow). Aerial photograph captured by NPI in 2011 and accessed via TopoSvalbard (toposvalbard.npolar.no). (f) Geometric ridge networks (bottom left of image, white arrows) in front of Hørbyebreen (78.75°N, 16.35°E) interpreted as CSRs and zig-zag eskers by Evans et al. (2022). Ice flow was broadly from NW to SE. Note the sinuous esker in the top right of the image (yellow arrow). Aerial photograph captured by NPI in 2011 and accessed via TopoSvalbard (toposvalbard.npolar.no).

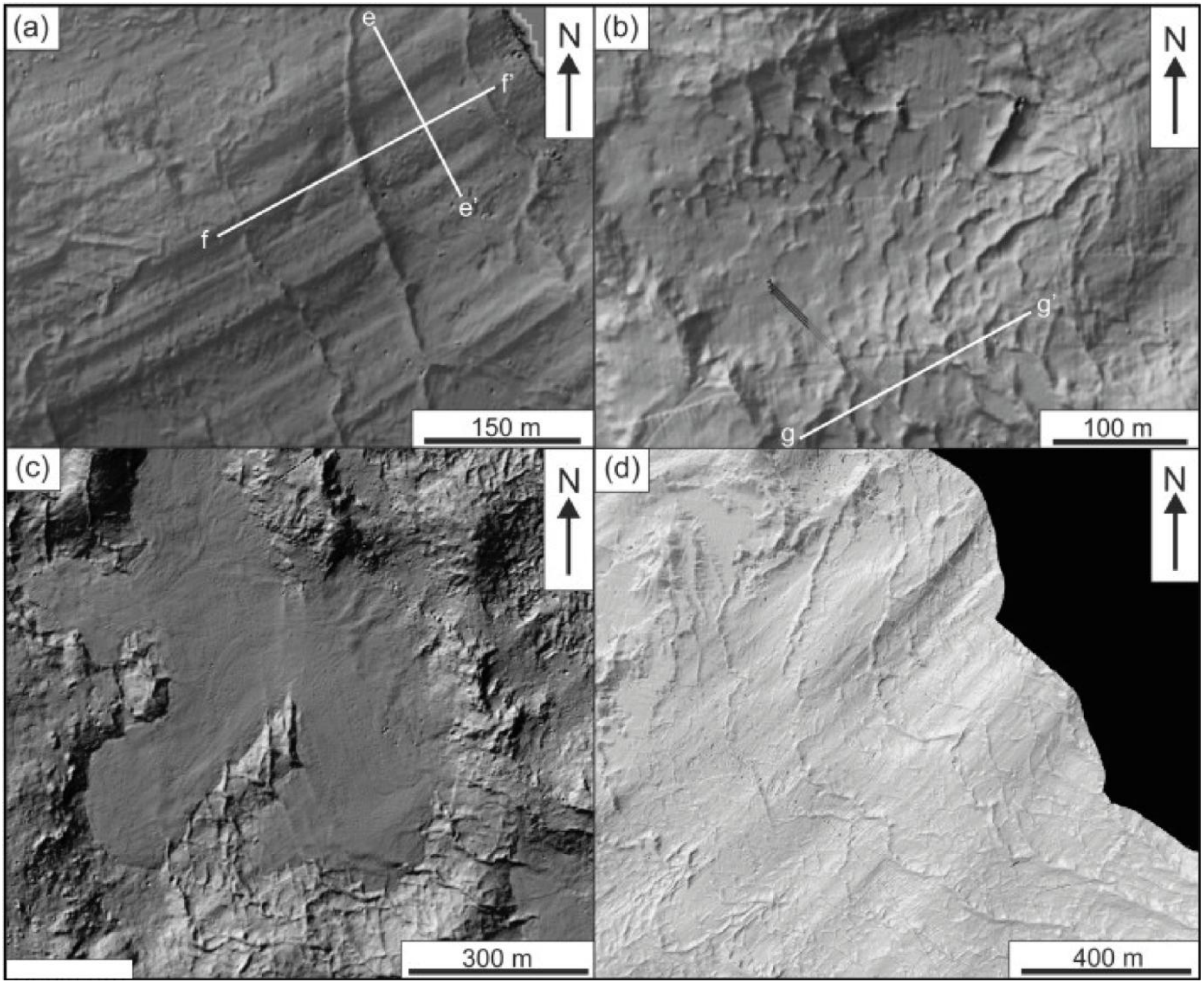

Figure 16 Examples of seafloor surge landforms in Tempelfjorden in front of Tunabreen (78.43°N, 17.31°E) from Flink et al. (2015) at ~40 m depth. (a) Glacial lineations; (b) Crevasse-squeeze ridges (CSRs); (c) Debris-flow lobe covering older CSRs. (d) Annual retreat moraines.

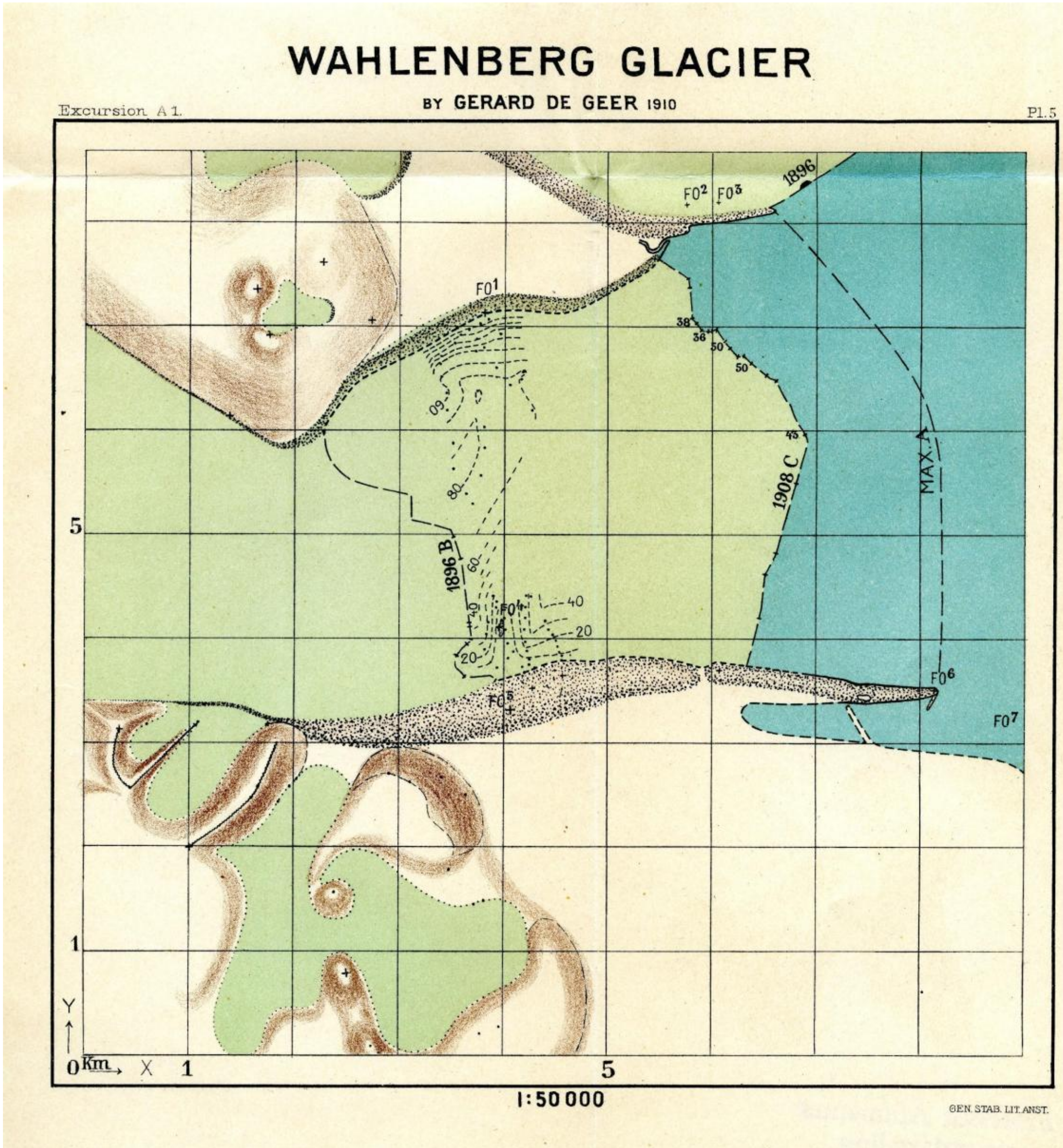

Figure 17 Historical map of the Wahlenbergbreen terminus (78.47°N, 14.20°E) from repeat mapping in the early 1900s (de Geer, 1910). An outline from their previous expedition in 1896 is drawn 3–4 km behind the 1908 terminus position, indicating an ongoing surge that is also visible through extensive crevassing in photographs from the latter year.

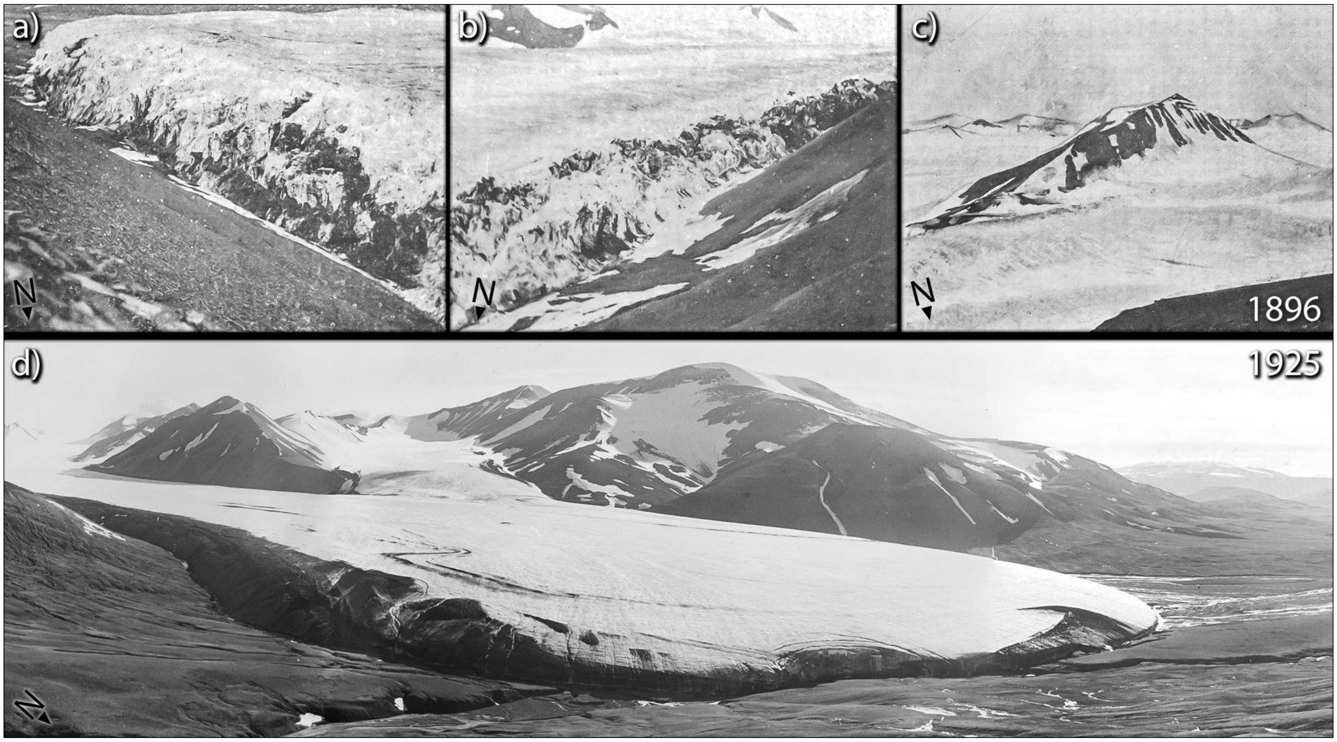

Figure 18 Historical photographs from Drønbreen (78.13°N, 18.82°E), central Svalbard, indicating a surge around 1896 (a-c) and subsequent quiescence in 1925 (d). Photographs (a-c) are from Garwood and Gregory (1898), and (d) taken by Adolf Hoel, kept at the Norwegian Polar Institute (NPI) library.

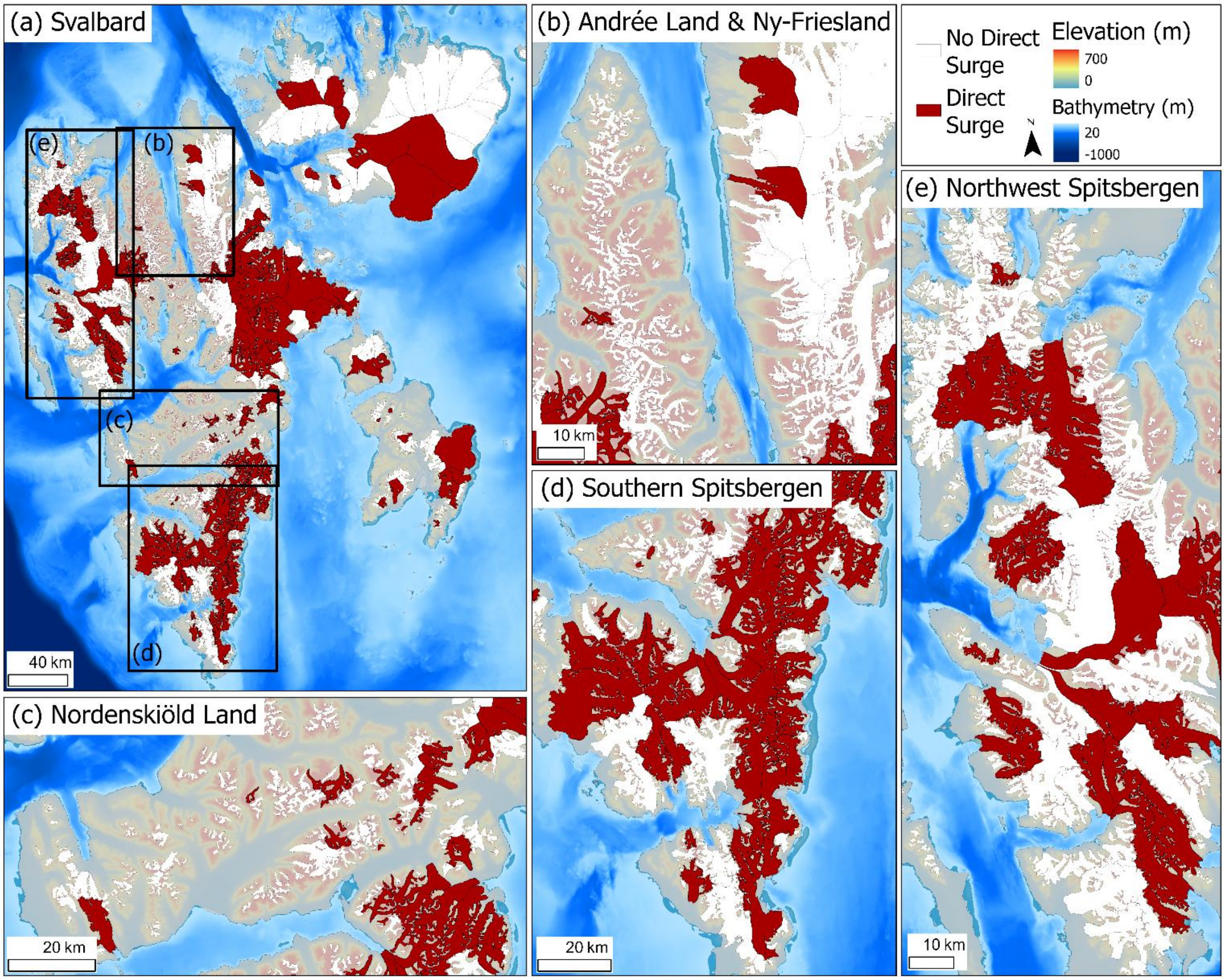

Figure 19 (a) Spatial distribution of glaciers directly observed to surge in Svalbard (red). Regions consisting of several small glaciers are expanded for (b) Andrée Land & Ny Friesland, (c) Nordenskiöld Land, (d) Southern Spitsbergen, and (e) Northwest Spistbergen. Bathymetry data is taken from the International Bathymetric Chart of the Arctic Ocean (IBCAO) (Jakobsson et al., 2024).

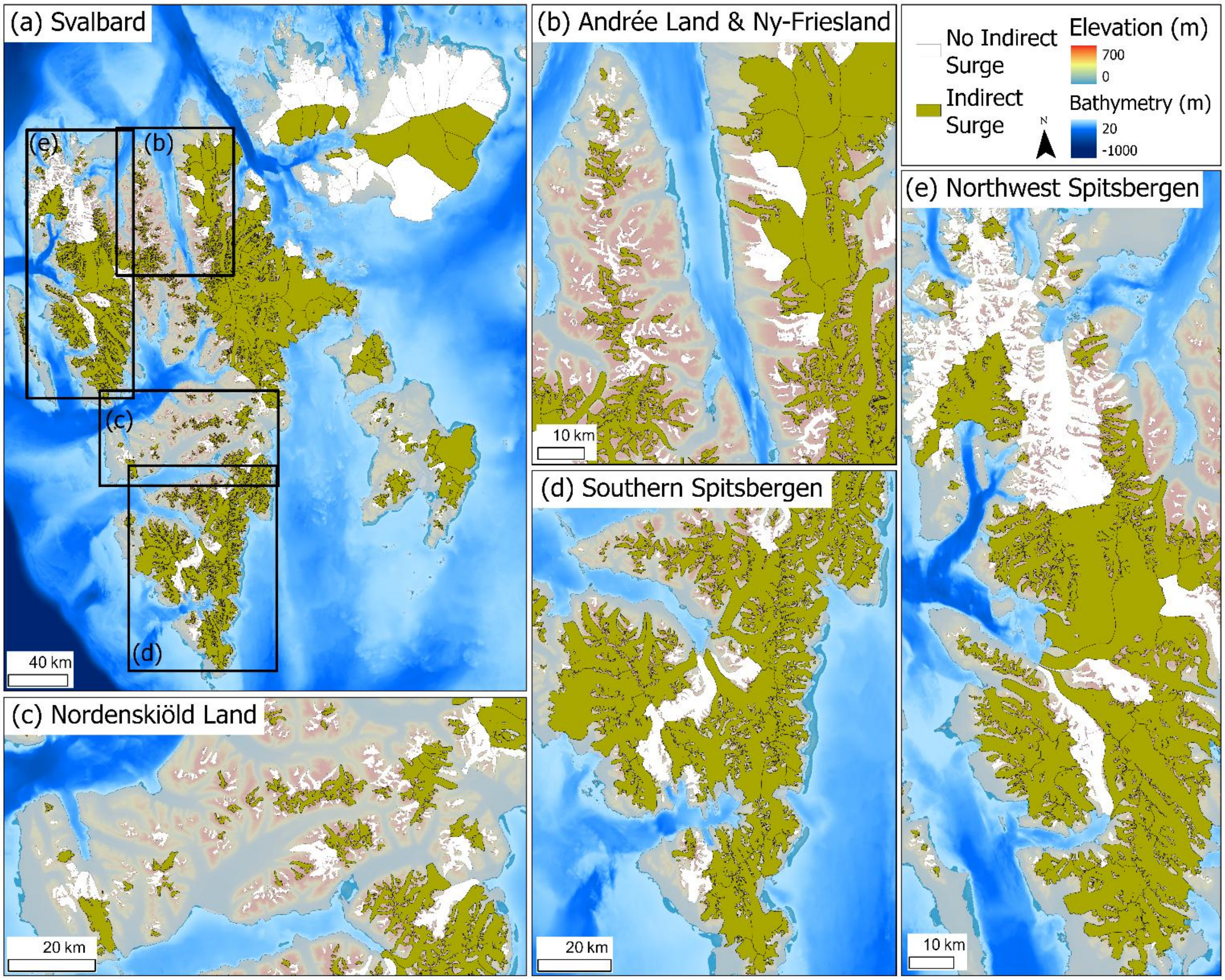

Figure 20 (a) Spatial distribution of glaciers indirectly (e.g. landforms, historical records) observed to surge in Svalbard (brown). Regions consisting of several small glaciers are expanded for (b) Andrée Land & Ny Friesland, (c) Nordenskiöld Land, (d) Southern Spitsbergen, and (e) Northwest Spistbergen. Bathymetry data is taken from the International Bathymetric Chart of the Arctic Ocean (IBCAO) (Jakobsson et al., 2024).

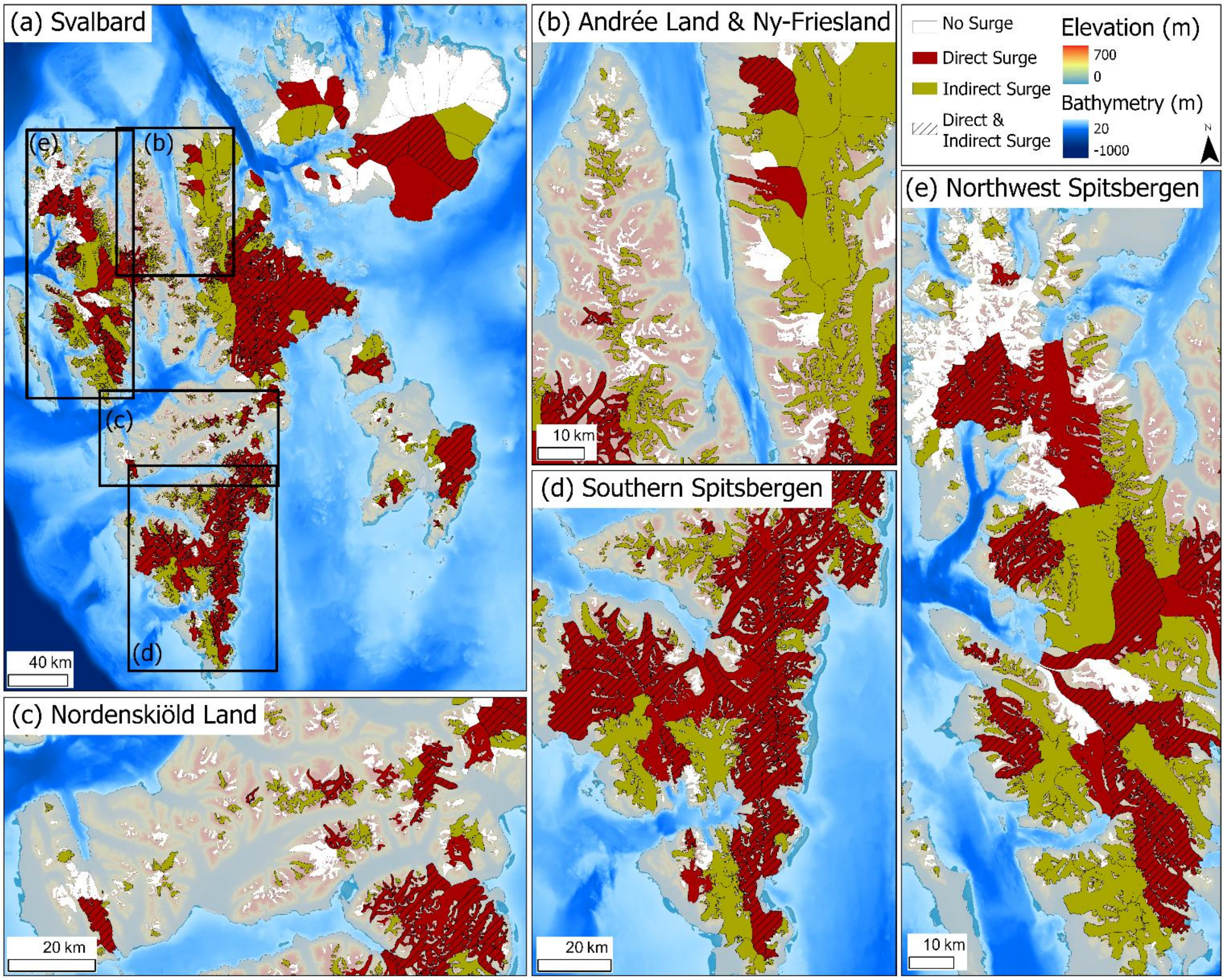

Figure 21 (a) Spatial distribution of all glaciers directly (red) and indirectly (brown) observed to surge in Svalbard. Glaciers that have been directly and indirectly observed to surge are rendered with hatching across their catchments. Regions consisting of several small glaciers are expanded for (b) Andrée Land & Ny Friesland, (c) Nordenskiöld Land, (d) Southern Spitsbergen, and (e) Northwest Spistbergen. Bathymetry data is taken from the International Bathymetric Chart of the Arctic Ocean (IBCAO) (Jakobsson et al., 2024).

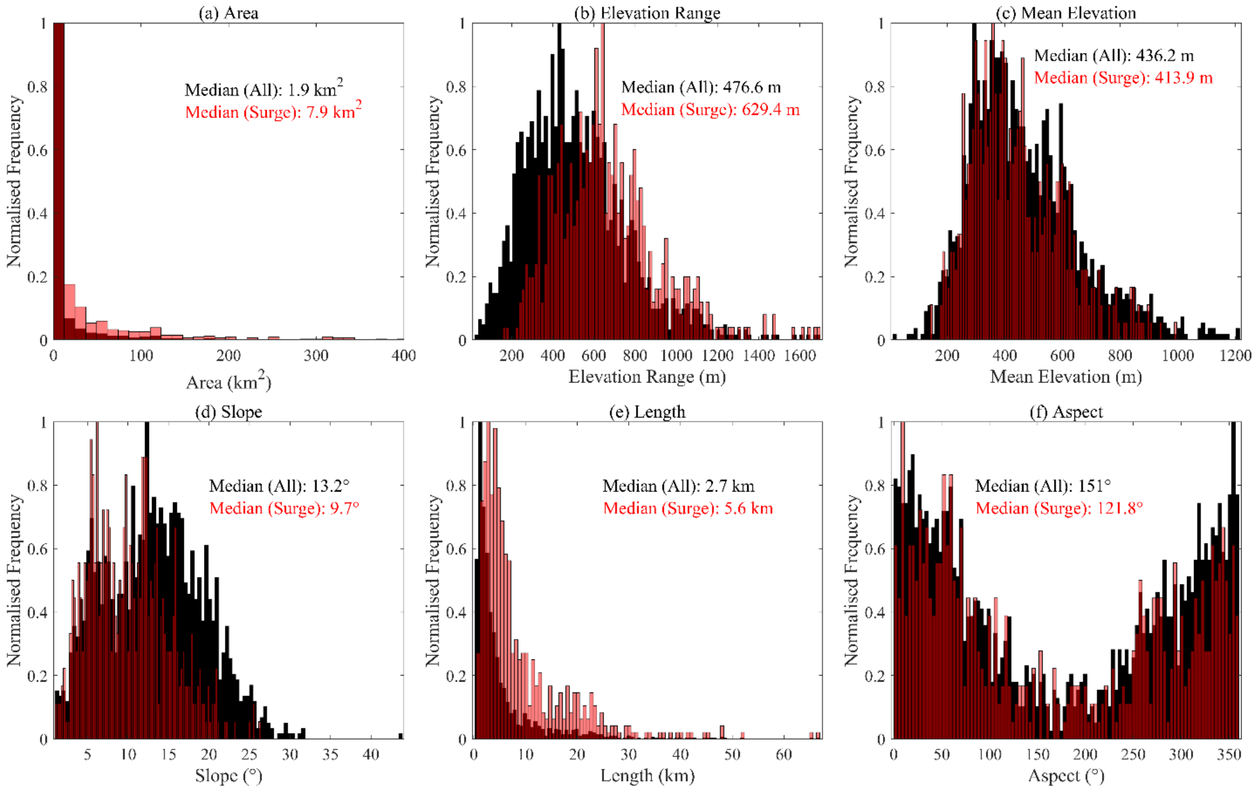

Figure 22 The characteristics of glaciers directly observed to surge (red) and all glaciers in Svalbard (black), including (a) area (km^2), (b) elevation range (m), (c) mean elevation (m), (d) Slope (°), (e) length (m), and (f) aspect (°). The glacier characteristics are taken from the RGI7.0 database.

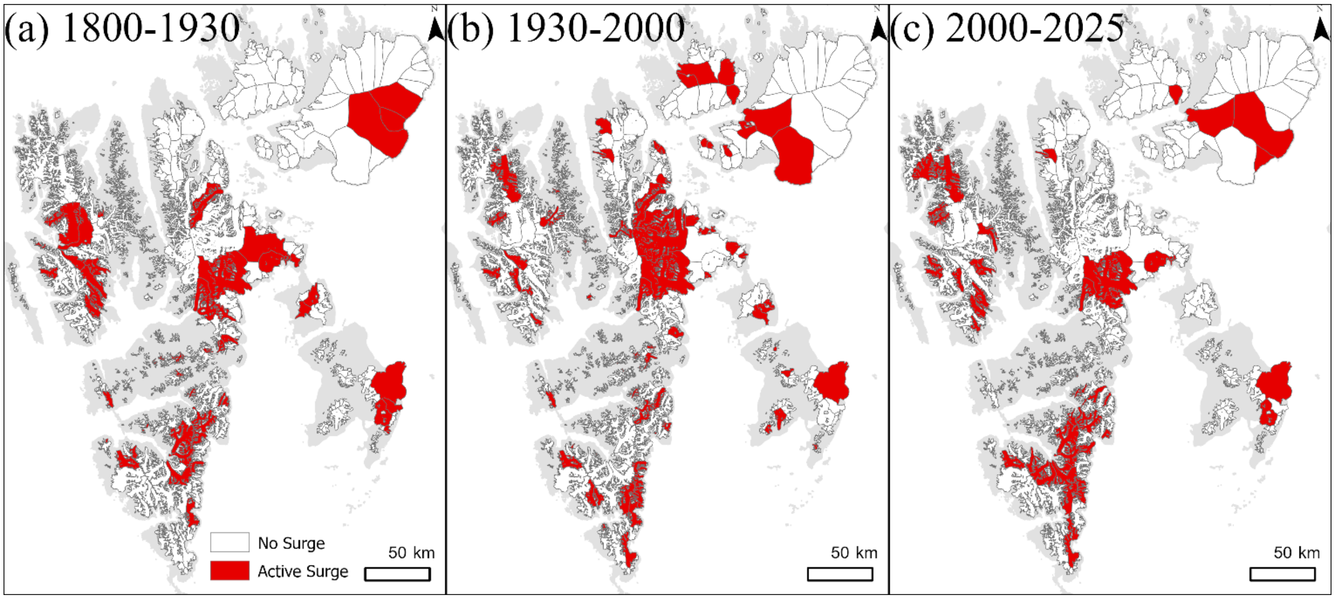

Figure 23 Glaciers with evidence of active surging for differing epochs: (a) 1800-1930, (b) 1930-2000, and (c) 2000-2025 based on available, but likely incomplete, data. Active surges are shown in red.

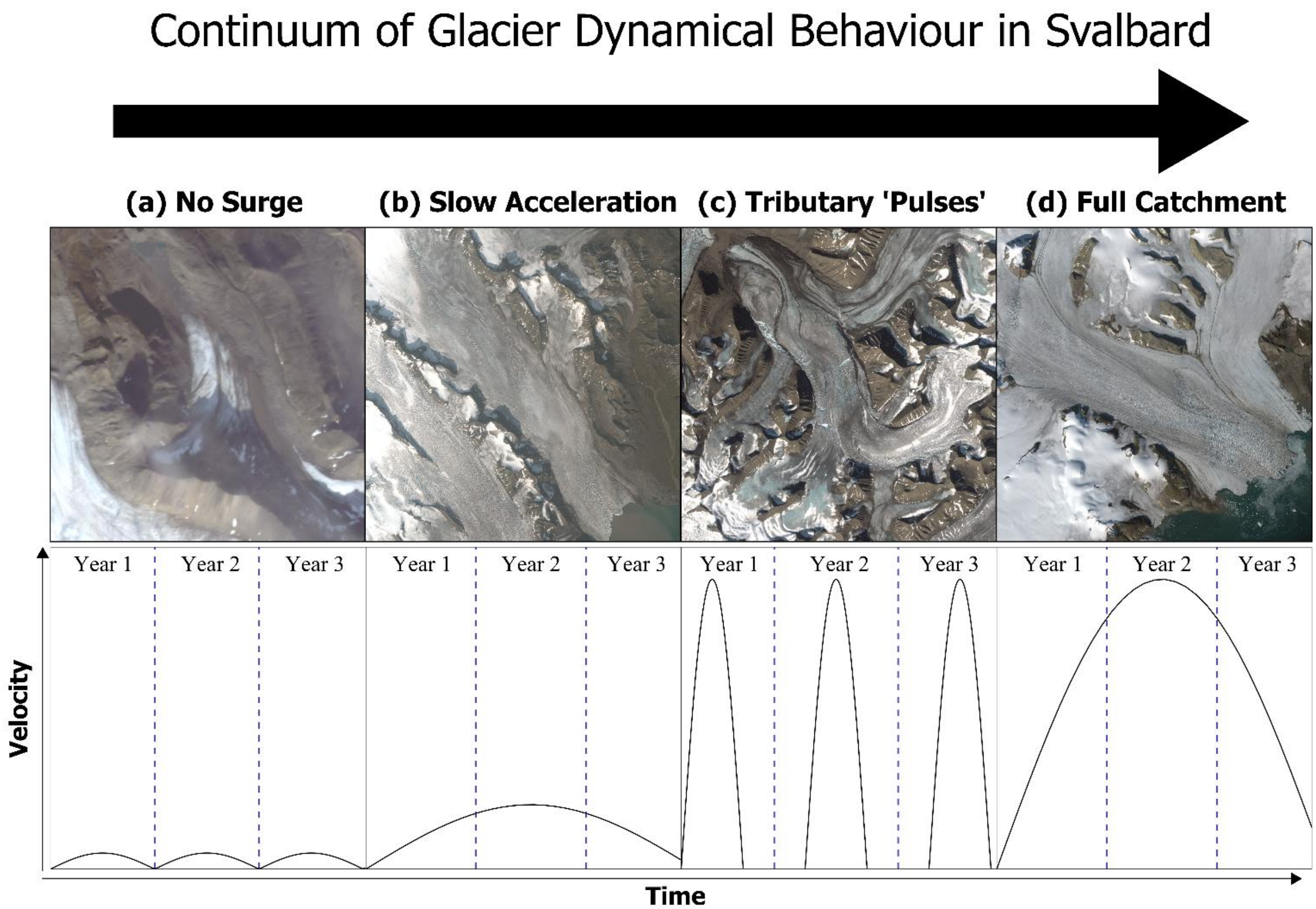

Figure 24 The continuum of glacier dynamical behaviour in Svalbard, consisting of two end-members, glaciers that do not surge and those that undergo full-catchments surges. In the top row, Landsat 8 optical images of representative glaciers are presented, and in the bottom row, illustrative velocity profiles are shown over three years, with each year demarcated by a dashed line. The surge behaviours shown here are just a collection of a wider set of behaviours observed in Svalbard. (a) Small glaciers are typically cold-based and do not surge, hence they represent an end-member of this continuum. (b) Some glaciers undergo a 'slow acceleration' but do not fully surge (e.g. pictured Sveabreen). The timescale of this process will vary with glacier size, meltwater availability, and other local environmental factors. A three-year time series is presented here and has been observed at glaciers such as Hansbreen (see Figure 25e). (c) Moving along the continuum, glacier systems with several tributaries (e.g pictured Paulabreen) are characterised by 'Tributary Pulses'. In theory, these pulses may occur on all glaciers and not just those with several tributaries but given the long quiescence periods in Svalbard (40-150 years), this pulse-like behaviour has mostly been observed at the confluence of several glaciers. (d) A 'Full Catchment' surge represents an end-member type and has been observed at glaciers such as Negribreen (pictured). Again, the temporal period of the surge can be longer (or shorter).

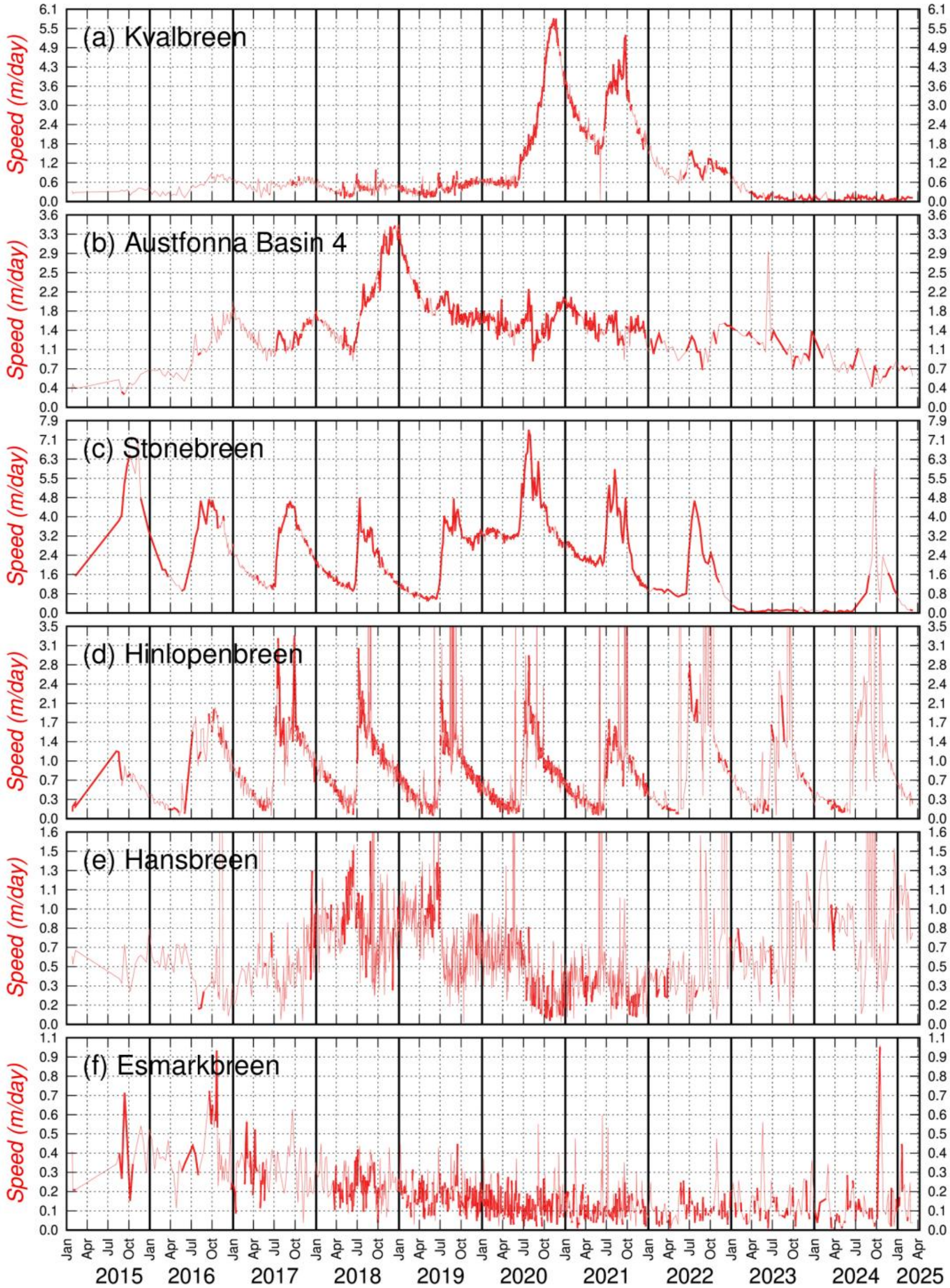

Figure 25 Velocity time series of glaciers in Svalbard from 2015 to 2025 (10 years), generated using Sentinel-1 feature-tracking. The time series demonstrates various surge-type behaviours ranging from: (a) Kvalbreen (77.56°N, 17.92°E; well defined surge), (b) Austfonna Basin-4 (79.62°N, 25.58°E; surge with marked speed-up), (c) Stonebreen (77.74°N, 23.97°E; seasonal cyclicity with a surge), (d) Hinlopenbreen (79.08°N, 18.99°E; seasonal cyclic behaviour), (e) Hansbreen (77.02°N, 15.63°E; low frequency multi-year cycles of fast and slow flow), and (f) Esmarkbreen (78.31°N, 13.85°E; apparent multi-year slowdown).

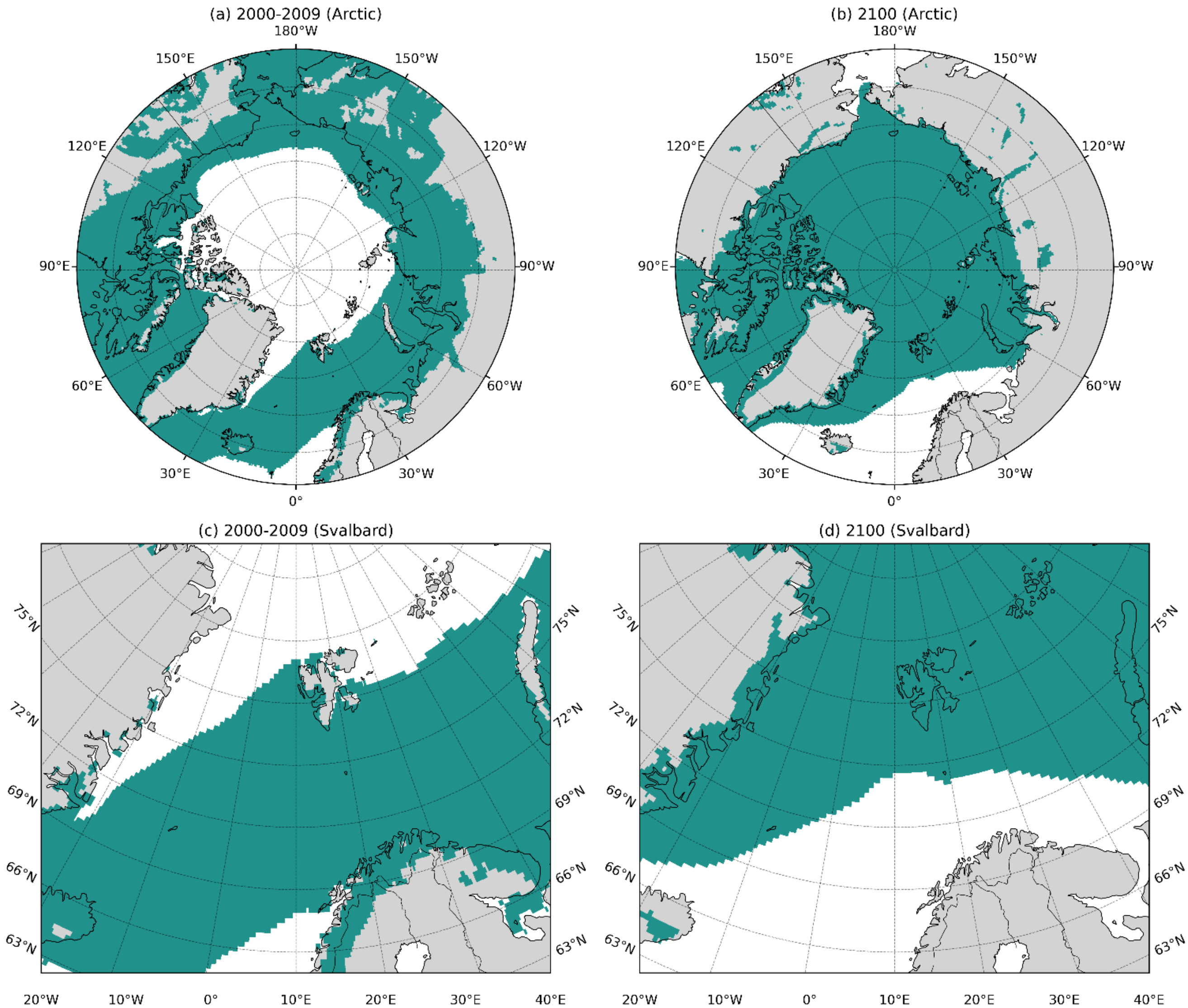

Figure 26 Climatic envelope (green) encapsulating surge-type glaciers, derived from Sevestre and Benn (2015) and calculated from ERA5 reanalysis data. The panels show the present-day climatic envelope across (a) the Arctic and (c) focused on Svalbard and the surrounding ocean. Also shown is the envelope simulated out to 2100 based on projections from Gutiérrez et al. (2021) for both (b) the Arctic and (d) Svalbard and the surrounding ocean.

References

Alexander, A., Kruusmaa, M., Tuhtan, J. A., Hodson, A. J., Schuler, T. V., Kääb, A. (2020a). Pressure and inertia sensing drifters for glacial hydrology flow path measurements. Cryosphere, 14, 1009-1023. https://doi.org/10.5194/tc-14-1009-2020

Alexander, A., Obu, J., Schuler, T.V., Kääb, A., Christiansen, H.H. (2020b). Subglacial permafrost dynamics and erosion inside subglacial channels driven by surface events in Svalbard, Cryosphere, 14, 4217-4231. https://doi.org/10.5194/tc-14-4217-2020

Aradóttir, N., Ingólfsson, Ó., Noormets, R., Benediktsson, Í.Ö., Ben-Yehoshua, D., Håkansson, L., Schomacker, A. (2019). Glacial geomorphology of Trygghamna, western Svalbard - Integrating terrestrial and submarine archives for a better understanding of past glacial dynamics. Geomorphology, 344, 75-89. https://doi.org/10.1016/j.geomorph.2019.07.007

Andreassen, K., Winsborrow, M.C.M., Bjarnadottir, L.R., Ruther, D.C. (2014). Ice stream retreat dynamics inferred from an assemblage of landforms in the northern Barents Sea, Quaternary Science Reviews, 92, 246-257. https://doi.org/10.1016/j.quascirev.2013.09.015

Aschwanden, A., Bueler, E., Khroulev, C., Blatter, H. (2012). An enthalpy formulation for glaciers and ice sheets, Journal of Glaciology, 58, 441-457. https://doi.org/10.3189/2012JoG11J088

Aster, R. C., Winberry, J. P. (2017). Glacial seismology. Reports on Progress in Physics, 80, 126801. https://doi.org/10.1088/1361-6633/aa8473

Bælum, K., Benn, D. I. (2011). Thermal structure and drainage system of a small valley glacier (Tellbreen, Svalbard), investigated by ground penetrating radar. Cryosphere, 5, 139-149. https://doi.org/10.5194/tc-5-139-2011

Bahr, D.B., Pfeffer, W.T., Kaser, G. (2015). A review of volume-area scaling of glaciers, Review of Geophysics, 53, 95-140. https://doi.org/10.1002/2014RG000470

Bamber, J.L. (1989). Ice/bed interface and englacial properties of Svalbard ice masses deduced from airborne radio echo-sounding data, Journal of Glaciology, 35, 30-37. https://doi.org/10.3189/002214389793701392

Barrett, B. E., Murray, T., Clark, R., Matsuoka, K. (2008). Distribution and character of water in a surge-type glacier revealed by multifrequency and multipolarization ground-penetrating radar. Journal of Geophysical Research: Earth Surface, 113. https://doi.org/10.1029/2007JF000972

Bartholomaus, T. C., Larsen, C. F., O'Neel, S., West, M. E. (2012). Calving seismicity from iceberg–sea surface interactions. Journal of Geophysical Research: Earth Surface, 117. https://doi.org/10.1029/2012JF002513

Bartholomaus, T.C., Amundson, J.M., Walter, J.I., O'Neel, S., West, M.E., Larsen, C. F. (2015). Subglacial discharge at tidewater glaciers revealed by seismic tremor, Geophysical Research Letters, 42, 6391–6398. https://doi.org/10.1002/2015GL064590

Barzycka, B., Błaszczyk, M., Grabiec, M., Jania, J. (2019). Glacier facies of Vestfonna (Svalbard) based on SAR images and GPR measurements. Remote Sensing of Environment, 221, 373-385. https://doi.org/10.1016/j.rse.2018.11.020

Barzycka, B., Grabiec, M., Błaszczyk, M., Ignatiuk, D., Laska, M., Hagen, J.O., Jania, J. (2020). Changes of glacier facies on Hornsund glaciers (Svalbard) during the decade 2007-2017, Remote Sensing of Environment, 251, 1-22. https://doi.org/10.1016/j.rse.2020.112060

Ben-Yehoshua, D., Aradóttir, N., Farnsworth, W.R., Benediktsson, Í.Ö., Ingólfsson, Ó. (2023). Formation of crevasse-squeeze ridges at Trygghamma, Svalbard, Earth Surface Processes and Landforms, 48, 2334-2348. https://doi.org/10.1002/esp.5631

Benn, D.I., Kristensen, L., Gulley, J.D. (2009). Surge propagation constrained by a persistent subglacial conduit, Bakaninbreen-Paulabreen, Svalbard, Annals of Glaciology, 50, 81-86. https://doi.org/10.3189/172756409789624337

Benn, D.I., Fowler, A.C., Hewitt, I., Sevestre, H. (2019a). A general theory of glacier surges, Journal of Glaciology, 65, 701-716. https://doi.org/10.1017/jog.2019.62

Benn, D.I., Jones, R.L., Luckman, A., Fürst, J.J., Hewitt, I., Sommer, C. (2019b). Mass and enthalpy budget evolution during the surge of a polythermal glacier: A test of theory, Journal of Glaciology, 65, 717-731. https://doi.org/10.1017/jog.2019.63

Benn, D.I., Hewitt, I.J., Luckman, A.J. (2022). Enthalpy balance theory unifies diverse glacier surge behaviour, Annals of Glaciology, 63, 88-94. https://doi.org/10.1017/aog.2023.23

Bennett, M. R., Hambrey, M. J., Huddart, D., Ghienne, J. F. (1996). The formation of a geometrical ridge network by the surge-type glacier Kongsvegen, Svalbard. Journal of Quaternary Science: Published for the Quaternary Research Association, 11(6), 437-449. https://doi.org/10.1002/(SICI)1099-1417(199611/12)11:6<437::AID-JQS269>3.0.CO;2-J

Bevan, S., Luckman, A., Murray, T., Sykes, H., Kohler, J. (2007). Positive mass balance during the late 20th century on Austfonna, Svalbard, revealed using satellite radar interferometry, Annals of Glaciology, 46, 117-122. https://doi.org/10.3189/172756407782871477

Bintanja, R. (2018). The impact of Arctic warming on increased rainfall, Scientific Reports, 8, 16001. https://doi.org/10.1038/s41598-018-34450-3

Bjarnadóttir, L.R., Winsborrow, M.C.M, Andreassen, K. (2014). Deglaciation of the central Barents Sea, Quaternary Science Reviews, 92, 208-226, https://doi.org/10.1016/j.quascirev.2013.09.012

Björnsson, H., Gjessing, Y., Hamran, S-E., Hagen, J.O., Liestøl, O., Pálsson, F., Erlingsson, B. (1996). The thermal regime of sub-polar glaciers mapped by multi-frequency radio-echo sounding, Journal of Glaciology, 42, 23-32. https://doi.org/10.3189/S0022143000030495

Błaszczyk, M., Jania, J.A., Ciepły, M., Grabiec, M., Ignatiuk, D., Kolondra, L., Kruss, A., Luks, B., Moskalik, M., Pastusiak, T., Strzelewicz, A., Walczowski, W., Wawrzyniak, T. (2021). Factors controlling terminus position of Hansbreen, a tidewater glacier in Svalbard, Journal of Geophysical Research: Earth Surface, 126, 1-20. https://doi.org/10.1029/2020JF005763

Bouchayer, C., Aiken, J.M., Thøgersen, K., Renard, F., Schuler, T.V. (2022). A machine learning framework to automate the classification of surge-type glaciers in Svalbard, Journal of Geophysical Research: Earth Surface, 127, 1-26. https://doi.org/10.1029/2022JF006597

Bouchayer, C., Nanni, U., Lefeuvre, P-M., Hult, J., Schmidt, L.S., Kohler, J., Renard, F., Schuler, T.V. (2024). Multi-scale variations of subglacial hydro-mechanical conditions at Kongsvegen glacier, Svalbard, Cryosphere, 18, 2939-2968. https://doi.org/10.5194/tc-18-2939-2024

Boulton, G.S., Van Der Meer, J.J.M., Hart, J., Beets, D., Ruegg, G.H.J., Van Der Wateren, F.M., Jarvis, J. (1996). Till and moraine emplacement in a deforming bed surge – An example from a marine environment, Quaternary Science Reviews, 15, 961-987. https://doi.org/10.1016/0277-3791(95)00091-7

Boulton, G.S., van der Meer, J.J.M., Beets, D.J., Hart, J.K., Ruegg, G.H.J. (1999). The sedimentary and structural evolution of a recent push moraine complex: Holmströmbreen, Spitsbergen. Quaternary Science Reviews,, 18, 339-371. https://doi.org/10.1016/S0277-3791(98)00068-7

Brandt, O., Kohler, J., Lüthje, M. (2008). Spatial mapping of multi-year superimposed ice on the glacier Kongsvegen, Svalbard, Journal of Glaciology, 54, 73-80. https://doi.org/10.3189/002214308784409080

Clarke, G.K.C. (1976). Thermal regulation of glacier surging, Journal of Glaciology, 74, 231-250. https://doi.org/10.3189/S0022143000031567

Chandler, B.M.P., Lovell, H., Boston, C.M., Lukas, S., Barr, I.D., Benediktsson, Í.Ö., Benn, D.I., Clark, C.D., Darvill, C.M., Evans, D.J.A., Ewertowski, M.W., Loibl, D., Margold, M., Otto, J-C., Roberts, D.H., Stokes, C.R., Storrar, R.D., Stroeven, A.P. (2018). Glacial geomorphological mapping: A review of approaches and frameworks for best practice, Earth Science Reviews, 185, 806-846. https://doi.org/10.1016/j.earscirev.2018.07.015

Christoffersen, P., Piotrowski, J. A., & Larsen, N. K. (2005). Basal processes beneath an Arctic glacier and their geomorphic imprint after a surge, Elisebreen, Svalbard. Quaternary Research, 64, 125-137. https://doi.org/10.1016/j.yqres.2005.05.009

Cichowicz, A. (1983). Icequakes and glacier motion: the Hans Glacier, Spitsbergen, Pure and Applied Geophysics, 121, 27-38. https://doi.org/10.1007/BF02590118

Commission scientifique du Nord (1852). *Voyages de la commission scientifique du Nord, en Scandinavie, en Laponie, au Spitzberg et aux Féroë pendant les années 1838, 1839 et 1840*. Vol. 1. Paris: Gide et J. Baudry, p. 300. Available at: https://archive.org/details/FOLSC0948_1NOR/page/n273/mode/2up [Accessed 6 Apr. 2025].

Conway, W.M. (1897). The First Crossing of Spitsbergen, The Geographical Journal, 9, 353-365. https://doi.org/10.2307/1774475

Crary, A.P. (1955). A brief study of ice tremors. Bulletin of the Seismological Society of America, 45, 1-9. https://doi.org/10.1785/BSSA0450010001

Croot DG (1988) Glaciotectonics and surging glaciers: a correlation based on Vestspitsbergen, Svalbard, Norway. In: Croot DG (ed) Glaciotectonics: forms and processes. Balkema, Amsterdam, pp 49–62.

Dachauer, A., Hann, R., Hodson, A.J. (2021). Aerodynamic roughness length of crevassed tidewater glaciers from UAV mapping, Cryosphere, 15, 5513-5528. https://doi.org/10.5194/tc-15-5513-2021

de Geer, G. (1910). Guide de l'excursion au Spitsberg: Excursion A1 (Guide to excursions on Spitsbergen: Excursion A1), paper presented at XI International Geological Congress. Exec. Comm., Stockholm.

Delf, R., Bingham, R.G., Curtis, A., Singh, S., Giannopoulos, A., Schwarz, B., Borstad, C.P. (2022). Reanalysis of polythermal glacier thermal structure using radar diffraction focusing, Journal of Geophysical Research: Earth Surface, 127, e2021JF006382. https://doi.org/10.1029/2021JF006382

Dowdeswell, J.A. Collin, R.L. (1990). Fast-flowing outlet glaciers on Svalbard ice caps, Geology, 18, 778-781. https://doi.org/10.1130/0091-7613(1990)018%3C0778:FFOGOS%3E2.3.CO;2

Dowdeswell, J.A., Bamber, J.L. (1995). On the glaciology of Edgeøya and Barentsøya, Svalbard, Polar Research, 14, 105-122. https://doi.org/10.3402/polar.v14i2.6658

Dowdeswell, J.A., Hamilton, G.S., Hagen, J.O. (1991). The duration of the active phase on surge-type glaciers: Contrasts between Svalbard and other regions, Journal of Glaciology, 37, 388-400. https://doi.org/10.3189/S0022143000005827

Dowdeswell, J.A., Hodgkins, R., Nuttall, A-M., Hagen, J.O., Hamilton, G.S. (1995). Mass balance change as a control on the frequency and occurrence of glacier surges in Svalbard, Norwegian High Arctic, Geophysical Research Letters, 22, 2909-2912. https://doi.org/10.1029/95GL02821

Dunse, T., Schuler, T.V., Hagen, J.O., Eiken, T., Brandt, O., Høgda, K.A. (2009). Recent fluctuations in the extent of the firn area of Austfonna, Svalbard, inferred from GPR. Annals of Glaciology, 50, 155-162. https://doi.org/10.3189/172756409787769780

Dunse, T., Schuler, T.V., Hagen, J.O., Reijmer, C.H. (2012). Seasonal speed-up of two outlet glaciers of Austfonna, Svalbard, inferred from continuous GPS measurements, Cryosphere, 6, 453-466. https://doi.org/10.5194/tc-6-453-2012

Dunse, T., Schellenberger, T., Hagen, J. O., Kääb, A., Schuler, T. V., & Reijmer, C. H. (2015). Glacier-surge mechanisms promoted by a hydro-thermodynamic feedback to summer melt. Cryosphere, 9, 197-215. https://doi.org/10.5194/tc-9-197-2015

Dyrda, M., Kułak, A., Trześniowski, Z., Trześniowski, M., Trześniowski, T., Worek, C., Ziętara, K. (2023). Spectral ground penetrating radar - An innovative tool for multispectral subsurface probing and modelling, NSG2023 29th European Meeting of Environmental and Engineering Geophysics, 1-5. https://doi.org/10.3997/2214-4609.202320038

Eiken, T., Sund, M. (2012). Photogrammetric methods applied to Svalbard glaciers: Accuracies and challenges, Polar Research, 31, 18671. http://dx.doi.org/10.3402/polar.v31i0.18671

Eiken, T., Hagen, J.O., Melvold, K. (1997). Kinematic GPS survey of geometry changes on Svalbard glaciers, Annals of Glaciology, 24, 157-163. https://doi.org/10.3189/S0260305500012106

Evans, D.J.A., Rea, B.R. (1999). Geomorphology and sedimentology of surging glaciers: A land-systems approach, Annals of Glaciology, 28, 75-82. https://doi.org/10.3189/172756499781821823

Evans, D.J.A. (2005). Glacial landsystems, London, Arnold.

Evans, D.J.A., Ewertowski, M., Roberts, D.H., Tomczyk, A.M. (2022). The historical emergence of a geometric and sinuous ridge network at the Hørbyebreen polythermal glacier snout, Svalbard and its use in the interpretation of ancient glacial landforms, Geomorphology, 406, 1-22. https://doi.org/10.1016/j.geomorph.2022.108213

Farnsworth, W.R., Ingólfsson, Ó., Retelle, M., Schomacker, A. (2016). Over 400 previously undocumented Svalbard surge-type glaciers identified, Geomorphology, 264, 52-60. https://doi.org/10.1016/j.geomorph.2016.03.025

Farnsworth, W.R., Allaart, L., Ingólfsson, Ó., Alexanderson, H., Forwick, M., Noormets, R., Retelle, M., Schomacker, A. (200). Holocene glacial history of Svalbard: Status, perspectives and challenges, Earth Science Reviews, 208, 103249. https://doi.org/10.1016/j.earscirev.2020.103249

Fichtner, A., Hofstede, C., Kennett, B. L., Svensson, A., Westhoff, J., Walter, F., ... & Eisen, O. (2025). Hidden cascades of seismic ice stream deformation. Science, 387(6736), 858-864. https://doi.org/10.1126/science.adp8094

Flink, A.E., Noormets, R. (2018). Submarine glacial landforms and sedimentary environments in Vaigattbogen, Marine Geology, 402, 244-263. https://doi.org/10.1016/j.margeo.2017.07.019

Flink, A.E., Noormets, R., Kirchner, N., Benn, D.I., Luckman, A., Lovell, H. (2015). The evolution of a submarine landform record following recent and multiple surges of Tunabreen glacier, Svalbard, Quaternary Science Reviews, 108, 37-50. https://doi.org/10.1016/j.quascirev.2014.11.006

Flink, A.E., Noormets, R., Fransner, O., Hogan, K.A., ORegan, M., Jakobsson, M. (2017). Past ice flow in Wahlenbergfjorden and its implications for late Quaternary ice sheet dynamics in northeastern Svalbard. Quaternary Science Reviews, 163,162-179. https://doi.org/10.1016/j.quascirev.2017.03.021

Flink, A.E., Hill, P., Noormets, R., Kirchner, N. (2018). Holocene glacial evolution of Mohnbukta in eastern Spitsbergen. Boreas, 47, 390-409. https://doi.org/10.1111/bor.12277

Fowler, A.C. (1987). A theory of glacier surges, Journal of Geophysical Research: Solid Earth, 92, 9111-9120. https://doi.org/10.1029/JB092iB09p09111

Fowler, A.C., Murray, T., Ng, F.S.L. (2001). Thermally controlled glacier surging, Journal of Glaciology, 47, 527-538. https://doi.org/10.3189/172756501781831792

Friedl, Peter; Seehaus, Thorsten; Braun, Matthias (2021): Sentinel-1 ice surface velocities of Svalbard. V. 1.0. GFZ Data Services. https://doi.org/10.5880/fidgeo.2021.016

Fürst, J.J., Navarro, F., Gillet-Chaulet, F., Huss, M., Moholdt, G., Fettweis, X., Lang, C., Seehaus, T., Ai, S., Benham, T.J., Benn, D.I., Björnsson, H., Dowdeswell, J.A., Grabiec, M., Kohler, J., Lavrentiev, I., Lindbäck, K., Melvold, K., Pettersson, R., Rippin, D., Saintenoy, A., Sánchez-Gámez, P., Schuler, T.V., Sevestre, H., Vasilenko, E., Braun, M.H. (2018). The ice-free topography of Svalbard, Geophysical Research Letters, 45, 11760-11769. https://doi.org/10.1029/2018GL079734

Gajek, W., Trojanowski, J., Malinowski, M. (2017). Automating long-term glacier dynamics monitoring using single-station seismological observations and fuzzy logic classification: a case study from Spitsbergen, Journal of Glaciology, 63, 581-592. https://doi.org/10.1017/jog.2017.25

Gajek, W., Gräff, D., Hellmann, S., Rempel, A. W., Walter, F. (2021). Diurnal expansion and contraction of englacial fracture networks revealed by seismic shear wave splitting, Communications Earth & Environment, 2, 209. https://doi.org/10.1038/s43247-021-00279-4

Gajek, W., Köhler, A., Wuestefeld, A., & Hanssen, A. (2024). Hornsund 2023–2024 geophone seismic data (FROST). *Dataset*. https://doi.org/10.25171/InstGeoph_PAS_IGData_FROST_geophone_seismic_data_Hornsund_2023_2024

Gajek W., Luckman A., Harcourt W. D, Pearce D. M., Hann R. (2025) Utilising seismic station internal GPS for tracking surging glacier sliding velocity. Journal of Glaciology, 71, e40. https://doi.org/10.1017/jog.2025.30

Gardner, A.S., Greene, C.A., Kennedy, J.H., Fahnestock, M.A., Liukis, M., López, L.A., Lei, Y., Scambos, T.A., Dehecq, A. (2025). ITS_LIVE global glacier velocity data in near real time, EGUsphere [preprint]. https://doi.org/10.5194/egusphere-2025-392

Garwood, E. J., Gregory, J. W. (1898). Contributions to the glacial geology of Spitsbergen, Quarterly Journal of the Geological Society, 54, 197–227. https://doi.org/10.1144/GSL.JGS.1898.054.01-04.1

Geyman, E.C., van Pelt, W.J.J., Maloof, A.C., Aas, H.F., Kohler, J. (2022). Historical glacier change on Svalbard predicts doubling of mass loss by 2100, Nature, 601, 374-379. https://doi.org/10.1038/s41586-021-04314-4

Gilbert, A., Gimbert, F., Thørgersen, K., Schuler, T.V., Kääb, A. (2022). A consistent framework for coupling basal friction with subglacial hydrology on hard-bedded glaciers, Geophysical Research Letters, 49, e2021gl097507. https://doi.org/10.1029/2021GL097507

Gillet-Chaulet, F., Hindmarsh, R. C., Corr, H. F., King, E. C., Jenkins, A. (2011). In-situ quantification of ice rheology and direct measurement of the Raymond Effect at Summit, Greenland using a phase-sensitive radar. Geophysical Research Letters, 38, L24503. https://doi.org/10.1029/2011GL049843

Gimbert, F., Tsai, V. C., Amundson, J. M., Bartholomaus, T. C., Walter, J. I. (2016). Subseasonal changes observed in subglacial channel pressure, size, and sediment transport. Geophysical Research Letters, 43(8), 3786-3794. https://doi.org/10.1002/2016GL068337

Girod, L., Nuth, C., Kääb, A., Etzelmüller, B., Kohler, J. (2017). Terrain changes from images acquired on opportunistic flights by SfM photogrammetry, Cryosphere, 11, 827-840. https://doi.org/10.5194/tc-11-827-2017

Glasser, N.F., Coulson, S.J., Hodkinson, I.D., Webb, N.R. (2004). Photographic evidence of the return period of a Svalbard surge-type glacier: A tributary of Pedersenbreen, Kongsfjord, Journal of Glaciology, 50, 307-308. https://doi.org/10.3189/172756504781830060

Górski, M., Teisseyre, R. (1991). Seismic events in Hornsund, Spitsbergen, Polish Polar Research, 12, 345-352.

Gräff, D., & Walter, F. (2021). Changing friction at the base of an Alpine glacier, Scientific reports, 11, 10872. https://doi.org/10.1038/s41598-021-90176-9

Gräff, D., Lipovsky, B. P., Vieli, A., Dachauer, A., Jackson, R., Farinotti, D., ... & Williams, E. F. (2025). Calving-driven fjord dynamics resolved by seafloor fibre sensing. Nature, 644(8076), 404-412. https://doi.org/10.1038/s41586-025-09347-7

Gregory, J. W., Garwood, M., Trevor-Battye, M. (1897). The First Crossing of Spitsbergen: Discussion. The Geographical Journal, 9, 365–368. https://doi.org/10.2307/1774476

Gripp, K. (1929). Glaciologische und geologische Ergebnisse der Hamburgischen Spitzbergen-Expedition 1927. Abhandlungen aus dem Gebiete der Naturwissenschaften, 22(3/4), 145-249.

Guillet, G., Benn, D.I., King, O., Shean, D., Mannerfelt, E.S., Hugonnet, R. (2025). Global detection of glacier surges from surface velocities, elevation change and SAR backscatter data between 2000 and 2024: A test of surge mechanism theories, Journal of Glaciology, 71, e88. https://doi.org/10.1017/jog.2025.10065

Gutiérrez, J.M., Jones, R.G., Narisma, G.T., Alves, L.M., Amjad, M., Gorodetskaya, I.V., Grose, M., Klutse, N.A.B., Krakovska, S., Li, J., Martinez-Castro, D., Mearns, L.O., Mernild, S.H., Ngo-Duc, T., van den Hurk, B., Yoon, J-H. (2021). Atlas. In Climate Change 2021: The Physical Science Basis. Contribution of Working Group I to the Sixth Assessment Report of the Intergovernmental Panel on Climate Change [Masson-Delmotte, V., Zhai, P., Pirano, A., Connors, S.L., Péan, C., Berger, S., Caud, N., Chen, Y., Goldfarb, L., Gomis, M.I., Huang, M., Leitzell, K., Lonnoy, E., Matthews, J.B.R., Maycock, T.K., Waterfield, T., Yelekçi, O., Yu, R., Zhou, B. (eds.)]. Cambridge University Press, Cambridge, United Kingdom and New York, NY, USA, pp. 1927–2058, doi: https://doi.org/10.1017/9781009157896.021

Haas, C. , Happ, L. , Landy, J. and Krumpen, T. (2024): Campaign Report: IceBird Summer 2023 - Polar 5 / C. Haas (editor) , [Other]

Haga, O.N., McNabb, R., Nuth, C., Altena, B., Schellenberger, T., Kääb, A. (2020). From high friction zone to frontal collapse: Dynamics of an ongoing tidewater glacier surge, Negribreen, Svalbard, Journal of Glaciology, 66, 742-754, https://doi.org/10.1017/jog.2020.43

Hagen, J.O., Liestøl, O., Roland, E., Jørgensen, T. (1993). Glacier Atlas of Svalbard and Jan Mayen, Norwegian Polar Institute, Oslo, Norway.

Hagen J.O., Eiken, T., Kohler, J., Melvold, K. (2005). Geometry changes on Svalbard glaciers: Mass-balance or dynamic response, Annals of Glaciology, 42, 255-261. https://doi.org/10.3189/172756405781812763

Hald, M., Dahlgren, T., Olsen, T.E., Lebesbye, E., (2001). Late Holocene palaeooceanography in Van Mijenfjorden, Svalbard. Polar Research, 20, 23-35. https://doi.org/10.3402/polar.v20i1.6497

Hamberg, A. (1894). En resa till norra Ishafvet sommaren 1892. Ymer, 14:25–61.

Hamilton, G.S., Dowdeswell, J.A. (1996). Controls on glacier surging in Svalbard, Journal of Glaciology, 42, 157-168. https://doi.org/10.3189/S0022143000030616

Hann, R., Altstädter, B., Betlem, P., Deja, K., Dragańska-Deja K., Ewertowski, M., Hartvich, F., Jonassen, M., Lampert, A., Laska, M., Sobota, I., Storvold, R., Tomczyk, A., Wojtysiak, K. Zagórski P. (2021). Scientific Applications of Unmanned Vehicles in Svalbard. SESS Report 2020, Svalbard Integrated Arctic Earth Observing System. doi.org/10.5281/zenodo.4293283

Hann, R., Betlem, P., Deja, K., Hartvich, F., Jonassen, M., Lampert, A., Laska, M., Sobota, I., Storvold, R., Zagórski P. (2022). Update to Scientific Applications of Unmanned Vehicles in Svalbard. SESS Report 2021, Svalbard Integrated Arctic Earth Observing System. doi.org/10.5281/zenodo.5751959

Hann, R., Betlem, P., Deja, K., Ewertowski, M., Harm-Altstädter, B., Jonassen, M., Lampert, A., Laska, M., Sobota, I., Storvold, R., Tomczyk, A., & Zagorski, P. (2023). Practical Guidelines for Scientific Application of Uncrewed Aerial Vehicles in Svalbard (UAV Svalbard 3). In SESS report 2022 - The State of Environmental Science in Svalbard - an annual report (pp. 142–152). Svalbard Integrated Arctic Earth Observing System. https://doi.org/10.5281/zenodo.7371141

Hann, R., Rodes, N. Gajek, W. Pearce, D., Harcourt, W.D. (2024). Drone-based mapping of calving rates of Borebreen in Svalbard, https://doi.org/10.18710/B553MB, DataverseNO, V1

Hansen, S. (2003). From surge-type to non-surge-type glacier behaviour: Midre Lovénbreen, Svalbard, Annals of Glaciology, 36, 97-102. https://doi.org/10.3189/172756403781816383

Hanssen-Bauer, I., Førland, E.J., Hisdal, H., Mayer, S., Sandø, A.B., Sorteberg, A. (eds) (2019) Climate in Svalbard 2100 - a knowledge base for climate adaptation. Norway, Norwegian Centre of Climate Services (NCCS) for Norwegian Environment Agency (Miljødirektoratet), 208pp. (NCCS report 1/2019). DOI: http://dx.doi.org/10.25607/OBP-888

Harcourt, W.D., Robertson, D.A., Macfarlane, D.G., Rea, B.R., Spagnolo, M., Benn, D.I., James, M.R., (2022). Glacier monitoring using real-aperture 94 GHz radar. Annals of Glaciology, 63, 116-120. https://doi.org/10.1017/aog.2023.30

Harcourt, W.D., Gajek, W., Pearce, D., Hann, R., Luckman, A., Rea, B.R., Benn, D.I., James, M.R., Spagnolo, M., Nanni, U. (2024). Surge initiation at the terminus of Borebreen (Svalbard): Drivers and impact on calving. EGU General Assembly 2024, Vienna, Austria. https://doi.org/10.5194/egusphere-egu24-1505

Harcourt, W.D., Pearce, D.M., Gajek, W., Lovell, H., Luckman, A., Benn, D., Kohler, J., Kääb, A., Hann, R. (2025a). Surging glaciers in Svalbard: Current knowledge and perspectives for monitoring (SvalSurge). In SESS report 2024 - The State of Environmental Science in Svalbard - an annual report (pp. 84–105). Svalbard Integrated Arctic Earth Observing System. https://doi.org/10.5281/zenodo.14425522

Harcourt, W.D., Pearce, D., Gajek, W., Lovell, H., Mannerfelt, E.S., Kääb, A., Benn, D., Luckman, A., Hann, R., Kohler, J. (2025b). Svalbard Surge Database 2024 (RGI2000-v7.0-G-07) [Data set]. Zenodo. https://doi.org/10.5281/zenodo.18033216

Hart, J.K., Watts, R.J. (1997). A comparison of the styles of deformation associated with two recent push moraines, south van Keulenfjorden, Svalbard, Earth Surface Processes and Landforms, 22, 1089-1107. https://doi.org/10.1002/(SICI)1096-9837(199712)22:12<1089::AID-ESP804>3.0.CO;2-8

Hart, J.K., Martinez, K., Ong, R., Riddoch, A., Rose, K.C., [adhy, P. (2006). A wireless multi-sensor subglacial probe: Design and preliminary results, Journal of Glaciology, 52, 389-397. https://doi.org/10.3189/172756506781828575

Hatherton, T., Evison, F.F. (1962). A special mechanism for some Antarctic earthquakes, New Zealand Journal of Geology and Geophysics, 5, 864-873. https://doi.org/10.1080/00288306.1962.10417642

Herreid, S., Truffer, M. (2015). Automated detection of unstable glacier flow and a spectrum of speedup behavior in the Alaska Range, Journal of Geophysical Research: Earth Surface, 121, 64-81. https://doi.org/10.1002/2015JF003502

Hodgkins, R., Dowdeswell, J.A. (1994). Tectonic processes in Svalbard tide-water glacier surges: Evidence from structural glaciology, Journal of Glaciology, 40, 553-560. https://doi.org/10.3189/S0022143000012430

Hodgkins, R., Hagen, J.O., Hamran, S-E. (1999). 20th century mass balance and thermal regime change at Scott Turnerbreen, Svalbard, Annals of Glaciology, 28, 216-220. https://doi.org/10.3189/172756499781821986

Hodgkins, R., Fox, A., Nuttall., A-M. (2007). Geometry change between 1990 and 2003 at Finsterwalderbreen, a Svalbard surge-type glacier, from GPS profiling, Annals of Glaciology, 46, 131-135. https://doi.org/10.3189/172756407782871189

Hoel, A. 1914: Exploration du Nord-ouest Spitsbergen entreprise sous les auspices de S.A.S. le Prince de Monaco par la Mission Isachsen. Troisieme partie. RPsultats des campagnes scienrifiques accomplies sur son yachtpar ler Prince Souuerain de Monaco, farc. XLII, 1-160.

Holmlund, P., Martinsson, T. (2016). Den norsk-brittisk-svenska Antarktisexpeditionen (NSBX). In: J. Hedberg, ed., Frusna ögonblick: Svensk polarfotografi 1861–1980. Stockholm: Art and Theory Publishing, pp.216–229.

Hopwood, M.J., Carroll, D., Dunse, T., Hodson, A., Holding, J.M., Iriarte, J.L., Ribeiro, S., Achterberg, E.P., Cantoni, C., Carlson, D.F., Chierici, M., Clarke, J.S., Cozzi, S., Fransson, A., Juul-Pedersen, T., Winding, M.H.S., Meire, L. (2020). Review article: How does glacier discharge affect marine biogeochemistry and primary production in the Arctic, Cryosphere, 14, 1347-1383. https://doi.org/10.5194/tc-14-1347-2020

How, P., Benn, D.I., Hulton, N.R.J., Hubbard, B., Luckman, A., Sevestre, H., van Pelt, W.J.J., Lindbäck, K., Kohler, J., Boot, W. (2017). Rapidly changing subglacial hydrological pathways at a tidewater glacier revealed through simultaneous observations of water pressure, supraglacial lakes, meltwater plumes and surface velocities, Cryosphere, 11, 2691-2710. https://doi.org/10.5194/tc-11-2691-2017

Howe, J.A., Husum, K., Inall, M.E., Coogan, J., Luckman, A., Arosio, R., Abernethy, C., Verchili, D. (2019). Autonomous underwater vehicle (AUV) observations of recent tidewater glacier retreat, western Svalbard, Marine Geology, 417. https://doi.org/10.1016/j.margeo.2019.106009

Hudson, T.S., Baird, A.F., Kendall, J.M., Kufner, S.K., Brisbourne, A.M., Smith, A.M., Butcher, A., Chalari, A., Clarke, A. (2021). Distributed Acoustic Sensing (DAS) for natural microseismicity studies: A case study from Antarctica. Journal of Geophysical Research: Solid Earth, 126, e2020JB021493. https://doi.org/10.1029/2020JB021493

Hugonnet, R., McNabb, R., Berthier, E., Menounos, B., Nuth, C., Girod, L., Farinotti, D., Huss, M., Dussaillant, I., Brun, F., Kääb, A. (2021a). Accelerated global glacier mass loss in the early twenty-first century, Nature, 592, 726-731. https://doi.org/10.1038/s41586-021-03436-z

Hugonnet, R., McNabb, R., Berthier, E., Menounos, B., Nuth, C., Girod, L., Farinotti, D., Huss, M., Dussaillant, I., Brun, F., Kääb, A. (2021b). Accelerated global glacier mass loss in the early twenty-first century - Dataset. [dataset]. Theia. https://doi.org/10.6096/13

Inall, M.E., Sundfjord, A., Cottier, F., Korte, M-L., Slater, D.A., Venables, E.J., Coogan, J. (2024). Mixing, water transformation, and melting close to a tidewater glacier, Geophysical Research Letters, 51, e2024GL108421, https://doi.org/10.1029/2024GL108421

Ingólfsson, Ó., Landvik, J.Y. (2013). The Svalbard-Barents ice-sheet - Historical, current and future perspectives, Quaternary Science Reviews, 64, 33-60. https://doi.org/10.1016/j.quascirev.2012.11.034

Isaksen, K., Nordli, Ø., Ivanov, B., Køltzow, M.A.Ø., Aaboe, S., Gjelten, H.M., Mezghani, A., Eastwood, S., Førland, E., Benestad, R.E., Hanssen-Bauer, I., Brækan, R., Sviashchennikov, P., Demin, V., Revina, A., Karandasheva, T. (2022). Exceptional warming over the Barents area, Scientific Reports, 12, 9371. https://doi.org/10.1038/s41598-022-13568-5

Jakobsson, M., Mohammad, R., Karlsson, M., Salas-Romero, S., Vacek, F., Heinze, F., Bringensparr, C., Castro, C.F., Johnson, P., Kinney, J., Cardigos, S., Bogonko, M., Accettella, D., Amblas, D., An, L., Bohan, A., Brandt, A., Bünz, S., Canals, M., Casamor, J.L., Coakley, B., Cornish, N., Danielson, S., Demarte, M., Di Franco, D., Dickson, M-L., Dorschel, B., Dowdeswell, J.A., Dreutter, S., Freman, A.C., Hall, J.K., Hally, B., Holland, D., Hongm J.K., Ivaldi, R., Knutz, P.C., Krawczyk, D.W., Kristofferson, Y., Lastras, G., Leck, C., Lucchi, R.G., Masetti, G., Morlighem, M., Muchowski, J., Nielsen, T., Noormets, R., Plaza-Faverola, A., Prescott, M.M., Purser, A., Rasmussen, T.L., Rebesco, M., Rignot, E., Rysgaard, S., Silyakova, A., Snoeijs-Leijonmalm, P., Sørensen, A., Straneo, F., Sutherland, D.A., Tate, A.J., Travaglini, P., Trenholm, N., van Wijk, E., Wallace, L., Willis, J.K., Wood, M., Zimmerman, M., Zinglersen, K.B., Mayer, L. (2024). The International Bathymetric Chart of the Arctic Ocean version 5.0, Scientific Reports, 11, 1420. https://doi.org/10.1038/s41597-024-04278-w

Jania, J., Mochnacki, D., & Gadek, B. (1996). The thermal structure of Hansbreen, a tidewater glacier in southern Spitsbergen, Svalbard. Polar Research, 15(1), 53–66. https://doi.org/10.1111/j.1751-8369.1996.tb00458.x

Jenssen, R-O.R., Vickers, H., Ricker, R., Malnes, E., Jacobsen, S. (2024). Drone-mounted snow radar system - Quantitative field validation of terrestrial snow measurements, Proceedings of the International Snow Science Workshop, Tromsø, Norway, 1073-1078.

Jiskoot, H., Boyle, P., Murray, T. (1998). The incidence of glacier surging in Svalbard: Evidence from multivariate statistics, Computers and Geoscience, 24, 387-399. https://doi.org/10.1016/S0098-3004(98)00033-8

Jiskoot, H., Murray, T., Boyle, P. (2000). Controls on the distribution of surge-type glaciers in Svalbard, Journal of Glaciology, 46, 412-422. https://doi.org/10.3189/172756500781833115

Kääb, A., Jacquemart, M., Gilbert, A., Leinss, S., Girod, L., Huggel, C., Falaschi, D., Ugalde, F., Petrakov, Chernomorets, S., Dokukin, M., Paul, F., Gascoin, S., Berthier, E., Kargel, J.S. (2021). Sudden large-volume detachments of low-angle mountain glaciers - more frequent than thought?, Cryosphere, 15, 1751-1785. https://doi.org/10.5194/tc-15-1751-2021

Kääb, A., Bazilova, V., Leclercq, P.W., Mannerfelt, E.S., Strozzi, T. (2023). Global clustering of recent glacier surges from radar backscatter data, 2017-2022, Journal of Glaciology, 69, 1515-1523. https://doi.org/10.1017/jog.2023.35

Kachniarz, K., Grabiec, M., Wróbel, K., & Ignatiuk, D. (2025). Glacier internal structure revealed by automatic image processing-powered classification of radar images. Applied Geomatics, 1-16. https://doi.org/10.1007/s12518-025-00635-5

Kamb, B. (1987). Glacier surge mechanism based on linked cavity configuration of the basal water conduit system, Journal of Geophysical Research: Solid Earth, 92, 9083-9200. https://doi.org/10.1029/JB092iB09p09083

Kamb, B., Raymond, C.F., Harrison, W.D., Engelhardt, H., Echelmeyer, K.A., Humphrey, N., Brugman, M.M., Pfeffer, T. (1985). Glacier surge mechanism: 1982-1983 surge of Variegated Glacier, Alaska, Science, 227, 469-479. https://doi.org/10.1126/science.227.4686.469

Karušs, J., Lamsters, K., Ješkins, J., Sobota, I., Džeriņš, P. (2022). UAV and GPR data integration in glacier geometry reconstruction: a case study from Irenebreen, Svalbard. Remote Sensing, 14, 456. https://doi.org/10.3390/rs14030456

Kavan, J., Tallentire, G.D., Demidionov, M., Dudek, J., Strzelecki, M.C. (2022). Fifty years of tidewater glacier surface elevation and retreat dynamics along the south-east coast of Spitsbergen (Svalbard Archipelago), Remote Sensing, 13, 354. https://doi.org/10.3390/rs14020354.

Kavan, J., Luláková, P., Małecki, J., Strzelecki, C. (2024). Capturing the transition from marine to land-terminating glacier from the 126-year retreat history of Nordenskiöldbreen, Svalbard, Journal of Glaciology, 70, e70. https://doi.org/10.1017/jog.2023.92

Kempf, P., Forwick, M., Laberg, J.S., Vorren, T.O. (2013). Late Weichselian and Holocene sedimentary palaeoenvironment and glacial activity in the high-arctic van Keulenfjorden, Spitsbergen, Holocene, 23, 1607-1618. https://doi.org/10.1177/0959683613499055

King, O., Hambrey, M.J., Irvine-Flynn, T.D.L., Holt, T.O. (2016). The structural, geometric and volumetric changes of a polythermal Arctic glacier during a surge cycle: Comfortlessbreen, Svalbard, Earth Surface Processes and Landforms, 41, 162-177. https://doi.org/10.1002/esp.3796

Kingslake, J., Hindmarsh, R.C.A., Aðalgeirsdóttir, G., Conway, H., Corr, H.F.J., Gillet-Chaulet, F., Martín, C., King, E.C., Mulvaney, R., Pritchard, H.D. (2014). Full-depth englacial vertical ice sheet velocities measured using phase-sensitive radar. Journal of Geophysical Research: Earth Surface, 119, 2604-2618.

Kleber, G.E., Magerl, L., Turchyn, A.V., Schloemer, S., Trimmer, M., Zhu, Y., Hodson, A. (2025). Proglacial methane emissions driven by meltwater and groundwater flushing in a high-Arctic glacial catchment, Biogeosciences, 22, 659-674. https://doi.org/10.5194/bg-22-659-2025

Koch, M., Seehaus, T., Friedl, P., Braun, M. (2023). Automated detection of glacier surges from Sentinel-1 surface velocity time series – An example from Svalbard, Remote Sensing, 15, 1545. https://doi.org/10.3390/rs15061545

Köhler, A., Nuth, C., Schweitzer, J., Weidle, C., Gibbons, S.J. (2015). Regional passive seismic monitoring reveals dynamic glacier activity on Spitsbergen, Svalbard, Polar Research, 34, 26178. https://doi.org/10.3402/polar.v34.26178

Köhler, A., Nuth, C., Kohler, J., Berthier, E., Weidle, C., Schweitzer, J. (2016). A 15 year record of frontal glacier ablation rates estimated from seismic data, Geophysical Research Letters, 43, 12155-12164. https://doi.org/10.1002/2016GL070589

Köhler, A., Pętlicki, M., Lefeuvre, P-M., Buscaino, G., Nuth, C., Weidle, C. (2019). Contribution of calving to frontal ablation quantified from seismic and hydroacoustic observations calibrated with lidar volume measurements, Cryosphere, 13, 3117-3137. https://doi.org/10.5194/tc-13-3117-2019.

Köhler, A., Gajek, W., Malinowski, M., Schweitzer, J., Majdanski, M., Geissler, W. H., Chamarczuk, M., & Wuestefeld, A. (2020). Seismological monitoring of Svalbard's cryosphere: current status and knowledge gaps. In SESS report 2019 - The State of Environmental Science in Svalbard - an annual report (pp. 136–159). Svalbard Integrated Arctic Earth Observing System. https://doi.org/10.5281/zenodo.4704584

Kolar, J., Haas, C., Helm, V. (2025): 2023 Glacier surface elevation data from airborne laser scanner survey in Svalbard [dataset]. PANGAEA, https://doi.org/10.1594/PANGAEA.974592

Kotlyakov, V.M., Macheret, Y.Y. (1987). Radio echo-sounding of sub-Polar glaciers in Svalbard: Some problems and results of Soviet studies, Annals of Glaciology, 9, 151-159. https://doi.org/10.3189/S0260305500000537

Kristensen, L., Benn, D.I. (2012). A surge of the glaciers Skobreen-Paulabreen, Svalbard, observed by time-lapse photographs and remote sensing data, Polar Research, 31, 1-9. https://doi.org/10.3402/polar.v31i0.11106

Kristensen, L., Benn, D.I., Hormones, A., Ottesen, D. (2009). Mud aprons in front of Svalbard surge moraines: Evidence of subglacial deforming layers or proglacial glaciotectonics?, Geomorphology, 111, 206-221. https://doi.org/10.1016/j.geomorph.2009.04.022

Kulessa, B., Murray, T. (2003). Slug-test derived differences in bed hydraulic properties between a surge-type and a non-surge-type Svalbard glacier, Annals of Glaciology, 36, 103-209. https://doi.org/10.3189/172756403781816257

Kurjanski, B., Rea, B.R., Spagnolo, M., Winsborrow, M., Cornwell, D., Andreassen, K., Howell, J. (2019). Morphological evidence for marine ice stream shutdown, central Barents Sea. Marine Geology, 414, 64-76. https://doi.org/10.1016/j.margeo.2019.05.001

Langley, K., Hamran, S-E., Høgda, K.A., Storvold, R., Brandt, O., Hagen, J.O., Kohler, J. (2007). Use of C-band ground penetrating radar to determine backscatter sources within glaciers, IEEE Transactions on Geoscience and Remote Sensing, 45, 1236-1246. https://doi.org/10.1109/TGRS.2007.892600

Langley, K., Lacroix, P., Hamran, S-E., Brandt, O. (2009). Sources of backscatter at 5.3 GHz from a superimposed ice and firn area revealed by multi-frequency GPR and cores, Journal of Glaciology, 55, 373-383. https://doi.org/10.3189/002214309788608660

Larsen, D.J., Geirsdóttir, Á., Miller, G.H. (2015). Precise chronology of Little Ice Age expansion and repetitive surges of Langjökull, central Iceland, Geology, 43, 167-170. https://doi.org/10.1130/G36185.1

Larsen, E., Lyså, A., Rubensdotter, L., Farnsworth, W.R., Jensen, M., Nadeau, M.J., Ottesen, D. (2018). Lateglacial and Holocene glacier activity in the van Mijenfjorden area, western Svalbard, Arktos, 4. https://doi.org/10.1007/s41063-018-0042-2

Leclercq, P.W., Kääb, A., Altena, B. (2021). Brief communication: Detection of glacier surge activity using cloud computing of Sentinel-1 radar data, Cryosphere, 15, 4901-4907. https://doi.org/10.5194/tc-15-4901-2021.

Lefauconnier, B., Hagen, J.O. (1991). Surging and calving glaciers in eastern Svalbard, Norsk Polarinstitutt, Meddelelser NR. 116.

Lei, Y., Gardner, A.S., Agram, P. (2022). Processing methodology for the ITS_LIVE Sentinel-1 ice velocity products, Earth System Science Data, 14, 5111-5137. https://doi.org/10.5194/essd-14-5111-2022.

Lewandowska, H., & Teisseyre, R. (1964). Investigations of the ice microtremors on Spitsbergen in 1962. Biul Inf Komisji Wypraw Geof PAN, 37, 1-5.

Li, T., Heidler, K., Mou, L., Ignéczi, Á., Zhu, X.X., Bamber, J.L. (2024). A high-resolution calving front data product for marine-terminating glaciers in Svalbard, Earth System Science Data, 16, 919-939. https://doi.org/10.5194/essd-16-919-2024.

Li, T., Hofer, S., Moholdt, G., Igneczi, A., Heidler, K., Zhu, X.X., Bamber, J. (2025). Pervasive glacier retreats across Svalbard from 1985 to 2023, Nature Communications, 16, 1-11. https://doi.org/10.1038/s41467-025-55948-1

Lliboutry, L. (1968). General theory of subglacial cavitation and sliding of temperate glaciers, Journal of Glaciology, 7, 21-58. https://doi.org/10.3189/S0022143000020396

Lok, L. B., Brennan, P. V., Nicholls, K. W., & Corr, H. F. (2014). ApRES: Autonomous phase-sensitive FMCW radar, for basal monitoring and imaging of Antarctic ice shelves, IET Colloquium on Antennas, Wireless and Electromagnetics, 7. https://doi.org/10.1049/ic.2014.0019

López, Y.Á., Garcia-Fernandez, M., Alvarez-Narciandi, G., Andrés, F.L.H. (2022). Unmanned aerial vehicle-based ground-penetrating radar systems: A review. IEEE Geoscience and Remote Sensing Magazine, 10, 66-86. https://doi.org/10.1109/MGRS.2022.3160664

Lovell, H., Boston, C.M. (2017). Glacitectonic composite ridge systems and surge-type glaciers: An updated correlation based on Svalbard, Norway, Arktos, 3. https://doi.org/10.1007/s41063-017-0028-5.

Lovell, H., Fleming, E.J. (2023). Structural evolution during a surge in the Paulabreen glacier system, Svalbard, Journal of Glaciology, 69, 141-152. https://doi.org/10.1017/jog.2022.53

Lovell, H., Fleming, E.J., Benn, D.I., Hubbard, B., Lukas, S., Naegeli, K. (2015a). Former dynamic behaviour of a cold-based valley glacier on Svalbard revealed by basal ice and structural glaciology investigations. Journal of Glaciology, 61, 309-328. https://doi.org/10.3189/2015JoG14J120

Lovell, H., Fleming, E.J., Benn, D.I., Hubbard, B., Lukas, S., Rea, B.R., Noormets, R., Flink, A.E. (2015b). Debris entrainment and landform genesis during tidewater glacier surges, Journal of Geophysical Research: Earth Surface, 120, 1574-1595. https://doi.org/10.1002/2015JF003509

Lovell, H., Benn, D.I., Lukas, S., Spagnolo, M., Cook, S.J., Swift, D.A., Clark, C.D., Yde, J.C., Watts, T. (2018a). Geomorphological investigation of multiphase glacitectonic composite ridge systems in Svalbard, Geomorphology, 300, 176-188. https://doi.org/10.1016/j.geomorph.2017.10.024

Lovell, H., Benn, D.I., Lukas, S., Ottesen, D., Luckman, A., Hardiman, M., Barr, I.D., Boston, C.M., Sevestre, H. (2018b). Multiple late Holocene surges of a high-Arctic tidewater glacier system in Svalbard, Quaternary Science Reviews, 201, 162-185. https://doi.org/10.1016/j.quascirev.2018.10.024

Lovell, H., Benn, D.I., Jiskoot, H., Stokes, C.R., Flowers, G.E., Guillet, G., Mannerfelt, E.S., Falaschi, D., Kääb, A., King, O., Benediktsson, Í.Ö., Bhambri, R., Lv, M., Muhammad, S., Luckman, A. (In Press). Glacier surging and surge-related hazards in a changing climate, Nature Reviews Earth and Environment.

Luckman, A., Murray, T., Strozzi, T. (2002). Surface flow evolution throughout a glacier surge measured by satellite radar interferometry, Geophysical research Letters, 29, 2095. https://doi.org/10.1029/2001GL014570

Luckman, A., Benn, D.I., Cottier, F., Bevan, S., Nilsen, F., Inall, M. (2015). Calving rates at tidewater glaciers vary strongly with ocean temperature, Nature Communications, 8566, 8566. https://doi.org/10.1038/ncomms9566

Lyså, A., Larsen, E.A., Høgaas, F., Jensen, M.A., Klug, M., Rubensdotter, L., Szczuciński, W. (2018). A temporary glacier-surge ice-dammed lake, Braganzavågen, Svalbard, Boreas, 47, 837-854. https://doi.org/10.1111/bor.12302

Makinson, K., & Anker, P. G. (2014). The BAS ice-shelf hot-water drill: design, methods and tools. Annals of Glaciology, 55(68), 44-52. https://doi.org/10.3189/2014AoG68A030

Małecki, J., Faucherre, S., Strzelecki, M.C. (2013). Post-surge geometry and thermal structure of Hørbyebreen, central Spitsbergen, Polish Polar Research, 34, 305-321. https://doi.org/10.2478/popore−2013−0019

Mannerfelt, E.S., Hodson, A.J., Håkansson, L., Lovell, H. (2024). Dynamic LIA advances hastened the demise of small valley glaciers in central Svalbard, Arctic Science, 10, 815-833. https://doi.org/10.1139/as-2024-0024

Mannerfelt, E.S., Schellenberger, T, Kääb, A.M. (2025). Tracking glacier surge evolution using interferometric SAR coherence – examples from Svalbard. Journal of Glaciology, 71, e43. https://doi.org/10.1017/jog.2025.27

Mansell, D., Luckman, A., Murray, T. (2012). Dynamics of tidewater surge-type glaciers in northwest Svalbard, Journal of Glaciology, 58, 110-118. https://doi.org/10.3189/2012JoG11J058.

McCerery, R., Davies, B.J., Lovell, H., Pearce, D.A., Calvo-Ryan, R., Małecki, J., Woodward, J. (2024). Terrestrial glacial geomorphology of surge-type and non-surge-type glaciers on Svalbard, Journal of Maps, 20, 2362277. https://doi.org/10.1080/17445647.2024.2362277

McCerery, R., Davies, B.J., Lovell, H., Calvo-Ryan, R., Pearce, D.A., Małecki, J., Woodward, J. (2025). Landsystem models from remote and field based geomorphological mapping reveal diverse glacier dynamics on Svalbard, Geomorphology, 484, 109854. https://doi.org/10.1016/j.geomorph.2025.109854

McCrystall, M.R., Stroeve, J., Serreze, M., Forbes, B.C., Screen, J.A. (2021). New climate models reveal faster and larger increases in Arctic precipitation than previously projected, Nature Communications, 12, 6765. https://doi.org/10.1038/s41467-021-27031-y

McMillan, M., Shepherd, A., Gourmelen, N., Dehecq, A., Leeson, A., Ridout, A., Flament, T., Hogg, A., Gilbert, L., Benham, T., van den Broeke, M., Dowdeswell, J.A., Fettweis, X., Noël, B., Strozzi, T. (2014). Rapid dynamic activation of a marine-based Arctic ice cap, Geophys Research Letters, 41, 8902-8909. https://doi.org/10.1002/2014GL062255.

Meier, M.F., Post, A. (1969). What are glacier surges?, Canadian Journal of Earth Sciences, 6, 807-817. https://doi.org/10.1139/e69-081

Melvold, K., Hagen, J.O. (1998). Evolution of a surge-type glacier in its quiescent phase: Kongsvegen, Spitsbergen, 1964-95, Journal of Glaciology, 44, 394-404. https://doi.org/10.3189/S0022143000002720.

Mikesell, T. D., van Wijk, K., Haney, M. M., Bradford, J. H., Marshall, H. P., & Harper, J. T. (2012). Monitoring glacier surface seismicity in time and space using Rayleigh waves. Journal of Geophysical Research: Earth Surface, 117, F02020. https://doi.org/10.1029/2011JF002259

Minchew, B.M., Meyer, C.R. (2020). Dilation of subglacial sediment governs incipient surge motion in glaciers with deformable beds, Proceedings of the Royal Society A, 476, 20200033. https://doi.org/10.1098/rspa.2020.0033

Morris, A., Moholdt, G., Gray, L. (2020). Spread of Svalbard glacier mass loss to Barents Sea margins revealed by CryoSat-2, Journal of Geophysical Research: Earth Surface, 125, 1-20. https://doi.org/10.1029/2019JF005357

Murray, T., Porter, P.R. (2001). Basal conditions beneath a soft-bedded polythermal surge-type glacier: Bakaninbreen, Svalbard, Quaternary International, 86, 103-116. https://doi.org/10.1016/S1040-6182(01)00053-2

Murray, T., Booth, A.D. (2010). Imaging glacial sediment inclusions in 3-D using ground-penetrating radar at Kongsvegen, Svalbard, Journal of Quaternary Science, 25, 754-761. https://doi.org/10.1002/jqs.1351

Murray, T., Gooch, D.L., Stuart, G.W. (1997). Structures within the surge front at Bakaninbreen, Svalbard, using ground-penetrating radar, Annals of Glaciology, 24, 122-129. https://doi.org/10.3189/S0260305500012040

Murray, T., Dowdeswell, J.A., Drewry, D.J., Frearson, I. (1998). Geometric evolution and ice dynamics during a surge of Bakaninbreen, Svalbard, Journal of Glaciology, 44, 263-272. https://doi.org/10.3189/S0022143000002604

Murray, T., Stuart, G.W., Miller, P.J., Woodward, J., Smith, A.M., Porter, P. R., Jiskoot, H. (2000). Glacier surge propagation by thermal evolution at the bed. Journal of Geophysical Research: Solid Earth, 105, 13491-13507. https://doi.org/10.1029/2000JB900066

Murray, T., Strozzi, T., Luckman, A., Jiskoot, H., Christakos, P. (2003a). Is there a single surge mechanism? Contrasts in dynamics between glacier surges in Svalbard and other regions, Journal of Geophysical Research: Solid Earth, 108, 2237. https://doi.org/10.1029/2002JB001906

Murray, T., Luckman, A., Strozzi, T., Nuttall, A-M., (2003b). The initiation of glacier surging at Fridtjovbreen, Svalbard, Annals of Glaciology, 36, 110-116. https://doi.org/10.3189/172756403781816275.

Murray, T., James, T.D., Macheret, Y., Lavrentiev, I., Glazovsky, A., Sykes, H. (2012). Geometric changes in a tidewater glacier in Svalbard during its surge cycle, Arctic Antarctic, and Alpine Research, 44, 359-367. https://doi.org/10.1657/1938-4246-44.3.359.

Nanni, U., Gimbert, F., Vincent, C., Gräff, D., Walter, F., Piard, L., & Moreau, L. (2020). Quantification of seasonal and diurnal dynamics of subglacial channels using seismic observations on an Alpine glacier, Cryosphere, 14, 1475-1496. https://doi.org/10.5194/tc-14-1475-2020

Nanni, U., Bouchayer, C., Åkesson,H., Lefeuvre, P-M., Mannerfelt, E.S., Köhler, A., Gagliardini, O., Kohler, J., Schmidt, L.S., Hult, J., Renard, F., Schuler, T.V. (2025). Observed positive feedback between surface ablation and crevasse formation drives glacier acceleration and potential surge, Nature Communications, 15, 11227. https://doi.org/10.1038/s41467-025-66349-9

Navarro, F., & Eisen, O. (2009). 11 Ground-penetrating radar in glaciological applications. Remote sensing of glaciers: Techniques for topographic, spatial and thematic mapping of glaciers, 195-229. https://doi.org/10.1201/b10155

Navarro, F. J., Martín-Español, A., Lapazaran, J. J., Grabiec, M., Otero, J., Vasilenko, E. V., & Puczko, D. (2014). Ice volume estimates from ground-penetrating radar surveys, Wedel Jarlsberg Land glaciers, Svalbard, Arctic, Antarctic, and Alpine Research, 46, 394-406. https://doi.org/10.1657/1938-4246-46.2.394

Nuth, C., Moholdt, G., Kohler, J., Hagen, J.O., Kääb, A. (2010). Svalbard glacier elevation changes and contribution to sea level rise, Journal of Geophysical Research, 115, F01008. https://doi.org/10.1029/2008JF001223

Nuth, C., Gilbert, A., Köhler, A., McNabb, R., Schellenberger, T., Sevestre, H., Weidle, C., Girod, L., Luckman, A., Kääb, A. (2019). Dynamic vulnerability revealed in the collapse of an Arctic tidewater glacier, Scientific Reports, 9, 5541. https://doi.org/10.1038/s41598-019-41117-0.

Nuttall, A-M., Hagen, J.O., Dowdeswell, J. (1997). Quiescent-phase changes in velocity and geometry of Finsterwalderbreen, a surge-type glacier in Svalbard, Annals of Glaciology, 24, 249-254. https://doi.org/10.3189/S0260305500012258.

Ødegård, R.S., Hamran, S-E., Bø, P.H., Etzelmüller, B., Vatne, G., Sollid, J.L. (1992). Thermal regime of a valley glacier, Erikbreen, northern Spitsbergen, Polar Research, 11, 69-79. https://doi.org/10.3402/polar.v11i2.6718

Ødegård, R.S., Hagen, J.O., Hamran, S-E. (1997). Comparison of radio-echo sounding (30-1000 MHz) and high-resolution borehole-temperature measurements at Finsterwalderbreen, southern Spitsbergen, Svalbard, Annals of Glaciology, 24, 262-267. https://doi.org/10.3189/S0260305500012271

Oerlemans, J. (2018). Modelling the late Holocene and future evolution of Monacobreen, northern Spitsbergen, Cryosphere, 12, 3001-3015. https://doi.org/10.5194/tc-12-3001-2018.

Onarheim, I.H., Eldevik, T., Smedsrud, L.H., Stroeve, J.C. (2018). Seasonal and regional manifestation of Arctic sea ice loss, Journal of Climate, 31, 4917-4932. https://doi.org/10.1175/JCLI-D-17-0427.1

Osika, A., Jania, J. (2024). Geomorphological and historical records of the surge-type behaviour of Hansbreen (Svalbard). Journal of Glaciology, 65, e31. https://doi.org/10.1017/aog.2024.32

Ottesen, D., Dowdeswell, J.A. (2006). Assemblages of submarine landforms produced by tidewater glaciers in Svalbard, Journal of Geophysical Research: Earth Surface, 11, F01016. https://doi.org/10.1029/2005JF000330

Ottesen, D., Dowdeswell, J.A., Benn, D.I., Kristensen, L., Christiansen, H.H., Christensen, O., Hansen, L., Lebesbye, E., Forwick, M., Vorren, T.O. (2008). Submarine landforms characteristic of glacier surges in two Spitsbergen fjords, Quaternary Science Reviews, 27, 1583-1599. https://doi.org/10.1016/j.quascirev.2008.05.007

Ottesen, D., Dowdeswell, J.A., Bellec, V.K., Bjarnadóttir, L.R. (2017). The geomorphic imprint of glacier surges into open-marine waters: Examples from eastern Svalbard. Marine Geology, Volume 392, 1-29, https://doi.org/10.1016/j.margeo.2017.08.007

Ødegård, R. S., Hagen, J. O., & Hamran, S.-E. (1997). Comparison of radio-echo sounding (30–1000 MHz) and high-resolution borehole-temperature measurements at Finsterwalderbreen, southern Spitsbergen, Svalbard. Annals of Glaciology, 24, 262–267.

Pętlicki, M., Ciepły, M., Jania, J. A., Promińska, A., Kinnard, C. (2015). Calving of a tidewater glacier driven by melting at the waterline, Journal of Glaciology, 61, 851-863. https://doi.org/10.3189/2015JoG15J062

Pickell, DJ and Hawley, RL (2024) Performance characterization of a new, low-cost multi-GNSS instrument for the cryosphere. Journal of Glaciology 70(e41). https://doi.org/10.1017/jog.2023.97

Podolskiy, E.A., Walter, F. (2016). Cryoseismology, Reviews of Geophysics, 54, 708-758. https://doi.org/10.1002/2016RG000526

Podolskiy, E.A., Murai, Y., Kanna, N., Sugiyama, S. (2021). Ocean-bottom and surface seismometers reveal continuous glacial tremor and slip, Nature Communications, 12, 3929. https://doi.org/10.1038/s41467-021-24142-4

Pohjola, V.A., Christoffersen, P., Kolondra, L., Moore, J.C., Pettersson, R., Schäfer, M., Strozzi, T., Reijmer, C.H. (2011). Spatial distribution and change in the surface ice-velocity field of Vestfonna ice cap, Nordaustlandet, Svalbard, 1995-2010 using geodetic and satellite interferometry data, Geografiska Annaler: Series A, Physical geography, 93, 323-335. https://doi.org/10.1111/j.1468-0459.2011.00441.x

Porter, P.R., Murray, T., Dowdeswell, J.A. (1997). Sediment deformation and basal dynamics beneath a glacier surge front: Bakaninbreen, Svalbard, Annals of Glaciology, 24, 21-26. https://doi.org/10.3189/S0260305500011873

Porter, P.R., Murray, T. (2001). Mechanical and hydraulic properties of till beneath Bakaninbreen, Svalbard, Journal of Glaciology, 47, 167-175. https://doi.org/10.3189/172756501781832304

Porter, P. R. (2011), Subglacial borehole instrumentation, in `Encyclopedia of Snow, Ice and Glaciers', Springer, 1091-1095.

Prior-Jones, M. R., Bagshaw, E. A., Lees, J., Clare, L., Burrow, S., Werder, M. A., ... & Hubbard, B. (2021). Cryoegg: development and field trials of a wireless subglacial probe for deep, fast-moving ice. Journal of Glaciology, 67(264), 627-640. https://doi.org/10.1017/jog.2021.16

Quincey, D.J., Glasser, N.F., Cook, S.J., Luckman, A. (2015). Heterogeneity in Karakoram glacier surges, Journal of Geophysical Research: Earth Surface,120, 1288-1300. https://doi.org/10.1002/2015JF003515

Rantanen, M., Karpechko, A.Y., Lipponen, A., Nordling, K., Hyvärinen, O., Ruosteenoja, K., Vihma, T., Laaksonen, A. (2022). The Arctic has warmed nearly four times faster than the globe since 1979, Communications Earth & Environment, 3, 168. https://doi.org/10.1038/s43247-022-00498-3

Raymond, C.F. (1987). How do glaciers surge? A review, Journal of Geophysical Research: Solid Earth, 92, 9121-9134. https://doi.org/10.1029/JB092iB09p09121

Raymond, C.F., Malone, S. (1986). Propagating strain anomalies during mini-surges of Variegated Glacier, Alaska, USA, Journal of Glaciology, 32, 178-191. https://doi.org/10.3189/S0022143000015495

Rea, B.R., Evans, D.J.A. (2011). An assessment of surge-induced crevassing and the formation of crevasse squeeze ridges, Journal of Geophysical Research: Earth Surface, 16, F04005. https://doi.org/10.1029/2011JF001970

RGI 7.0 Consortium (2023). Randolph Glacier Inventory - A Dataset of Global Glacier Outlines, Version 7.0. Boulder, Colorado USA. NSIDC: National Snow and Ice Data Center. doi:10.5067/f6jmovy5navz. Online access: https://doi.org/10.5067/f6jmovy5navz.

Rieke, O., Årthun, M., Dörr, J.S. (2023). Rapid sea ice changes in the future Barents Sea, Cryosphere, 17, 1445-1456. https://doi.org/10.5194/tc-17-1445-2023

Roberson, S., Hubbard, B. (2010). Application of borehole optical televiewing to investigating the 3-D structure of glaciers: Implications for the formation of longitudinal debris ridges, midre Lovénbreen, Svalbard, Journal of Glaciology, 56, 143-156. https://doi.org/10.3189/002214310791190802

Robsinson, P., Dowdeswell, J.A. (2011). Submarine landforms and the behavior of a surging ice cap since the last glacial maximum: The open-marine setting of eastern Austfonna, Svalbard, Marine Geology, 286, 82-94. https://doi.org/10.1016/j.margeo.2011.06.004

Rolstad, C., Amlien, J., Hagen, J.O., Lundén, B. (1997). Visible and near-infrared digital images for determination of ice velocities and surface elevation during a surge on Osbornebreen, a tidewater glacier in Svalbard, Annals of Glaciology, 24, 255-261. https://doi.org/10.3189/S026030550001226X

Röösli, C., Walter, F., Husen, S., Andrews, L.C., Lüthi, M.P., Catania, G.A., Kissling, E. (2014). Sustained seismic tremors and icequakes detected in the ablation zone of the Greenland ice sheet, Journal of Glaciology, 60, 563-575. https://doi.org/10.3189/2014JoG13J210

Røthe, T.O., Bakke, J., Vasskog, K., Gjerde, M., D'Andrea, W.J., Bradley, R.S. (2015). Arctic Holocene glacier fluctuations reconstructed from lake sediments at Mitrahalvøya, Spitsbergen, Quaternary Science Reviews, 109, 111-125. https://doi.org/10.1016/j.quascirev.2014.11.017

Röthlisberg, H. (1955). Studies in glacier physics on the Penny Ice Cap, Baffin Island, 1953: Part III: seismic sounding, Journal of Glaciology, 2, 539-552. https://doi.org/10.3189/002214355793702064

Saintenoy, A., Friedt, J. M., Booth, A. D., Tolle, F., Bernard, E., Laffly, D., Marlin, C., Griselin, M. (2013). Deriving Ice Thickness, Glacier Volume and Bedrock Morphology of Austre Lovénbreen (Svalbard) Using GPR, Near Surface Geophysics, 11, 253–262. https://doi.org/10.3997/1873-0604.2012040

Schomacker, A., Kjær, K.H. (2008). Quantification of dead-ice melting in ice-cored moraines at the high-Arctic glacier Holmströmbreen, Svalbard, Boreas, 37, 211-225. https://doi.org/10.1111/j.1502-3885.2007.00014.x

Schoof, C. (2005). The effect of cavitation on glacier sliding, Proceedings of the Royal Society A, 461, 609-627. https://doi.org/10.1098/rspa.2004.1350

Sevestre, H., Benn, D.I. (2015). Climatic and geometric controls on the global distribution of surge-type glaciers: Implications for a unifying model of surging, Journal of Glaciology, 61, 646-662. https://doi.org/10.3189/2015JoG14J136

Sevestre, H., Benn, D.I., Hulton, N.R.J., Bælum, K. (2015). Thermal structure of Svalbard glaciers and implications for thermal switch models of glacier surging, Journal of Geophysical Research: Earth Surface, 120, 2220-2236. https://doi.org/10.1002/2015JF003517

Sevestre, H., Benn, D.I., Luckman, A., Nuth, C., Kohler, J., Lindbäck, K., Pettersson, R. (2018). Tidewater glacier surges initiated at the terminus, Journal of Geophysical Research: Earth Surface, 123, 1035-1051. https://doi.org/10.1029/2017JF004358

Sharp, M. (1985). “Crevasse-fill” ridges - A landform type characteristics of surging glaciers?, Geografiska Annaler: Series A, Physical Geography, 67, 213-220. https://doi.org/10.1080/04353676.1985.11880147

Smith, A.M., Murray, T., Davison, B.M., Clough, A.F., Woodward, J., Jiskoot, H. (2002). Late surge glacial conditions on Bakaninbreen, Svalbard, and implications for surge termination, Journal of Geophysical Research: Solid Earth, 107, 2152. https://doi.org/10.1029/2001JB000475

Smith, M.W., Carrivick, J.L., Quincey, D.J. (2016). Structure from motion photogrammetry in physical geography, Progress in physical geography, 40, 247-275. https://doi.org/10.1177/03091333156158

Sochor, L., Seehaus, T., Braun, M.H. (2021). Increased ice thinning over Svalbard measured by ICESat/ICESat-2 laser altimetry, Remote Sensing, 13, 2089. https://doi.org/10.3390/rs13112089

Solbø, S., & Storvold, R. (2013). Mapping svalbard glaciers with the cryowing UAS. The International Archives of the Photogrammetry, Remote Sensing and Spatial Information Sciences, 40, 373-377.

Still, H., Odolinski, R., Bowman, M. H., Hulbe, C., & Prior, D. J. (2024). Observing glacier dynamics with low-cost, multi-GNSS positioning in Victoria Land, Antarctica. Journal of glaciology, 70, e31. https://doi.org/10.1017/jog.2023.101

Streuff, K., Forwick, M., Szczuciński, W., Andreassen, K., Ó Cofaigh, C. (2015). Submarine landform assemblages and sedimentary processes related to glacier surging in Kongsfjorden, Svalbard, Arktos, 1. https://doi.org/10.1007/s41063-015-0003-y

Streuff, K., Ó Cofaigh, C., Noormets, R., Lloyd, J. (2018). Submarine landform assemblages and sedimentary processes in front of Spitsbergen tidewater glaciers, Marine Geology, 402, 209-227. https://doi.org/10.1016/j.margeo.2017.09.006

Striberger, J., Björk, S., Benediktsson, Í.Ö., Snowball, I., Uvo, C.B., Ingólfsson, Ó., Kjær, K.H. (2011). Climatic control of the surge periodicity of an Icelandic outlet glacier, Journal of Quaternary Science, 26, 561-565. https://doi.org/10.1002/jqs.1527

Strozzi, T., Paul, F., Wiesmann, A., Schellenberger, T., Kääb, A. (2017). Circum-Arctic changes in the flow of glaciers and ice caps from satellite SAR data between the 1990s and 2017, Remote Sensing, 9, 947. https://doi.org/10.3390/rs9090947

Strozzi, T., Mannerfelt, E.S., Cartus, O., Santoro, M., Schellenberger, T., Kääb, A. (2025). Glacier surge activity over Svalbard from 1992 to 2025 interpreted using heritage satellite radar missions and Sentinel-1, Cryosphere Discussions. https://doi.org/10.5194/egusphere-2025-5011

Stuart, G., Murray, T., Brisbourne, A., Styles, P., Toon, S. (2005). Seismic emissions from a surging glacier: Bakaninbreen, Svalbard. Annals of Glaciology, 42, 151-157. https://doi.org/10.3189/172756405781812538

Sund, M. (2006). A surge of Skobreen, Svalbard, Polar Research, 25, 115-122. https://doi.org/10.3402/polar.v25i2.6241

Sund, M., Eiken, T. (2010). Recent surges on Blomstrandbreen, Comfortlessbreen and Nathorstbreen, Svalbard, Journal of Glaciology, 56, 182-184. https://doi.org/10.3189/002214310791190910

Sund, M., Eiken, T., Hagen, J.O., Kääb, A. (2009). Svalbard surge dynamics derived from geometric changes, Annals of Glaciology, 50, 50-60. https://doi.org/10.3189/172756409789624265

Sund, M., Lauknes, T.R., Eiken, T. (2014). Surge dynamics in the Nathorstbreen glacier system, Svalbard, Cryosphere, 8, 623-638. https://doi.org/10.5194/tc-8-623-2014

Swirad, Z.M., Johansson, A.M., Malnes, E. (2024). Extent, duration and timing of the sea ice cover in Hornsund, Svalbard, from 2014-2023, Cryosphere, 18, 895-910. https://doi.org/10.5194/tc-18-895-2024

Tedstone, A.J., Nienow, P.W., Gourmelen, N., Dehecq, A., Goldberg, D., Hanna, E. (2015). Decadal slowdown of a land-terminating sector of the Greenland Ice Sheet despite warming, Nature, 526, 692-695. https://doi.org/10.1038/nature15722

Temminghoff, M., Benn, D.I., Gulley, J.D., Sevestre, H. (2019). Characterization of the englacial and subglacial drainage system in a high Arctic cold glacier by speleological mapping and ground-penetrating radar, Geografiska Annaler: Series A, Physical Geography, 101, 98-117. https://doi.org/10.1080/04353676.2018.1545120

Terleth, Y., van Pelt, W.J.J., Pohjola, V.A., Pettersson, R. (2021). Complementary approaches towards a universal model of glacier surges, Frontiers in Earth Science, 9. https://doi.org/10.3389/feart.2021.732962

Thøgersen, K., Gilbert, A., Schuler, T.V., Malthe-Sørenssen, A. (2019). Rate-and-state friction explains glacier surge propagation, Nature Communications, 10, 2823. https://doi.org/10.1038/s41467-019-10506-4

Thøgersen, K., Gilbert, A., Bouchayer, C., Schuler, T.V. (2024). Glacier surges controlled by the close interplay between subglacial friction and drainage, Journal of Geophysical Research: Earth Surface, 129, E2023JF007441. https://doi.org/10.1029/2023JF007441

Trantow, T., Herzfeld, U.C. (2018). Crevasses as indicators of surge dynamics in the Bering Bagley glacier system, Alaska: Numerical experiments and comparison to image data analysis, Journal of Geophysical Research: Earth Surface, 123, 1615-1637. https://doi.org/10.1029/2017JF004341

Trantow, T., Herzfeld, U.C. (2025). Progression of the surge in the Negribreen glacier system from two years of ICESat-2 measurements, Journal of Glaciology, 71, e2. https://doi.org/10.1017/jog.2024.58

Truffer, M., Kääb, A., Harrison, W.D., Osipova, G.B., Nosenko, G.A., Espizua, L., Gilbert, A., Fischer, L., Huggel, C., Craw Burns, P.A., Lai, A.W. (2021): Chapter 13 - Glacier surges. In: W. Haeberli and C. Whiteman (Eds.), Snow and Ice-Related Hazards, Risks, and Disasters (Second Edition). Elsevier. 417-466. https://doi.org/10.1016/B978-0-12-817129-5.00003-2

Vallot, D., Adinugroho, S., Strand, R., How, P., Pettersson, R., Benn, D.I., Hulton, N.R. (2019). Automatic detection of calving events from time-lapse imagery at Tunabreen, Svalbard, Geoscientific Instrumentation, Methods and Data Systems, 8, 113-127. https://doi.org/10.5194/gi-8-113-2019

Van Pelt, W., Frank, T. (2025). New glacier thickness and bed topography maps for Svalbard, Cryosphere, 19, 1-17. https://doi.org/10.5194/tc-19-1-2025

Van Pelt, W., Pohjola, V., Pettersson, R., Marchenko, S., Kohler, J., Luks, B., Hagen, J.O., Schuler, T.V., Dunce, T., Noël, B., Reijmer, C. (2019). A long-term dataset of climatic mass balance, snow conditions, and runoff in Svalbard (1957-2018), Cryosphere, 13, 2259-2280. https://doi.org/10.5194/tc-13-2259-2019

Van Pelt, W.J.J., Schuler, T.V., Pohjola, V.A., Pettersson, R. (2021). Accelerating future mass loss of Svalbard glaciers from a multi-model ensemble, Journal of Glaciology, 67, 485-499. https://doi.org/10.1017/jog.2021.2

Van Wychen, W., Burgess, D., Kochtitzky, W., Nikolic, N., Copland, L., Gray, L. (2020). RADARSAT-2 derived glacier velocities and dynamic discharge estimates for the Canadian High Arctic: 2015-2020, Canadian Journal of Remote Sensing, 46, 695-714. https://doi.org/10.1080/07038992.2020.1859359

Walter, F., Roux, P., Roeoesli, C., Lecointre, A., Kilb, D., Roux, P.F. (2015). Using glacier seismicity for phase velocity measurements and Green's function retrieval, Geophysical Journal International, 201, 1722-1737. https://doi.org/10.1093/gji/ggv069

Walter, F., Gräff, D., Lindner, F., Paitz, P., Köpfli, M., Chmiel, M., Fichtner, A. (2020). Distributed acoustic sensing of microseismic sources and wave propagation in glaciated terrain. Nature Communications, 11, 2436. https://doi.org/10.1038/s41467-020-15824-6

Weaver, C.S., Malone, S.D. (1979). Seismic evidence for discrete glacier motion at the rock–ice interface, Journal of Glaciology, 23, 171-184. https://doi.org/10.3189/S0022143000029816

Weertman, J. (1957). On the sliding of glaciers, Journal of Glaciology, 3, 33-38. https://doi.org/10.3189/S0022143000024709

Werner, C., Strozzi, T., Wiesmann, A., Wegmüller, U. (2008). GAMMA’s portable radar interferometer. In: Proceedings of the 13th FIG International Symposium on Deformation Measurements and Analysis & 4th IAG Symposium on Geodesy for Geotechnical and Structural Engineering, Lisbon, Portugal, May 12–15, 2008.

Woodward, J., Murray, McCaig, A. (2002). Formation and reorientation of structure in the surge-type glacier Kongsvegen, Svalbard, Journal of Quaternary Science, 17, 201-209. https://doi.org/10.1002/jqs.673

Woodward, J., Murray, T., Clark, R.A., Stuart, G.W. (2003). Glacier surge mechanisms inferred from ground-penetrating radar: Kongsvegen, Svalbard, Journal of Glaciology, 49, 473-480. https://doi.org/10.3189/172756503781830458

Woodward, J., Burke, M.J. (2007). Applications of ground-penetrating radar to glacial and frozen materials. Journal of Environmental & Engineering Geophysics, 12, 69-85. https://doi.org/10.2113/JEEG12.1.69

Zagórski, P., Frydrych, K., Jania, J., Błaszczyk, M., Sund, M., Moskalik, M. (2023). Surges in three Svalbard glaciers derived from historic sources and geomorphic features, Annals of the American Association of Geographers, 113, 1835-1855. https://doi.org/10.1080/24694452.2023.2200487

Zemp, M., Jakob, L., Dussaillant, I., Nussbaumer, S.U., Gourmelen, N., Dubber, S., Geruo A., Abdullahi, S., Andreassen, L.M., Berthier, E., Bhattacharya, A., Blazquez, A., Vock, L.F.B., Bolch, T., Box, J., Braun, M.H., Brun, F., Cicero, E., Colgan, W., Eckert, N., Farinotti, D., Florentine, C., Floricioiu, D., Gardner, A., Harig, C., Hassan, J., Hugonnet, R., Huss, M., Jóhannesson, T., Liang, C-C. A., Ke, C-Q., Khan, S.A., King, O., Kneib, M., Krieger, L., Maussion, F., Mattea, E., McNabb, R., Menounos, B., Miles, E., Moholdt, G., Nilsson, J., Pálsson, F., Pfeffer, J., Piermattei, L., Plummer, S., Richter, A., Sasgen, I., Schuster, L., Seehaus, T., Shen, X., Sommer, C., Sutterley, T., Treichler, D., Velicogna, I., Wouters, B., Zekollari, H., Zheng, W. (2025). Community estimate of global glacier mass changes from 2000 to 2023, Nature, 639, 382-388. https://doi.org/10.1038/s41586-024-08545-z

Zhan, Z. (2019). Seismic noise interferometry reveals transverse drainage configuration beneath the surging Bering Glacier. Geophysical Research Letters, 46(9), 4747-4756. https://doi.org/10.1029/2019GL082411